FINITE ELEMENT MODELLING OF REINFORCED CONCRETE FRAME

A Thesis Report submitted in the partial fulfillment of

requirement for the award of the degree of

MASTER OF ENGINEERING

IN

STRUCTURES

Submitted By

Beena Kumari

Roll No. 800822011

Under the Supervision of

Dr. Naveen Kwatra

Associate Professor,
Department, of Civil Engineering
Thapar University, Patiala

DEPARTMENT OF CIVIL ENGINEERING

THAPAR UNIVERSITY,

PATIALA- 147004, (INDIA).

JULY-2010

FINITE ELEMENT MODELLING OF REINFORCED CONCRETE FRAME

A Thesis Report submitted in the partial fulfillment of

requirement for the award of the degree of

MASTER OF ENGINEERING

IN

STRUCTURES

Submitted By

Beena Kumari

Roll No. 800822011

Under the Supervision of

Dr. Naveen Kwatra

Associate Professor,
Department, of Civil Engineering
Thapar University, Patiala

DEPARTMENT OF CIVIL ENGINEERING

THAPAR UNIVERSITY,

PATIALA- 147004, (INDIA).

JULY-2010

CONTENTS

CERTIFICATE

This is to certify that the work presented in this thesis titled **"Finite Element Modelling of Reinforced Concrete Frame"** being submitted by **Beena Kumari** in partial fulfillment of requirements for the award of degree of **MASTER OF ENGINEERING IN STRUCTURES**, submitted in the **CIVIL ENGINEERING DEPARTMENT, THAPAR UNIVERSITY, PATIALA**, is an authentic record of the initial work carried out by her under the supervision of **Dr. Naveen Kwatra, Associate Professor,** DEPARTMENT OF CIVIL ENGINEERING, THAPAR UNIVERSITY, PATIALA.

The matter embodied in this report has not been submitted in part or full to any other university or institute for the award of any degree.

15/7/10

(Dr. Naveen Kwatra)

Associate Professor,

Deptt. of Civil Engineering,

Thapar University, Patiala.

Counter signed by:

15/7/10

(Dr. Maneek Kumar)

Professor & Head,

Deptt. Of Civil Engineering,

Thapar University, Patiala.

23/7/10

(Dr. R.K.Sharma)

Dean Academic Affairs

Thapar University,

Patiala.

ACKNOWLEDGEMENT

A special debt of gratitude is owned to my thesis supervisor, **Dr. Naveen Kwatra, Associate Professor**, for his gracious efforts and keen pursuit, which has remained as a valuable asset for the successful instrument of my thesis report. His dynamism and diligent enthusiasm has been highly helpful in keeping my spirit high. His flawless and forthright suggestions blended with an innate intelligent application have crowned my task with success.

My thanks are due to **Dr. Maneek Kumar, Professor and Head**, Department of Civil Engineering for their constant encouragement I would also like to thank Ar. Karamjit Singh Chahal, Head, Department of Architecture, GNDU, Amritsar for his unconditional help during my work.

I would like to give special word of thanks to my husband and my son Anshuman for their patience and constant moral support during the entire course of my work. I would also like to thank my parents for their blessings. My friends also deserve a special word of thanks.

I would also like to offer my sincere thanks to all faculty and non-teaching staff of Civil Engineering Department (CED), TU, Patiala for their assistance.

beenakumari

BEENA KUMARI

M.E. CIVIL (STRUCTURES)

ABSTRACT

To model the complex behaviour of reinforced concrete analytically in its non-linear zone is difficult. This has led engineers in the past to rely heavily on empirical formulas which were derived from numerous experiments for the design of reinforced concrete structures.

The Finite Element method makes it possible to take into account non-linear response. The FE method is an analytical tool which is able to model RCC or retrofitted structure and is able to calculate the non-linear behaviour of the structural members is Finite element method. For structural design and assessment of reinforced concrete members, the non-linear finite element (FE) analysis has become an important tool. The method can be used to study the behaviour of reinforced and pre-stressed concrete structures including both force and stress redistribution.

The Finite Element method allows complex analyses of the nonlinear response of RC structures to be carried out in a routine fashion. FEM helps in the investigation of the behaviour of the structure under different loading conditions, its load deflection behaviour and the cracks pattern.

In the present study, the non-linear response of RCC control frame and the retrofitted RCC frame using FE Modelling under the incremental loading has been carried out with the intention to investigate the relative importance of several factors in the non-linear finite element analysis of RCC frames. These include the variation in load displacement graph, the crack patterns, propagation of the cracks, the crack width and the effect of the non-linear behaviour of concrete and steel on the response of control frame and deformed frame.

.

LIST OF FIGURES

LIST OF TABLES

CHAPTER 1

INTRODUCTION

1.1 GENERAL

Reinforced Cement Concrete is one of the most important and widely used building materials being used in many types of engineering structures. The economy, the efficiency, the strength and the stiffness of reinforced concrete make it an attractive material for a wide range of structural applications. For its use as structural material, reinforced concrete structures must satisfy the following conditions:

- The structure must be strong and safe.
- The structure must be stiff and appear unblemished. Care must be taken to control deflections under service loads and to limit the crack width to an acceptable level.
- The structure must be economical.

The ultimate objective of design of any structure is the creation of a safe and economical structure. Reinforced concrete (RC) structures are commonly designed to satisfy criteria of serviceability and safety. To ensure the serviceability and safety requirement it is necessary to predict the cracking and the deflections of RC structures under service loads. In order to assess the margin of safety of RC structures against failure an accurate estimation of the ultimate load is essential and the prediction of the load-deformation behavior of the structure throughout the range of elastic and inelastic response is desirable.

But still the Reinforced concrete (RC) structures get damaged due to various reasons. In most of the cases damage occurred in the form of cracks, concrete spalling, and large deflection, etc. There are various factors which are responsible for these deteriorations, such as increasing load, corrosion of steel, earthquake, environmental effects and accidental impacts on the structure. Due to these reasons it again becomes very important to assess the behaviour of concrete (RC) structures under all possible loading conditions.

In addition, the rise in cost of structures encourages engineers to seek more economical alternative designs often resorting to innovative construction methods without lowering the safety of the structure. Intimately related to the increase in scale of modern structures is the extent and impact of disaster in terms of human and economical loss in the event of structural failure. As a result, careful and detailed structural safety analysis becomes more and more necessary. The objective of such an analysis is the investigation

of the behavior of the structure under all possible loading conditions, both, monotonic and cyclic, its time-dependent behavior, and, especially, its behavior under overloading. [1]

The existing building can become seismically deficient since seismic design code requirements are constantly upgraded and advancement in engineering knowledge. Further, Indian buildings built over past two decades are seismically deficient because of lack of awareness regarding seismic behaviour of structures. The widespread damage especially to RC buildings during earthquakes exposed the construction practices being adopted around the world, and generated a great demand for seismic evaluation and retrofitting of existing building stocks.

The static pushover analysis is becoming a popular tool for seismic performance evaluation of existing and new structures. The pushover analysis provides adequate information on seismic demands imposed by the design ground motion on the structural system and its components. The purpose of pushover analysis is to evaluate the expected performance of structural systems by estimating performance of a structural system by estimating its strength and deformation demands in design earthquakes by means of static inelastic analysis, and comparing these demands to available capacities at the performance levels of interest. The evaluation is based on an assessment of important performance parameters, including global drift, inter-story drift, inelastic element deformations and deformations between elements. The inelastic static pushover analysis can be viewed as a method for predicting seismic force and deformation demands, which accounts in an approximate manner for the redistribution of internal forces that no longer can be resisted within the elastic range of structural behavior [2].

Up-gradation of reinforced concrete structures is required for many different reasons. The concrete may have become structurally inadequate for example, due to deterioration of materials, poor initial design and/or construction, lack of maintenance, upgrading of design loads or accidental events such as earthquakes. That's why repair and rehabilitation has become an increasingly important challenge for the reinforced cement concrete structures in recent years. The major goals of the retrofitting are to strengthening the retrofitted structures for life safety and the protection of the structures. The existing deficient structures are retrofitted to improve their performance in the event of any natural disaster and to avoid large scale damage to life and property. Evaluation of behaviour of structures after retrofitting is more important.

1.1.1 IMPORTANCE OF FINITE ELEMENT MODELLING

To model the complex behaviour of reinforced concrete analytically in its non-linear zone is difficult. This has led engineers in the past to rely heavily on empirical formulas which were derived from numerous experiments for the design of reinforced concrete structures.

The Finite Element method makes it possible to take into account non-linear response. The FE method is an analytical tool which is able to model RCC or retrofitted structure and is able to calculate the non-linear behaviour of the structural members is Finite element method. For structural design and assessment of reinforced concrete members, the non-linear finite element (FE) analysis has become an important tool. The method can be used to study the behaviour of reinforced and pre-stressed concrete structures including both force and stress redistribution.

With the advent of digital computers and powerful methods of analysis, such as the finite element method many efforts to develop analytical solutions which would obviate the need for experiments have been undertaken by investigators. The finite element method has thus become a powerful computational tool, which allows complex analyses of the nonlinear response of RC structures to be carried out in a routine fashion [1].

FEM is useful for obtaining the load deflection behaviour and its crack patterns in various loading conditions.

1.1.2 NEED FOR EXPERIMENTATION

The results of any analytical model have to be verified by comparing them with experiments in the lab or with full-scale structure. The development of reliable analytical models can, however, reduce the number of required test specimens for the solution of a given problem; recognizing and conducting those tests are time-consuming and costly and often do not simulate exactly the loading and support conditions of the actual structure.

Experimentation is an excellent tool for the verification purpose but at the same time it is very difficult and un-economical to perform experiment on full scale structures. Experiments provide a firm basis for design equations, which are invaluable for design. Within the framework of developing advanced design and analysis methods for structures the need for experimental research continues. [3]

1.1.2.1EXPERIMENTAL NONLINEAR STATIC PUSHOVER ANALYSIS

As more and more emphasis is being laid on nonlinear analysis of RC framed structures subjected to earthquake excitation, the research and development on both non-linear static (pushover) analysis as well

as nonlinear dynamic (time history) analysis is in the forefront. Due to the prohibitive computational time and efforts required to perform a complete nonlinear dynamic analysis, researchers and designers all over the world are showing keen interest in nonlinear static pushover analysis. However, all these procedures require determination of nonlinear force-deformation curves that are generated from pushover analysis. This simplifies the structural model, but it provides insight information about the likely non-linear behavior of the structure. Therefore, it can be said that a very vital step towards a good performance estimation of the structure against earthquakes is the determination of correct load-deformation curve popularly known as "pushover curve" or "capacity curve".

The correct procedure to evaluate the characteristics can be judged by comparing the analytical results with those of the experiments. The experiment on full scale real life type structure is the best way to not only study the behavior of the structures under lateral seismic loading but these results can provide the best database to validate the analytical procedures [4].

In order to bridge this gap between experimental and analytical data, Reactor Safety Division (RSD), Bhabha Atomic Research Centre (BARC) conducted a national round robin exercise in which a full–scale four storeyed structure described as under was tested under lateral monotonically increasing Pushover loads at tower testing facility at Central Power Research Institute (CPRI), Bangalore. The test was conducted under gradually increasing monotonic lateral load in an inverted triangular pattern till failure [4].

- The existing site located at CPRI, Bangalore. The building is a four-storeyed with the storey height of 4.0m.
- The building was tested for pushover analysis. The block size is a square of 5m side with the four columns at the each corner which supports the beams over it.

One of the major objectives of this work was to test a real- life structure under pushover loads. In order to keep the structure as close to reality as possible, no special design for the structure as such was performed and instead a portion of a real life existing office building was selected. Thus the structure tested in this work was a replica of a part of an existing office building. The portion was deliberately selected so that it had certain eccentricities and was un-symmetric in plan. Also the column sizes and sections were varied along the storey as in the case of original real life structure.

Although the geometry of the structure tested in this work was kept same as the portion of the original structure, there were few major differences in the reinforcement detailing as mentioned below:

1. Although the original structure was detailed according to new conforming seismic detailing practice as per IS 13920 (BIS, 1993), the structure for the experiment followed the non-seismic detailing practice as per IS 456(BIS 2000). The reason for this is the fact that pushover analysis is mostly used for retrofit of old structures, which have not followed the seismic detailing practice. Consequently, special confining reinforcement as recommended by IS 13920(BIS, 1993) was not provided. Also no shear reinforcement in the beam- column joints was provided.
2. 2. Since the structure tested is replica of a small portion of the large original structure, the continuous reinforcement in the slab and beams were suitably modified to fit as per the requirement.

Experiments without analysis can lead to results that are difficult to interpret or understand, and there is little point in performing analysis without testing since the accuracy of the analysis cannot be verified. This experiment has provided a rare opportunity for the finite element analysis of a full scale real life structure mentioned above as it provided all the necessary data for the validation of analytical results in the shape of Push-Over curve, displacements at various floor levels and damage patterns at different loads.

1.2 OBJECTIVES

In the present study, the non-linear response of RCC control frame and the retrofitted RCC frame using FE Modelling under the incremental loading has been carried out with the intention to investigate the relative importance of several factors in the non-linear finite element analysis of RCC frames. These include the variation in load displacement graph, the crack patterns, propagation of the cracks, the crack width and the effect of size of the finite element mesh on the analytical results and the effect of the non-linear behaviour of concrete and steel on the response of control frame and deformed frame.

The following are the main objectives of the present study:

1. To study the response and load-carrying capacity of four storeyed RC frame using non-linear finite element analysis.
2. To model the reinforced cement concrete frame in first phase of study and model the same frame with FRP wrapping in second phase using finite element method.
3. To compare the results of the control frame and the damaged retrofitted frame with the experimental results of Push Over test.

1.3 SCOPE OF THE WORK

In the first phase of the present study of FE modelling of the control RCC frame under the incremental loads has been analyzed using ATENA software and the results so obtained have been compared with available experimental results from the Push Over test conducted at CPRI Banglore.

The control frame is analyzed using ATENA software up to the failure and the load deformation curves are plotted and the cracking behaviour is monitored. The control frame has been analyzed and results have been compared with the experimental results.

In the second phase of the study, FE modelling the stressed/damaged retrofitted RCC frame is analyzed. The frame retrofitted by using GFRP is modelled and analyzed. The results obtained from the analysis of FF model have been plotted in the shape of base-shear v/s deflection graphs at different floor levels. Comparisons are made by the load deflection curves and values. Deflection and cracking behaviour of the RCC frame are also studied.

The following parameters are proposed to be measured:

i) Nonlinear load-deflection behaviour.

ii) Study of crack patterns at different load steps.

iii) Level/type of damage and location of damage.

The effect on the above parameters due to use of the retrofitting materials like FRP for strengthening of the experimental frames (subjected to damage) is also studied.

1.4 ORGANIZATION OF THE THESIS

The thesis is organized as par detail given below:

Chapter 1: Introduces to the topic of thesis in brief.

Chapter 2: Discusses the literature review i.e. the work done by various researchers in the field of FE modelling of RCC structural members as well as retrofitted members.

Chapter 3: Deals with the details of the structure modelled in Atena in its first part. Second part comprises of FEM modelling, theory related to the ATENA, material modelling and analytical programming procedure steps involved in modelling of the control frame. It also deals with the description of the material behaviour of concrete, reinforced steel bars.

Chapter 4: In this chapter retrofitted frame has been discussed in detail. The theory related to retrofitting of the RCC elements and GFRP also discussed in brief.

Chapter 5: The results from the analysis, comparison between the analytical and the experimental results, results comparison between the control frame and damaged retrofitted frame and the cracking behaviour of the frame, all are discussed in. Comparison of results b/w control and retrofitted frame are discussed in second part of chapter.

Chapter 6: Finally, salient conclusions and recommendations of the present study are given in this chapter followed by the references.

CHAPTER 2

LITERATURE REVIEW

2.1 GENERAL

To provide a detailed review of the literature related to FE modelling and retrofitted reinforced cement concrete structures in its entirety would be difficult to address in this chapter. A brief review of previous studies on the application of the finite element method to the analysis of reinforced concrete structures and retrofitted structures is presented is this section.

This literature review focuses on recent contributions related to retrofitting techniques of the RCC structures, material used for retrofit and past efforts most closely related to the needs of the present work.

2.2 FINITE ELEMENT MODELLING AND THE STRENGTHENING OF RC MEMBERS

Amer M. Ibrahim et al., (2009) presented an analysis model for reinforced concrete beams externally reinforced with fiber reinforced polymer (FRP) laminates using finite elements method adopted by ANSYS. The finite element models are developed using a smeared cracking approach for concrete and three dimensional layered elements for the FRP composites. The results obtained from the ANSYS finite element analysis are compared with the experimental data for six beams with different conditions from researches (all beams are deficient of shear reinforcement). The comparisons are made for load-deflection curves at mid-span; and failure load. The results from finite element analysis were calculated at the same location as the experimental test of the beams. The accuracy of the finite element models is assessed by comparison with the experimental results, which are to be in good agreement. The load-deflection curves from the finite element analysis agree well with the experimental results in the linear range, but the finite elements results are slightly stiffer than that from the experimental results. The maximum difference in ultimate loads for all cases is 7.8%. [6]

Barbato M. et al., (2009) studied the efficient finite element modelling of reinforced concrete beams retrofitted with fibre reinforced polymers. This study presents a new simple and efficient two-dimensional frame finite element (FE) able to accurately estimate the load-carrying capacity of reinforced concrete (RC) beams flexurally strengthened with externally bonded fibre reinforced polymer (FRP) strips and plates. The proposed FE, denoted as FRP–FB beam, considers distributed plasticity with layer-discretization of the cross-sections in the context of a force-based (FB) formulation. The FRP–FB-beam element is able to model collapse due to

concrete crushing, reinforcing steel yielding, FRP rupture and FRP debonding. The FRP–FB-beam is used to predict the load-carrying capacity and the applied load-mid span deflection response of RC beams subjected to three- and four-point bending loading. Numerical simulations and experimental measurements are compared based on numerous tests available in the literature and published by different authors. The numerically simulated responses agree remarkably well with the corresponding experimental results. The major features of this frame FE are its simplicity, computational efficiency and weak requirements in terms of FE mesh refinement. These useful features are obtained together with accuracy in the response simulation comparable to more complex, advanced and computationally expensive FEs. Thus, the FRP–FB-beam is suitable for efficient and accurate modelling and analysis of flexural strengthening of RC frame structures with externally bonded FRP sheets/plates and for practical use in design-oriented parametric studies. [7]

Singhal H. (2009) analyzed three RCC retrofitted beams stressed at different levels in his research. In first phase of his research three beams are FE modelled on software ATENA. Results are analyzed and compared the stressed GFRP retrofitted beams at 60%, 75% and 90% with the results of control beam. The results showed that stressed retrofitted beam has higher ultimate load deflection than the control beam. In the second phase of this research is to compare the results with the experimental results and to try to identify the various effects on RCC structural members. The results show good agreement with the experimental results. Only the analytical results of the control beam showed some difference from experimental results whereas analytical results of the stressed retrofitted beam show nearly the same results as experimental results. [8]

Pannirselvam N. et al., (2008) presented the experimental work for Strength Modelling of Reinforced Concrete Beam with Externally Bonded Fibre Reinforcement Polymer. In this study, three different steel ratios are used with two different Glass Fibre Reinforced Polymer (GFRP) types and two different thicknesses in each type of GFRP were used. 15 beams were casted for this work in which 3 were used as a control beam and the remaining were fixed with the GFRP laminate on the soffit. Flexural test, using simple beam with two-point loading was adopted to study the performance of FRP plated beams in terms of flexural strength, deflection, ductility and was compared with the un-plated beams. The results obtained from this experiment showed that the beams strengthened with GFRP laminates exhibit better performance. The flexural strength

and ductility increase with increase in thickness of GFRP plate. The increase in first crack loads was up to 88.89% for 3 mm thick Woven Rovings GFRP plates and 100.00% for 5 mm WRGFRP plated beams and increase in ductility in terms of energy and deflection was found to be 56.01 and 64.69% respectively with 5 mm thick GFRP plated beam. Strength models were developed for predicting the flexural strength (ultimate load, service load) and ductility of FRP beams. [9]

Camata G. et al., (2007) presented a joint experimental–analytical investigation and studied the brittle failure modes of RCC members strengthened in flexure by FRP plates. Both mid span and plate end failure modes are studied. In the experimental work, four RC members were cast, two slabs and two beams. Out of these four members, one slab and one beam were tested as un-strengthened members and the other one slab and one beam were tested as a strengthened member. Same work can be done analytically. These RC members were modelled and analyzed through the finite element method. The finite element analyses are based on non-linear fracture mechanics. The FE model considers the actual crack pattern observed in the tests. The FEM uses both discrete and smeared crack discretization, because only a combination of the two crack model accurately traces the stiffness degradation of the strengthened members. The smeared crack mode was used for the beam concrete; the discrete crack model was used for the interfaces where delamination can be expected.

The strengthening of the RC beams was done with both CFRP and GFRP and notice the difference between these two materials. This paper shows how concrete cracking, adhesive behaviour, plate length, width and stiffness affect the failure mechanisms take place. The numerical and experimental work gave several results that show that debonding and concrete cover splitting failure modes occur always by crack propagation inside the concrete. For short FRP plates, failure starts at the plates end, while the longer FRP plates, failure starts at mid span. A comparison between CFRP and GFRP strengthening with the same axial stiffness but different contact area showed that increasing the plate width increases greatly the peak load and the deformation level of the strengthened beam. The analyses also indicated that an important parameter is the distance between flexural and shear cracks. [10]

Ferracuti et al., (2006) studied the numerical modelling for FRP-concrete delamination. A non-linear bond–slip model is presented for the study of delamination phenomenon. This research showed that FRP retrofit could be very useful to improve also the behaviour of the RC structure under both short term and long term service loadings. A non-linear interface law is adopted; the bonding between FRP plate and concrete is modelled by a non-linear interface law. A non-linear system of equations is then obtained via finite difference method. Newton–Raphson algorithm, different control parameters can be adopted in the various phases of delamination process (alternatively, force or displacements variables). Some numerical

simulations are presented, concerning different delamination test setups and bond lengths. The numerical results of this study agree well with experimental data reported in the literature. A non-linear shear stress–slip law is adopted for the interface, which takes non-linear behaviour of concrete cover into account. Finite difference method is used to solve the non-linear system of governing equations. It is also shown that, adopting classical delamination test setup, snap-back behaviour in the load–displacement curve occurs for bonded plate lengths greater than the minimum anchorage length. [11]

Mehri et al. (2005) reviews the results of some recent works conducted by the author on new methods of retrofitting the RC frames. On the local retrofit of RC members, it includes the work on the application of a new high performance fiber reinforced cementitious composite material. The composite can be applied either as a wet mix to the adhesive. The suitability of this technique of member retrofit to enhance the strength and ductility of the retrofitted member compared with other methods of local retrofit, such as steel plates and FRP laminates, is discussed. Other works reviewed in this paper include those carried out recently on global retrofit of RC frames using direct internal steel bracing. Results of inelastic pushover tests on scaled models of ductile RC frames, steel X and knee braces are presented which indicate that such bracings can increase the desired thickness or attached as precast sheets or strips to the face of the member using a suitable epoxy yield and strength capacities and reduce the global displacements of the frames to the desired levels. Also, the results of direct tensile tests on three full scale models of three different types of brace/RC frame connections are presented. Finally, the values of seismic behaviour factor, R, for this type of brace/frame system, evaluated from inelastic pushover analysis of dual systems of different heights and configurations are presented. It is concluded that .as for the global retrofit of the frame by steel bracing, addition of the bracing system through direct connections to the frame can enhance the stiffness and strength of the system. Both X braces and knee braces may be utilized to design or retrofit for a damage level earthquake. However, when designing or retrofitting for a collapse level earthquake for which ductile behaviour is necessary, the knee bracing system is most suitable.[12]

Perera et al., (2004) studied the adherence analysis of fiber reinforced polymer strengthened RC beams. In this paper, the effect of bonding between reinforced concrete and composite plates (CFRP) is discussed when epoxy adhesive is used. They compared the analytical and experimental results which came out from the works can be done in this paper. A test had been designed to characterize the behaviour of the adhesive connection between FRP and concrete. The test was based on the beam test, similar to the adherence test for steel reinforcement of concrete. In the same way, a numerical model based on finite elements has been developed to simulate the behaviour of RC members strengthened with FRP plates. The non-linear response of the strengthened members is determined through the development of numerical material non-linear constitutive models capable of simulating what happens experimentally. A

local failure occurred mainly determined by high shear bond stresses transmitted to the concrete from the plates via adhesive. Debonding started at the mid span at the concrete blocks ends and propagated from there to the intermediate areas of the blocks. In the analytical work, the model considers the position and increase of concrete cracks which has a very important influence on the overall response of the strengthened beam; it also affects the distribution of the stresses in the various locations of the member and the failure mechanism. In general, the model performs reasonably well in predicting the behaviour of the FRP strengthened beam. [13]

Supavirryakit et al., (2004) performed analytically the non-linear finite element analysis of reinforced concrete beam strengthened with externally bonded FRP plates. The finite element modelling of FRP-strengthened beams is demonstrated in this paper. The key for success of the analysis is the correct material models of concrete, steel and FRP. The concrete and reinforcing steel are modelled together by 8-node 2-D isoparametric plane stress RC element. The RC element considers the effect of cracks and reinforcing steel as being smeared over the entire element. Concrete cracks and steel bars are treated in a smeared manner. The FRP plate is modelled by 2D elastic element. The epoxy layer can also be modelled by 2D elastic elements. Stress-strain properties of cracked concrete consist of tensile stress model normal to crack, compressive stress model parallel to crack and shear stress model tangential to crack. Stress strain property of reinforcement is assumed to be elastic-hardening to account for the bond between concrete and steel bars. FRP is modelled as elastic-brittle material. The objective of the test was to investigate the effect of the bonded length on peeling mode of FRP. The results obtained from this analytical work that the finite element analysis can accurately predict the load deformation, load capacity and failure mode of the beam. It can also capture cracking process for the shear-flexural peeling and end peeling failures, similar to the experiment. [14]

Sanathakumar et al., (2004) performed the analysis of the retrofitted reinforced concrete shear beams using CFRP composites. This study presented the numerical study to simulate the behaviour of retrofitted reinforced concrete (RC) shear beams. The study was carried out on the control RC beam and retrofitted RC beams using carbon fibre reinforced plastic (CFRP) composites with ±45o and 90o fibre orientations. The effect of retrofitting on un-cracked and pre-cracked beams was studied too. The finite elements adopted by ANSYS were used in this study. A quarter of the full beam was used for modelling by taking advantage of the symmetry of the beam and loadings. The results obtained from this paper were the load deflection graph which showed good agreement with the experimental plots. There was a difference in behaviour between the un-cracked and pre-cracked retrofitted beams though not significant. This numerical modelling helps to track the crack formation and propagation especially in case of retrofitted beams in which the crack patterns cannot be seen by the experimental study due to wrapping of CFRP

composites. This numerical study can be used to predict the behaviour of retrofitted reinforced concrete beams more precisely by assigning appropriate material properties. The crack patterns in the beams were also presented. [15]

Cardone D.et al., (2004) an extensive program of shaking table tests on 1/4-scale three-dimensional R/C frames was jointly carried out by the Department of Structure, Soil Mechanics and Engineering Geology (DSGG) of the University of Basihcata, Italy, and the National Laboratory of Civil Engineering **(**LNEC), Portugal. It was aimed at evaluating the effectiveness of passive control bracing systems for the seismic retrofit of R/C frames designed for gravity loads only. Two different types of braces were considered, one based on the hysteretic behaviour of steel elements, the other on the super-elastic properties of Shape Memory Alloys (SMA). Different protection strategies were pursued, in order to fully exploit the high energy dissipation capacity of steel-based devices, on one hand, and the supplemental re-centring capacity of SMA-based devices, on the other hand. The experimental results confirmed the great potentials of both strategies and of the associated devices in limiting structural damage. The retrofitted model was subjected to table accelerations as high as three times the acceleration leading the unprotected model to collapse, with no significant damage to structural elements. Moreover, the re-centring capability of the SMA-based bracing system was able to recover the un-deforrned shape of the frame, when it was in a near-collapse condition. In this paper the experimenta1 behaviour of the non protected and of the protected structural models are described and compared. [16]

Yanga et al., (2003) performed an experiment on finite element modelling of concrete cover separation failure in FRP plated RC beams on the tension side of the reinforcement concrete beam. This paper deals with a fracture mechanics based finite element analysis of debonding failures. This study investigates the behaviour of an FRP plated RC beam using a discrete crack model based on FEA. In this research, only half of the beam was modelled accounting for its symmetry. Four node quadrilateral isoparametric elements and three node constant strain elements were used to model the concrete, adhesive and CFRP plate. The internal steel reinforcements were modelled using two-node truss elements. The concrete was modelled by near square elements to simplify the re-meshing process. The concrete cover on the tension face was modelled using four layers of elements. Both the adhesive and the CFRP plate were modelled using one layer of elements. The results obtained from this study, in a preliminary study was successfully simulated the concrete cover separation failure mode in FRP strengthened RC beams. Initial numerical results confirmed that the bonding of a plate leads to smaller and more closely spaced cracks than the un-strengthened beam. For plated beams, the cracking can have a significant effect on the stress distribution in the FRP plates. The stress distribution is uniform in the constant bending moment span only before major cracks are developed or close to the ultimate state. The length of the plate has a significant effect on

the failure mode. The numerical example showed that if all other parameters remain unchanged, a beam strengthened with a short plate is more likely to fail due to concrete cover separation and in a more brittle manner. [17]

Kachlakev et al. **(2001)** Finite element method (FEM) models are developed to simulate the behavior of four full-size beams from linear through nonlinear response and up to failure, using the ANSYS program (ANSYS 1998). Comparisons are made for load-strain plots at selected locations on the beams; load-deflection plots at mid-span; first cracking loads; loads at failure; and crack patterns at failure. The models are subsequently expanded to encompass the linear behavior of the Horsetail Creek Bridge. Modeling simplifications and assumptions developed during this research are presented. The study has compared strains from the FEM analysis with measured strains from load tests. Conclusions from the current research efforts and recommendations for future studies are included. [3]

Duthinh et al., (2001) conducted an experiment on strengthening of reinforced concrete beams using CFRP. The seven test beams were cast and strengthening externally with carbon fibre reinforced polymer (FRP) laminate after the concrete had cracked were tested under four-point bending. The results obtained from this experiment showed that CFRP is very effective for flexural strengthening. As the amount of steel reinforcement increases, the additional strength provided by the carbon FRP external reinforcement decreases. Compared to a beam reinforced heavily with steel only, the beams reinforced with both steel and carbon have adequate deformation capacity, in spite of their brittle mode of failure. [18]

Ma R. et al., (2000) performed A proof test was to investigate the improved seismic performance of parking structure columns retrofitted with carbon fiber composite jacketing. One full-scale square column with details simulating the typical existing parking structure columns designed following the pre-1971 codes was constructed and tested under constant axial load, cyclic shear and moment in double bending condition. Assessment analysis indicated that the column in 'as built' condition would suffer either a brittle shear failure or a premature failure due to lap-splice deterioration. Such failure modes could be avoided by the carbon fiber composite jacketing, which allowed the column to develop excellent hysteretic response with stable load carrying capacity and significantly improved ductility. [19]

Shahawy et al. (1995) assessed the effectiveness of external reinforcement in terms of the cracking moment, maximum moment, deflection, and crack patterns. Four beams (8"x12"x108") were tested using minimum steel reinforcement (two ½" diameter bars) and varying the layers of unidirectional CFRP. Also, non-linear finite element computer model was used to compare to the results of the experiment. The cracking moment of the CFRP repaired beams was much larger than that of the control beam. For one,

two, and three layers of GFRP, the cracking moment increased 12%, 61%, and 105%, respectively. The maximum moment also became larger and corresponded well to the theoretical data. A 13%, 66%, and 105% increase was observed for the three different layers. This showed the CFRP behaved similarly before and after cracking of the beam. The deflection and cracking patterns showed results similar to experiments. The deflection decreased inversely with the number of CFRP layers on each beam. This, alternatively, caused the stiffness to increase. The cracking patterns between the control and the CFRP repaired beams exhibited different patterns. The control had wider cracks while the repaired beams showed smaller cracks at relatively close spacing. This shows an enhanced concrete refinement due to the CFRP. [20]

2.3 Gaps in Research Area

Many experimental and analytical works has been done by many researchers in the area of strengthening and retrofitting the structural members with composite materials. The concept of retrofitting the structural members is rapidly growing due to enable the early identification of damage and provides warning for unsafe condition. Some researchers have also investigated or work on the area of the failure mode of the FRP strengthened structural members and some are work on the strengthening of the structural members with different FRP materials.

This research is concerned with the finite element modelling of the retrofitted the RC beam using the GFRP. The use of GFRP sheets for retrofitting and the strengthening of the reinforced concrete structural have been studied extensively in previous studies. However, many researchers performed experimentally and analytically the strengthening of the beams/columns but limited work is done on the study of RCC frames and in the field of stressed/damaged retrofitted structural members.

2.4 Closure

The literature review has suggested that use of a finite element modelling of the RCC control frame and retrofitted RCC frame is indeed feasible. So it has been decided to use ATENA for the FE modelling. With the help of this software study of RC frame has been done. ATENA also helps in FE modelling and meshing inside the surface of element. It gives the load deflection curve and gives the values of stresses and strains, crack width of the elements of the frame at every step.

CHAPTER 3

FINITE ELEMENT MODELLING OF RC FRAME

This chapter is intended to give a description of the structure that is to be FE modeled and analyzed to obtain the pushover curve analytically. In first part of the chapter the RC frame (experimentally analyzed at CPRI, Banglore) is described in detail. This chapter also discusses the theory related to ATENA and information about finite elements currently implemented in ATENA in its second part. All the necessary steps to create these models are explained in detail and the steps taken to generate the analytical load-deformation response of the model are discussed.

3.1 GENERAL

As more and more emphasis is being laid on nonlinear analysis of RC framed structures subjected to earthquake excitation, the research and development on both non-linear static (push over) analysis as well as nonlinear dynamic (time history) analysis is in the forefront. Due to the prohibitive computational time and efforts required to perform a complete nonlinear dynamic analysis, researchers and designers all over the world are showing keen interest in nonlinear static pushover analysis. However, all these procedures require determination of nonlinear force-deformation curves that are generated from pushover analysis. This simplifies the structural model, but it provides insight information about the likely non-linear behavior of the structure. Therefore, it can be said that a very vital step towards a good performance estimation of the structure against earthquakes is the determination of correct load-deformation curve popularly known as “pushover curve” or “capacity curve” [4].

The correct procedure to evaluate the characteristics can be judged by comparing the analytical results with those of the experiments. The experiment on full scale real life type structure is the best way to not only study the behavior of the structures under lateral seismic loading but these results can provide the best database to validate the analytical procedures.

3.2 GENERAL DESCRIPTION OF STRUCTURE

One of the major objectives of this work was to test a real- life structure under pushover loads. In order to keep the structure as close to reality as possible, no special design for the structure as such was performed and instead a portion of a real life existing office building was selected. Thus the structure tested in this work was a replica of a part of an existing office building. The portion was deliberately selected so that it

ertain eccentricities and was un-symmetric in plan (**Figure 3.1**). Also the column sizes and sections were varied along the storey as in the case of original real life structure. [4]

Although the geometry of the structure tested in this work was kept same as the portion of the original structure, there were few major differences in the reinforcement detailing as mentioned below:

1. Although the original structure was detailed according to new conforming seismic detailing practice as per IS 13920 (BIS, 1993), the structure for the experiment followed the non-seismic detailing practice as per IS 456(BIS 2000). The reason for this is the fact that pushover analysis is mostly used for retrofit of old structures, which have not followed the seismic detailing practice. Consequently, special confining reinforcement as recommended by IS 13920(BIS, 1993) was not provided. Also no shear reinforcement in the beam- column joints was provided.

2. Since the structure tested is replica of a small portion of the large original structure, the continuous reinforcement in the slab and beams were suitably modified to fit as per the requirement.

3. Another major difference is in the foundation system. In order to avoid any nonlinear behavior of the foundation, a raft foundation with a number of rock anchors were provided.

3.2.1 Material properties

The material used for construction is Reinforced concrete with M-20 grade concrete and fe-415 grade reinforcing steel. The Stress-Strain relationship used is as per I.S.456:2000. The basic material properties used are as follows:

Modulus of Elasticity of steel, E_s = 21,0000 MPa
Modulus of Elasticity of concrete, E_C = 22,360.68 MPa
Characteristic strength of concrete, f_{ck} = 20 MPa
Yield stress for steel, f_y =415 MPa
Ultimate strain in bending, ε_{cu} =0.0035

3.2.2 Model Geometry

The structure analyzed is a four-storied, one bay along X-direction and two bays along Y-direction moment-resisting frame of reinforced concrete with properties as specified above. The concrete floors are modeled as rigid. The details of the model are given as:

- Number of stories = 4

- Number of bays along X-direction =1
- Number of bays along Y-direction = 1
- Storey height = 4.0 meters
- Bay width along X-direction = 5.0 meters
- Bay width along Y-direction = 5.0 meters

3.2.3. Plan of Building

The plan of the building is shown in the Figure below. The bay width, column positions and beams positions can be seen here.

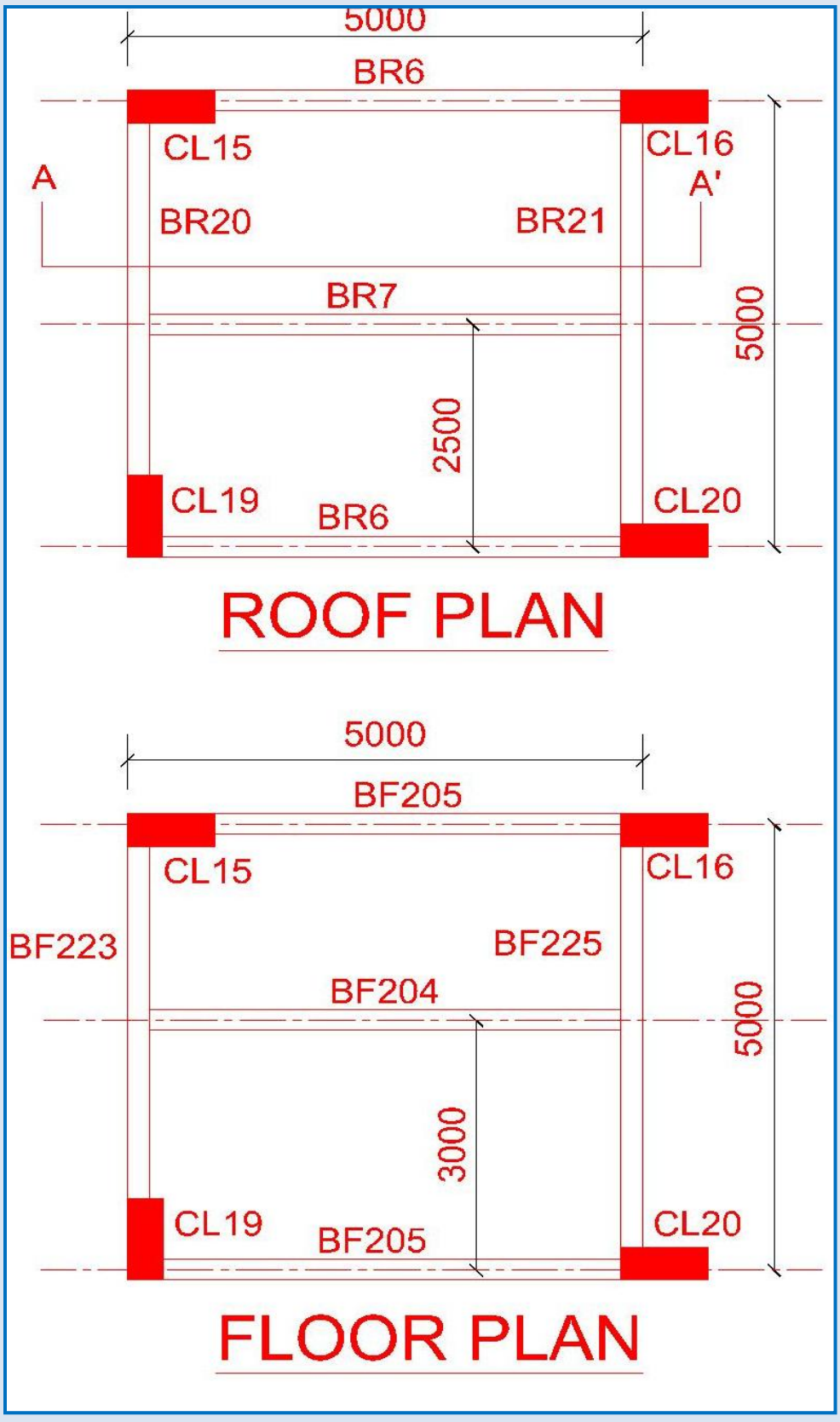

Figure 3.1 Roof Plan & Floor Plan of Structure [4]

3.2.4 ELEVATION OF BUILDING

The Figure 3.2 shows the sectional elevation of the structure. The storey heights, column lines, description of slabs etc. can be seen in this picture.

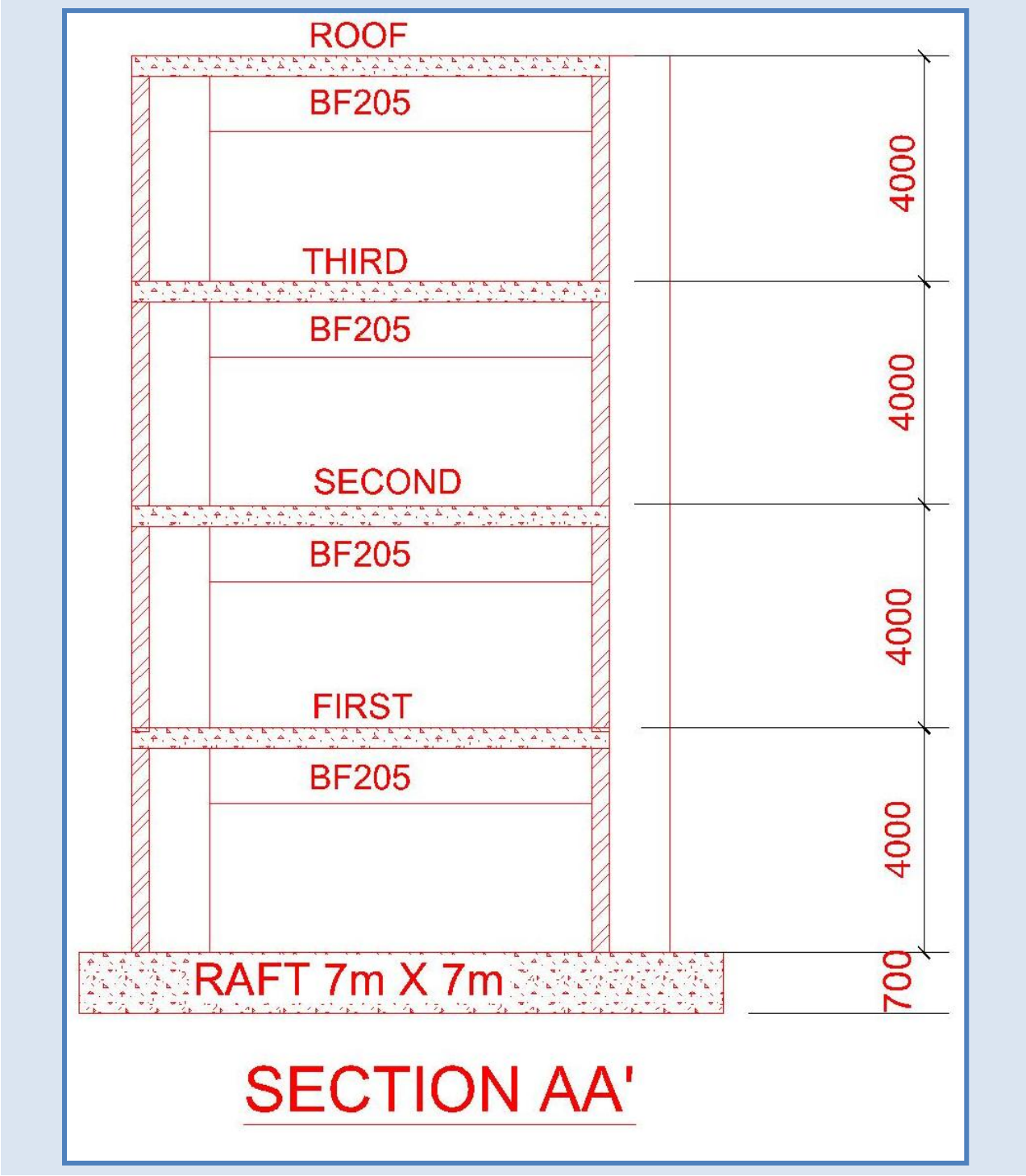

Figure 3.2.Sectional Elevation of the Structure [4]

3.2.5 SECTION DIMENSIONS

The structure is made of various sections whose dimensions are enlisted in table 3.1 below. In the identification column, 'B' stands for beam, 'F' stands for floor, and 'R' stands for roof. The first numeral after 'F' in 'BF' stands for the floor number and the rest two are used to identify the beam at the floor. Therefore, all 'BF' designations stand for the floor beams while 'BR' stands for roof beams. Similarly, 'CL' represents column while the first numeral after it stands for the floor to which that column is extending. The section dimensions are enlisted below:

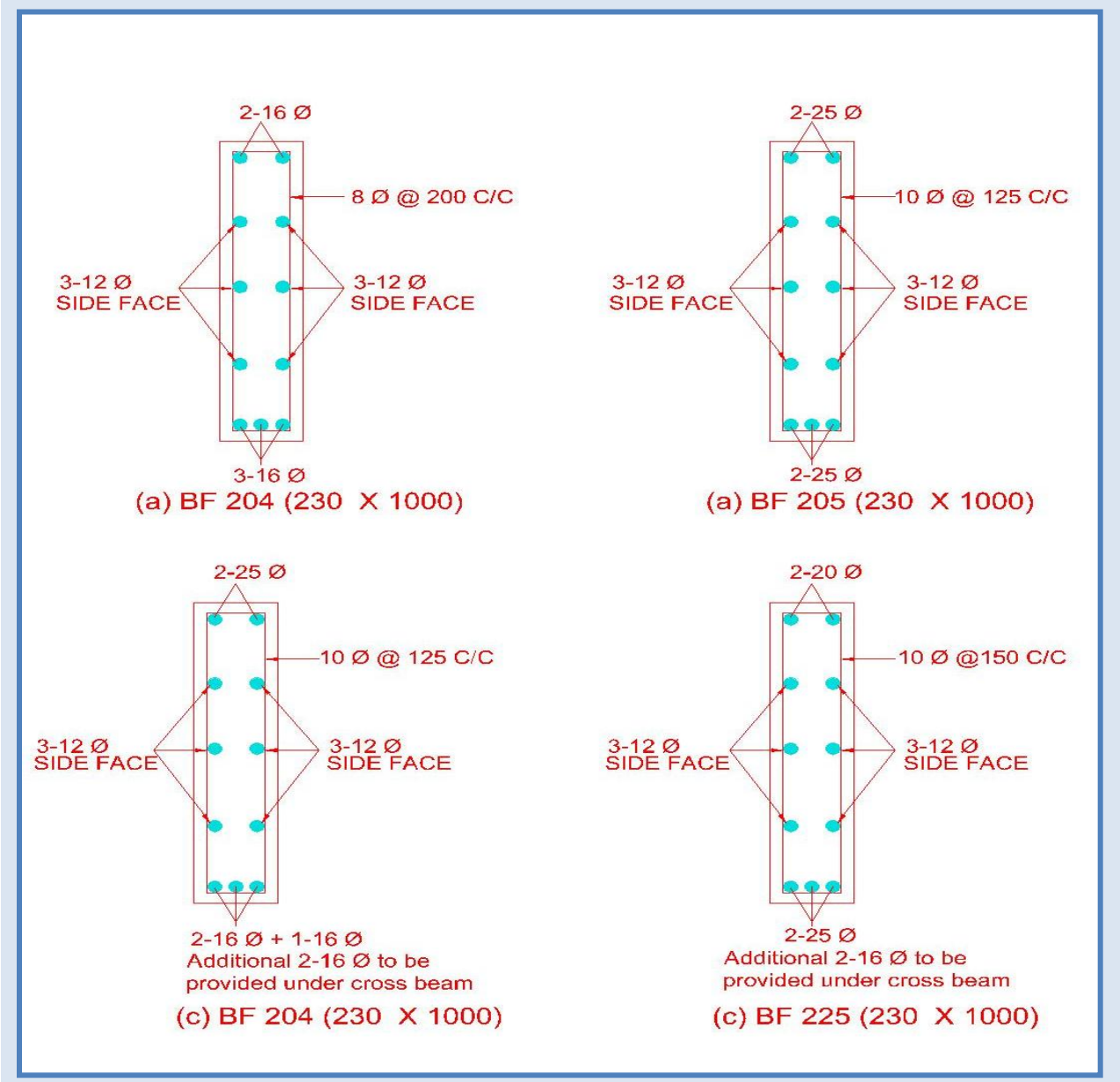

Figure 3.3 Detail of Floor Beams [4]

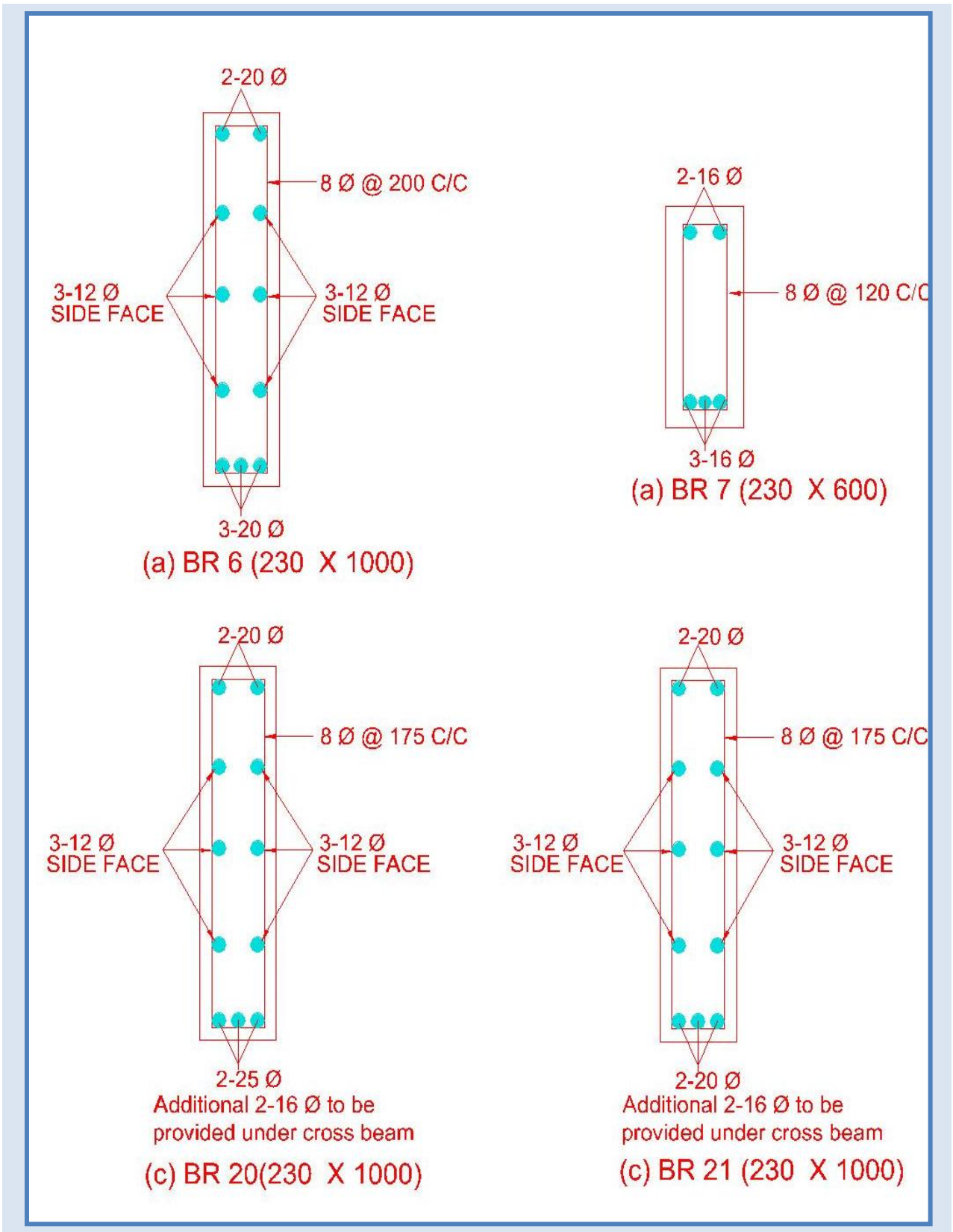

Figure 3.4 Detail of Roof Beams [4]

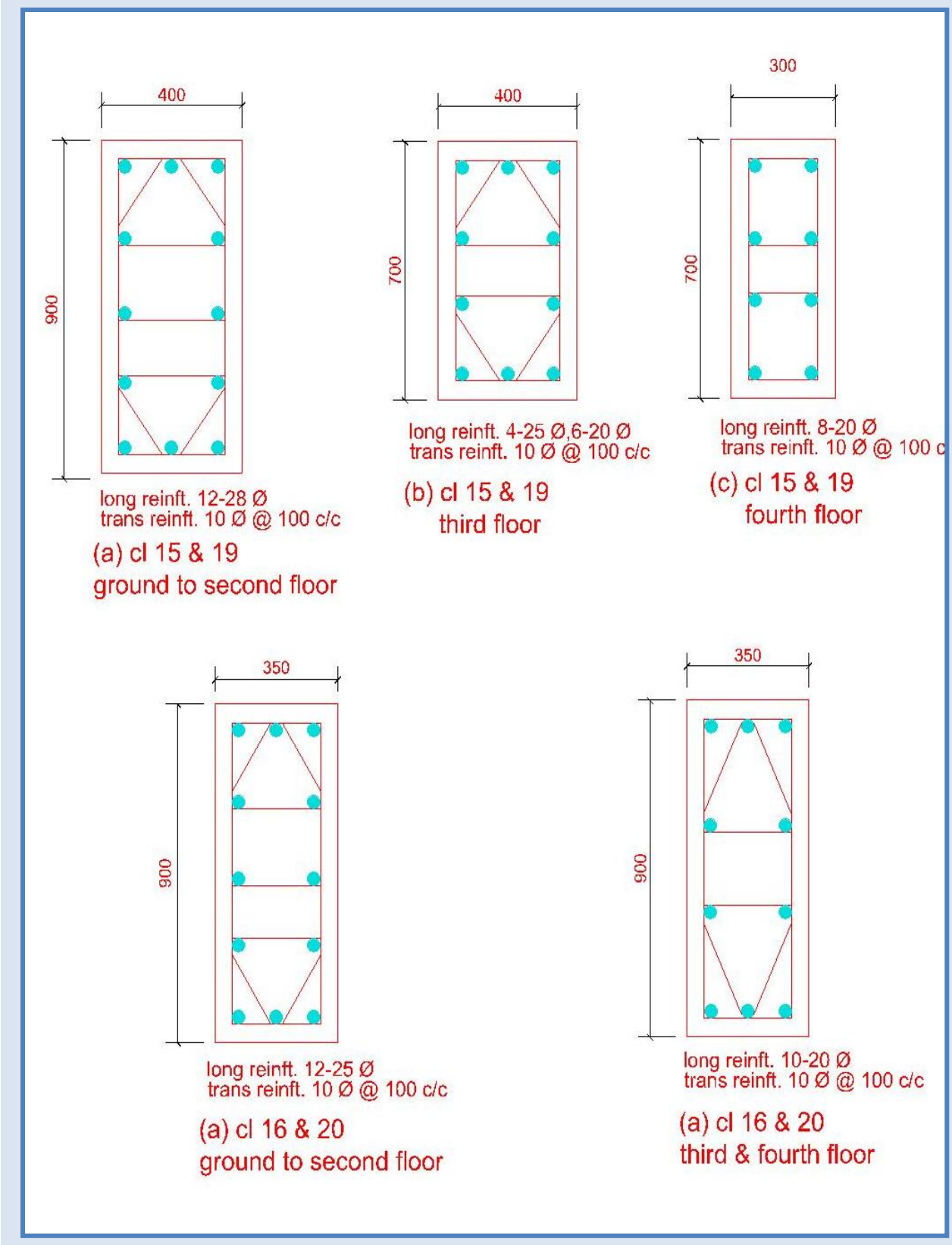

Figure 3.5 Detail of Columns [4]

3.2.6 Reinforcement Details

Detail reinforcement provided is as given in Table 3.1

Table 3.1 Detail of reinforcement [4]

Identification	B	D	Top Cover	Bottom Cover	Top steel nob-dia	Bottom steel stirrups	Dia of stirrups	Spacing of stirrups
BR6M	230	1000	35	35	2-20	3-20	8	200
BR6L	230	1000	35	35	3-20	3-20	8	200
BR6R	230	100	35	35	5-20	3-20	8	200
BR7MR	230	600	33	33	2-16	3-16	8	120
BR7L	230	600	33	33	2-16+1-20	3-16	8	120
BR20M	230	1000	35	37.50	2-20	2-25	8	175
BR20LR	230	1000	35	37.50	4-20	2-25	8	175
BR21M	230	1000	35	35	2-20	2-20	8	175
BR21LR	230	1000	35	35	3-20	2-20	8	175
BF204MR	230	1000	33	33	2-16	3-16	8	200
BF204L	230	1000	33	33	1-16+1-20	3-16	8	200
BF205M	230	1000	37.50	37.50	2-25	2-25	10	125
BF205L	230	1000	37.50	37.50	2-15+2-12	2-25	10	125
BF204R	230	1000	37.50	37.50	4-25	2-25	10	125
BF223M	230	1000	37.50	37.50	2-25	2-25+1-16	10	125
BF223LF	230	1000	37.50	37.50	4-25	2-25+1-16	10	125

BF225M	230	1000	35	37.50	2-20	2-25	10	150
BF224LR	230	1000	35	37.50	4-20	2-25	10	150
C15-G-2	400	900	54	54	12-28		10	100
C15-G-3	400	700	52.50	52.50	4-25+6-20		10	100
C15-G-R	300	700	50	50	8-20		10	100
C1620-G-2	350	900	52.50	52.50	12-25		10	100
C1620-G-R	350	900	50	50	10-20		10	100
C19-G-2	900	400	5	454	12-28		10	100
C19-G-3	700	400	52.50	52.50	4-25+6-20		10	100
C19-G-R	700	300	50	50	8-20		10	100

3.3 EXPERIMENT

3.3.1 LOADING PATTERN

Pushover loads can acceptably be applied in inverse triangular fashion, parabolic fashion or in the ratio of the first mode shape etc. In view of the existing tower test facility, it was found that the best possible control of loading would be through the inverse triangular loading. Therefore, the load on the structure was applied in an inverted triangular fashion. The ratio of force at "1st floor: 2nd floor: 3rd floor: 4th floor" was kept as "1:2:3:4" as shown in **Figure 3.6**

3.3.2 LOADING SEQUENCE

Due to the loading pattern, as discussed above , if P is the load on the first floor then the base shear would be equal to P+2P+3P+4P = 10P. The load on the structure was gradually increased in the steps of 1t at 1st floor, which resulted in a corresponding load step of 20t at 2nd floor, 30t at 3rd floor and 40t at 4th floor resulting in a load step of 10t in base shear. The base shear in the first step was 10t, in the second step 20t and so on till failure.

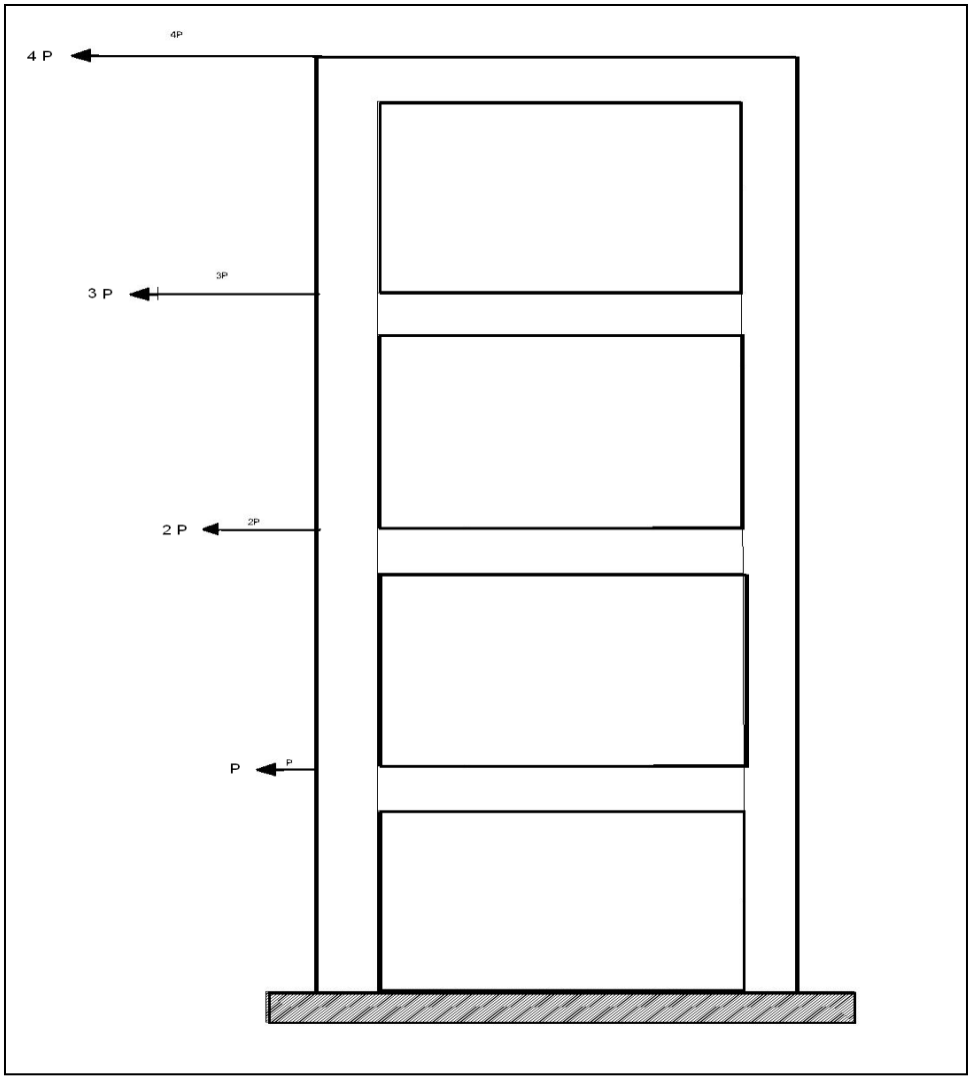

Figure3.6 Loading Pattern [4]

3.4 INTRODUCTION TO FE MODELLING

For structural design and assessment of reinforced concrete members, the non-linear finite element (FE) analysis has become an important tool. Over the last one or two decade numerical simulation of reinforced concrete structures and structural elements has become a major research area. A successful numerical simulation demands choosing suitable elements, formulating proper material models and selecting proper solution method.

3.4.1 Finite Element Method

The finite element method (FEM) or finite element analysis is a numerical technique for finding approximate solutions of partial differential equations (PDE) as well as of integral equations. The solution approach is based either on eliminating the differential equation completely (steady state problems), or

rendering the PDE into an approximating system of ordinary differential equations, which are then numerically integrated using standard techniques.

In solving partial differential equations, the primary challenge is to create an equation that approximates the equation to be studied, but is numerically stable, meaning that errors in the input data and intermediate calculations do not accumulate and cause the resulting output to be meaningless. The Finite Element Method is a good choice for solving partial differential equations over complex domains. [8]

3.5 FINITE ELEMENT MODELLING

The basic concept of FEM modelling is the subdivision of the mathematical model into disjoint (non-overlapping) components of simple geometry. The response of each element is expressed in terms of a finite number of degrees of freedom characterized as the value of an unknown function, or functions or at a set of nodal points. The response of the mathematical model is then considered to be the discrete model obtained by connecting or assembling the collection of all elements.

Within the framework of the finite element method reinforced concrete can be represented either by superimposition of the material models for the constituent parts (i.e., for concrete, for reinforcing steel and for FRP), or by a constitutive law for the composite concrete, embedded steel and composite FRP laminates considered as a continuum.

The finite element method is well suited for superimposition of the material models for the constituent parts of a composite material. Several constitutive models covering these effects are implemented in the computer code ATENA, which is a finite element package designed for computer simulation of concrete structures. The graphical user interface in ATENA provides an efficient and powerful environment for solving many anchoring problems. ATENA enables virtual testing of structures using computers, which is the present trend in the research and development world. Material models of this type can be employed for virtually all kinds of reinforced concrete structural members. Depending on the type of material modelling to be solved in ATENA, concrete can be represented by solid brick elements, the reinforcement is modelled by bar elements (discrete representation) and FRP is modelled by shell elements which are described in Chapter 4.

Geometry and shape of any mathematical element help in proper placement of the nodal points and materials properties helps in using proper modelling.

3.6 MATERIAL MODELS

The program system ATENA offers a variety of material models for different materials and purposes. The most important material models in ATENA for RCC structure are concrete and reinforcement. These

advanced models take into account all the important aspects of real material behaviour in tension and compression [5].

3.6.1 MODELLING OF CONCRETE

1) Geometry of the Concrete

Element geometric modelling of concrete has been done using 3D solid brick element with 8 up to 20 nodes in ATENA, shown in **Figure 3.7**

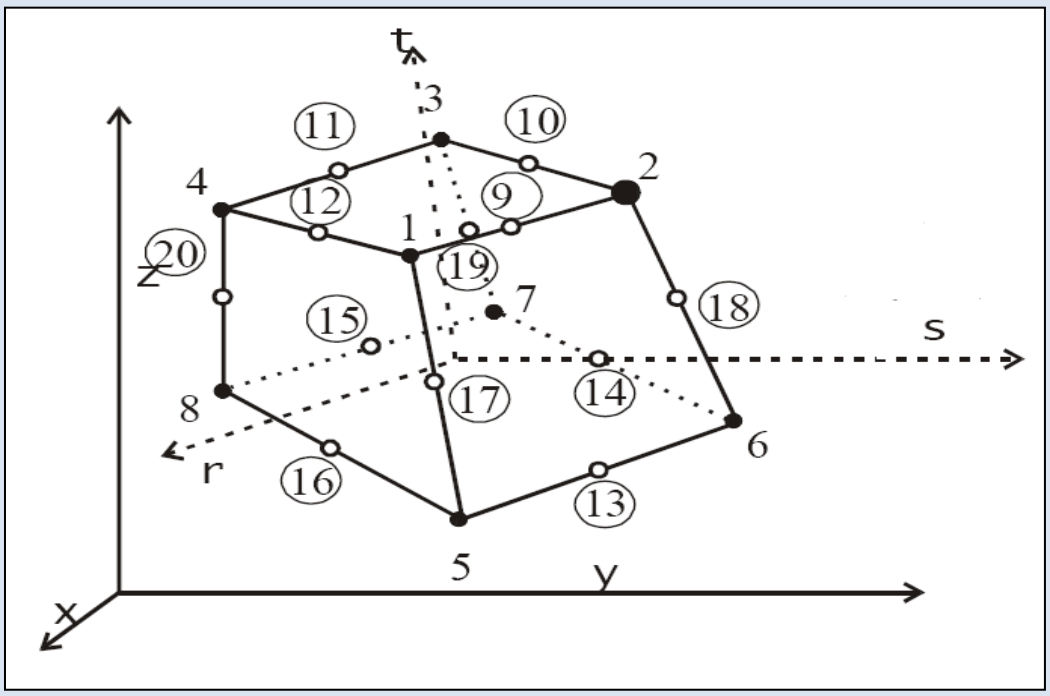

Figure 3.7 Geometry of Brick elements [5]

2) Element Properties

3D solid brick element having three degree of freedom at each node: translations in the nodal x, y and z directions. This is an isoparametric elements integrated by Gauss integration at integration points. This element is capable of plastic deformation, cracking in three orthogonal directions, and crushing. The most important aspect of this element is the treatment of non-linear material properties.

3) Element Interpolation function

3D solid brick element interpolation functions for all variants of the elements are given below:

$N_1 = (1/8)\ (1+r)\ (1+s)\ (1+t)$ $N_2 = (1/8)\ (1-r)\ (1+s)\ (1+t)$

$N_3 = (1/8)\ (1-r)\ (1-s)\ (1+t)$ $N_4 = (1/8)\ (1+r)\ (1-s)\ (1+t)$

N_5= (1/8) (1+r) (1+s) (1-t) N_6= (1/8) (1-r) (1+s) (1-t)

N_7= (1/8) (1-r) (1-s) (1-t) N_8= (1/8) (1+r) (1-s) (1-t)

3.6.2 MODELLING OF REINFORCEMENT

1) Geometry of the reinforcement

Reinforcement modelling could be discrete or smeared. In our work, a discrete modelling of reinforcement has been done. The reinforcement has been modelled using bar elements in ATENA.

2) Element Properties

Reinforcement steel is a 3D bar element, which has three degrees of freedom at each node; translations in the nodal x, y and z direction. Bar element is a uniaxial tension-compression element. The stress is assumed to be uniform over the entire element. Also plasticity, creep, swelling, large deflection and stress-stiffening capabilities are included in the element.

3) Element Shape Functions:

The shape functions in natural co-ordinate system for the three dimensional bar element without rotational degrees of freedom.

N_1= (1/2) (1+s) N_2= (1/2) (1-s)

3.7 STRESS-STRAIN RELATIONS FOR CONCRETE [5]

Concrete exhibits a large number of micro-cracks, especially, at the interface between coarser aggregates and mortar, even before subjected to any load. The presence of these micro-cracks has a great effect on the mechanical behaviour of concrete, since their propagation during loading contributes to the nonlinear behaviour at low stress levels and causes volume expansion near failure. Many of these micro-cracks are caused by segregation, shrinkage or thermal expansion of the mortar. Some micro-cracks may develop during loading because of the difference in stiffness between aggregates and mortar. Since the aggregate-mortar interface has a significantly lower tensile strength than mortar, it constitutes the weakest link in the composite system. This is the primary reason for the low tensile strength of concrete.

The response of a structure under load depends to a large extent on the stress-strain relation of the constituent materials and the magnitude of stress.

Since concrete is used mostly in compression, the **stress-strain relation** in compression is of primary interest **[5]**.

3.7.1 EQUIVALENT UNIAXIAL LAW

The nonlinear behaviour of concrete in the biaxial stress state is described by means of the so called effective stress σ_c^{ef}, and the equivalent uni-axial strain ε^{eq}. The effective stress is in most cases a principal stress.

The equivalent uni-axial strain is introduced in order to eliminate the Poisson's effect in the plane stress state. $\boldsymbol{\varepsilon^{eq} = \sigma_{ci} / E_{ci}}$

The equivalent uni-axial strain can be considered as the strain, that would be produced by the stress σ_{ci} in a uni-axial test with modulus associated E_{ci} with the direction *i*. Within this assumption, the nonlinearity representing damage is caused only by the governing stress σ_{ci}. The complete equivalent uni-axial stress-strain diagram for concrete is shown in **Figure3.8.**

The numbers of the diagram parts in **Figure 3.8**(material state numbers) are used in the results of the analysis to indicate the state of damage of concrete.

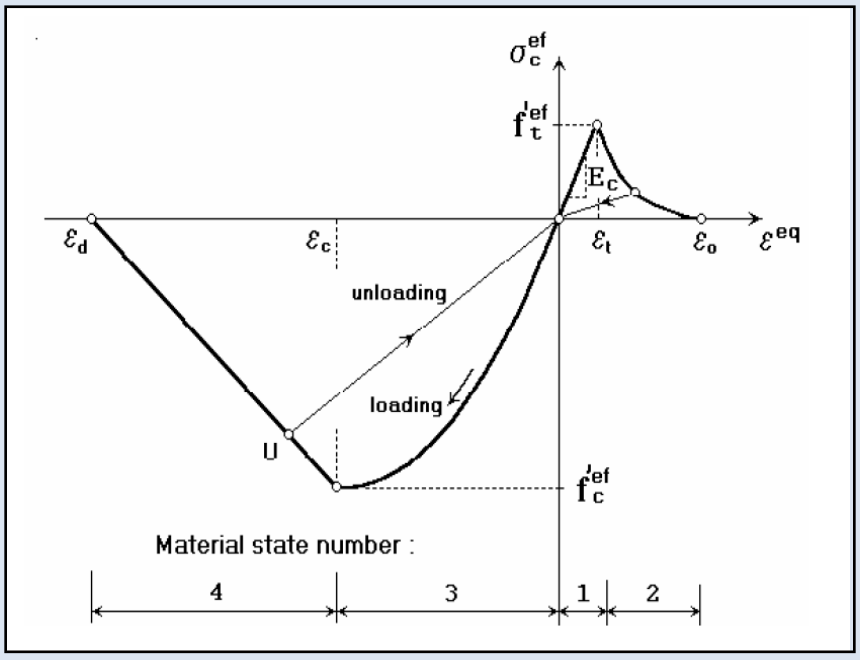

Figure 3.8 Uniaxial stress-strain law for concrete [5]

Unloading is a linear function to the origin. An example of the unloading point *U* is shown in **Figure 3.8**. Thus, the relation between stress σ_c^{ef} and strain ε^{eq} is not unique and depends on a load history. A

change from loading to unloading occurs, when the increment of the effective strain changes the sign. If subsequent reloading occurs the linear unloading path is followed until the last loading point *U* is reached again. Then, the loading function is resumed.

The peak values of stress in compression f'^{ef}_c and in tension f'^{ef}_t are calculated according to the biaxial stress state. Thus, the equivalent uni-axial stress-strain law reflects the biaxial stress state.

3.7.2 BIAXIAL STRESS FAILURE CRITERION OF CONCRETE

1) Compressive Failure

A biaxial stress failure criterion according to KUPFER et al. (1969) is used as shown in **Figure3.9**. In the compression-compression stress state the failure function is

$$\mathbf{f'^{ef}_c = [(1+3.65a)/(1+a)^2]f'_c;\quad a = (\sigma_{c1}/\sigma_{c2})} \qquad (3.1)$$

Where σ_{c1}, σ_{c2} are the principal stresses in concrete and f'_c is the uni-axial cylinder strength. In the biaxial stress state, the strength of concrete is predicted under the assumption of a proportional stress path.

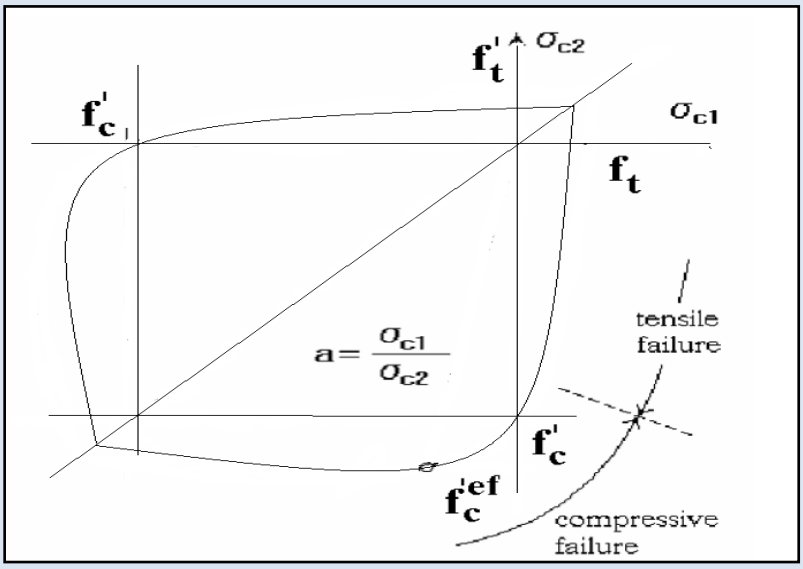

Figure 3.9 Biaxial failure functions for concrete [5]

In the tension-compression state, the failure function continues linearly from the point $\sigma_{c1} = 0$, $\sigma_{c2} = f'_c$, into the tension-compression region with the linearly decreasing strength:

$$\mathbf{f'^{ef}_c = f'_c r_{ec},\qquad r_{ec} = [1+ 5.3278(\sigma_{c1}/ f'_c)]} \qquad (3.2)$$

Where r_{ec} is the reduction factor of the compressive strength in the principal direction 2 due to the tensile stress in the principal direction 1.

2) Tensile failures

In the tension-tension state, the tensile strength is constant and equal to the uniaxial tensile strength f'_t. In the tension-compression state, the tensile strength is reduced by the relation:

$$f'^{ef}_t = f'_t \; r_{et} \qquad (3.3)$$

Where r_{et} is the reduction factor of the tensile strength in the direction 1 due to the compressive stress in the direction 2. The reduction function has one of the following forms.

$$r_{et} = 1 - 0.8\,(\sigma_{c2}/\, f'_c) \qquad (3.4)$$

$$r_{et} = [A + (A - 1)\,B]/\, AB;\; B = Kx + A;\; x = \sigma_{c2}/\, f'_c \qquad (3.5)$$

The relation in Eq. (3.4) is the linear decrease of the tensile strength and (3.5) is the hyperbolic decrease. Two predefined shapes of the hyperbola are given by the position of an intermediate point *r*, *x*. Constants *K* and *A* define the shape of the hyperbola. The values of the constants for the two positions of the intermediate point are given in the following table.

Type	***Point***		***Parameters***	
	r	**X**	**A**	**K**
A	0.5	0.4	0.75	1.125
B	0.5	0.2	1.0625	6.0208

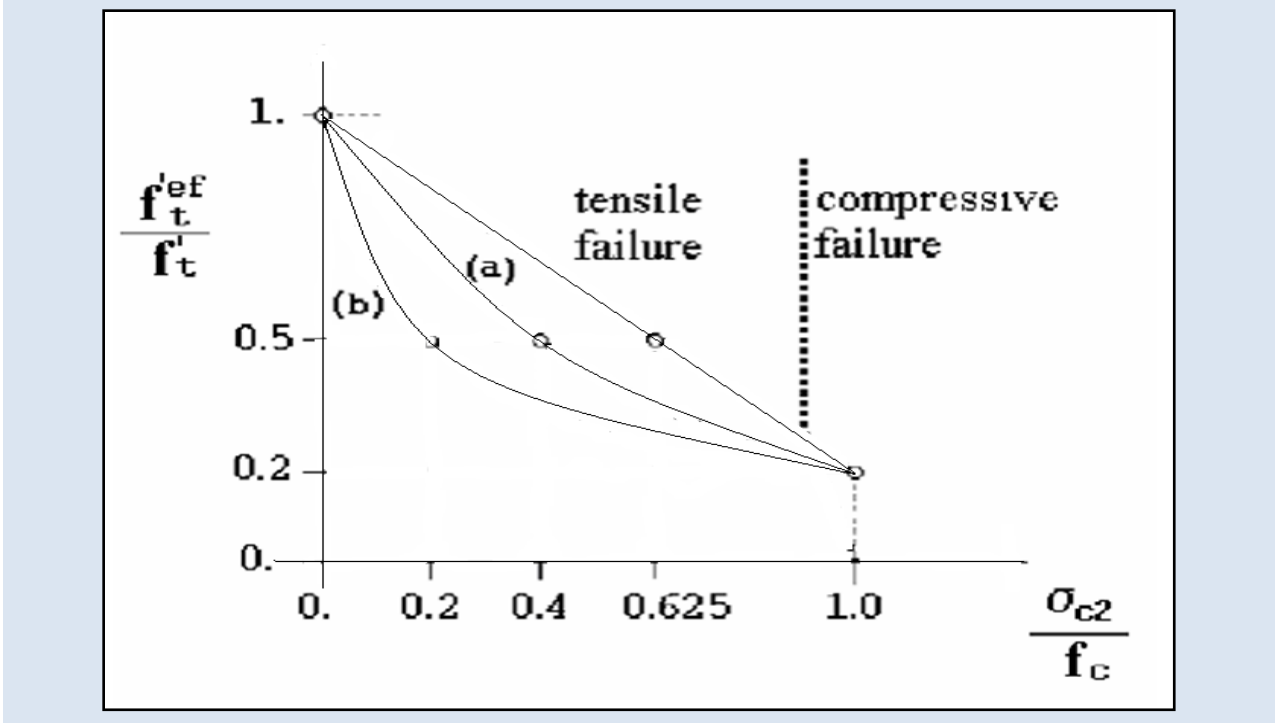

Figure 3.10 Tension-compression failure functions for concrete. **[5]**

3.7.3 TENSION BEFORE CRACKING

The behaviour of concrete in tension without cracks is assumed linear elastic. E_c *is* the initial elastic modulus of concrete, f'^{ef}_t is the effective tensile strength derived from the biaxial failure function already describe above.

$$\sigma_c^{ef} = E_c\, \varepsilon^{eq},\ 0 < \sigma_c < f'^{ef}_t$$

3.7.4 TENSION AFTER CRACKING

A fictitious crack model is based on a crack-opening law and fracture energy. This formulation is suitable for modelling of crack propagation in concrete. It is used in combination with the crack band. It is a region (band) of material, which represents a discrete failure plane in the finite element analysis. In tension it is a crack, in compression it is a plane of crushing. In reality these failure regions have some dimension. However, since according to the experiments, the dimensions of the failure regions are independent on the structural size, they are assumed as fictitious planes. In case of tensile cracks, this approach is known as rack the "crack band theory**", (*BAZANT OH 1983*).** Here is the same concept used also for the compression failure. The purpose of the failure band is to eliminate two deficiencies, which occur in connection with the application of the finite element model: element size effect and element orientation effect.

1) Element size effect.

The direction of the failure planes is assumed to be normal to the principal stresses in tension and compression, respectively. The failure bands (for tension L_t and for compression L_c) are defined as projections of the finite element dimensions on the failure planes.

2) Element Orientation Effect.

The element orientation effect is reduced, by further increasing of the failure band for skew meshes, by the following formula (proposed by (***CERVENKA et al. 1995*).**

$$L_t = \gamma L_t,\ L_c = \gamma L_c$$

$$\gamma = 1 + (\gamma^{max} - 1)\,(\theta/45), \qquad \theta\ \varepsilon\ (0; 45) \qquad (3.6)$$

An angle θ is the minimal angle (min (θ_1, θ_2)) between the direction of the normal to the failure plane and element sides. In case of a general quadrilateral element the element sides' directions are calculated as average side directions for the two opposite edges. The above formula is a linear interpolation between the factor γ=1.0 for the direction parallel with element sides, and $\gamma=\gamma^{max}$, for the direction inclined at 45o. The recommended (and default) value of γ max =1.5.

3.8 BEHAVIOUR OF CRACKED CONCRETE [5]

3.8.1 DESCRIPTION OF A CRACKED SECTION

The nonlinear response of concrete is often dominated by progressive cracking which results in localized failure. The structural member has cracked at discrete locations where the concrete tensile strength is exceeded.

At the cracked section all tension is carried by the steel reinforcement. Tensile stresses are, however, present in the concrete between the cracks, since some tension is transferred from steel to concrete through bond. The magnitude and distribution of bond stresses between the cracks determines the distribution of tensile stresses in the concrete and the reinforcing steel between the cracks.

Additional cracks can form between the initial cracks, if the tensile stress exceeds the concrete tensile strength between previously formed cracks. The final cracking state is reached when a tensile force of sufficient magnitude to form an additional crack between two existing cracks can no longer be transferred by bond from steel to concrete.

As the concrete reaches its tensile strength, primary cracks form. The number and the extent of cracks are controlled by the size and placement of the reinforcing steel. At the primary cracks the concrete stress drops to zero and the steel carries the entire tensile force. The concrete between the cracks, however, still carries some tensile stress, which decreases with increasing load magnitude. This drop in concrete tensile stress with increasing load is associated with the breakdown of bond between reinforcing steel and concrete. At this stage a secondary system of internal cracks, called bond cracks, develops around the reinforcing steel, which begins to slip relative to the surrounding concrete.

Since cracking is the major source of material nonlinearity in the serviceability range of reinforced concrete structures, realistic cracking models need to be developed in order to accurately predict the load-deformation behaviour of reinforced concrete members. The selection of a cracking model depends on the purpose of the finite element analysis. If overall load-deflection behaviour is of primary interest, without much concern for crack patterns and estimation of local stresses, the "smeared" crack model is probably the best choice. If detailed local behaviour is of interest, the adoption of a "discrete" crack model might be necessary. Unless special connecting elements and double nodes are introduced in the finite element discretization of the structure, the well established smeared crack model results in perfect bond between steel and concrete, because of the inherent continuity of the displacement field.

3.8.2 MODELLING OF CRACKS IN CONCRETE

The process of crack formation can be divided into three stages, **Figure 3.11**. The un-cracked stage is before a tensile strength is reached. The crack formation takes place in the process zone of a potential crack with decreasing tensile stress on a crack face due to a bridging effect. Finally, after a complete release of the stress, the crack opening continues without the stress.

The tension failure of concrete is characterized by a gradual growth of cracks, which join together and eventually disconnect larger parts of the structure. It is usually assumed that cracking formation is a brittle

process and that the strength in tension loading direction abruptly goes to zero after such cracks have formed.

Therefore, the formation of cracks is undoubtedly one of the most important non-linear phenomenon, which governs the behaviour of the concrete structures. In the finite element analysis of concrete structures, two principally different approaches have been employed for crack modelling. These are (a) discrete crack modelling (b) smeared crack modelling

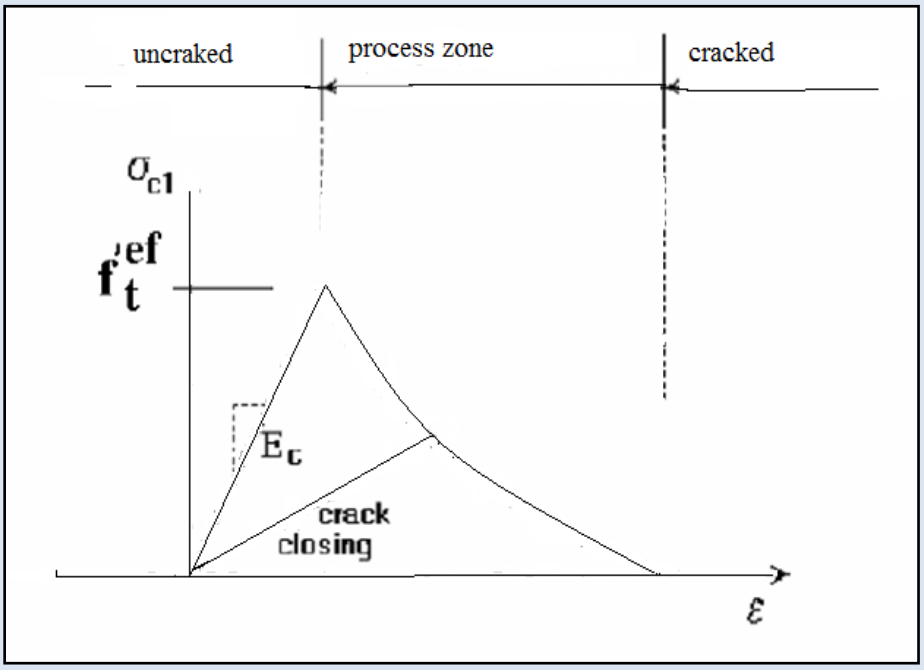

Figure3.11 Stages of Crack Opening [5]

.The discrete approach is physically attractive but this approach suffers from few drawbacks, such as**,** it employs a continuous change in nodal connectivity, which does not fit in the nature of finite element displacement method; the crack is considered to follow a predefined path along the element edges and excessive computational efforts are required. The second approach is the smeared crack approach. In this approach the cracks are assumed to be smeared out in a continuous fashion.

Within the smeared concept two options are available for crack models: the fixed crack model and the rotated crack model. In both models the crack is formed when the principal stress exceeds the tensile strength. It is assumed that the cracks are uniformly distributed within the material volume. This is reflected in the constitutive model by an introduction of orthotropy.

1) Fixed Crack Model

In the fixed crack model (***CERVENKA 1985, DARWIN 1974***) the crack direction is given by the principal stress direction at the moment of the crack initiation. During further loading this direction is fixed and represents the material axis of the orthotropy.

The principal stress and strain directions coincide in the un-cracked concrete, because of the assumption of isotropy in the concrete component. After cracking the orthotropy is introduced. The weak material axis m_1 is normal to the crack direction; the strong axis *m2* is parallel with the cracks. In a general case the principal strain axes ε_1 and ε_2 rotate and need not to coincide with the axes of the orthotropy *m1* and *m2*. This produces a shear stress on the crack face as shown in **Figure. 3.12**. The stress components σ_{c1} and σc2 denote, respectively, the stresses normal and parallel to the crack plane and, due to shear stress, they are not the principal stresses.

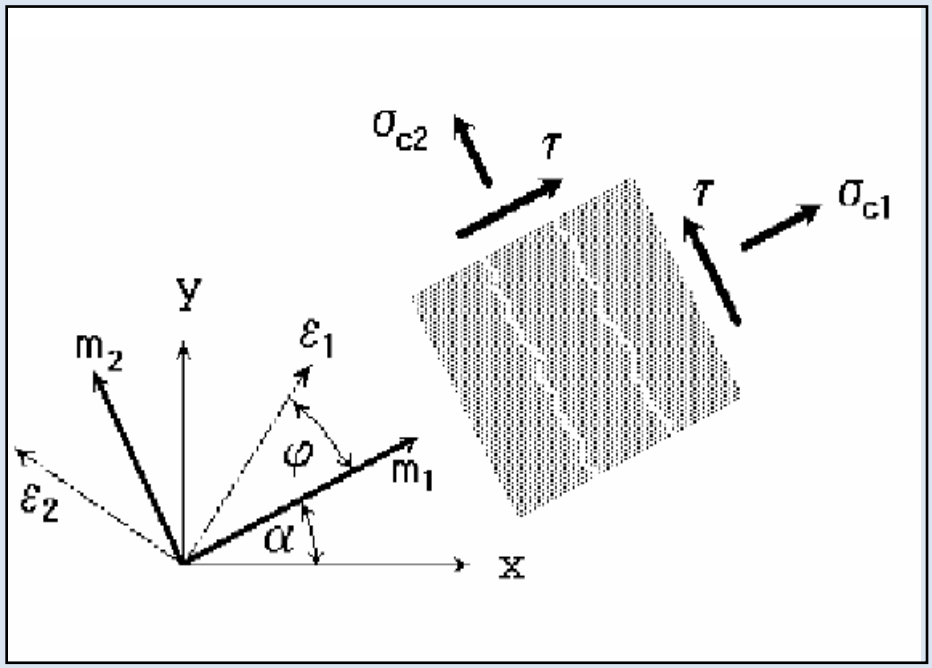

Figure 3.12 Fixed crack model Stress and strain state [5]

2) Rotated Crack Model

In the rotated crack model, the direction of the principal stress coincides with the direction of the principal strain. Thus, no shear strain occurs on the crack plane and only two normal stress components must be defined, as shown in **Figure 3.13.**

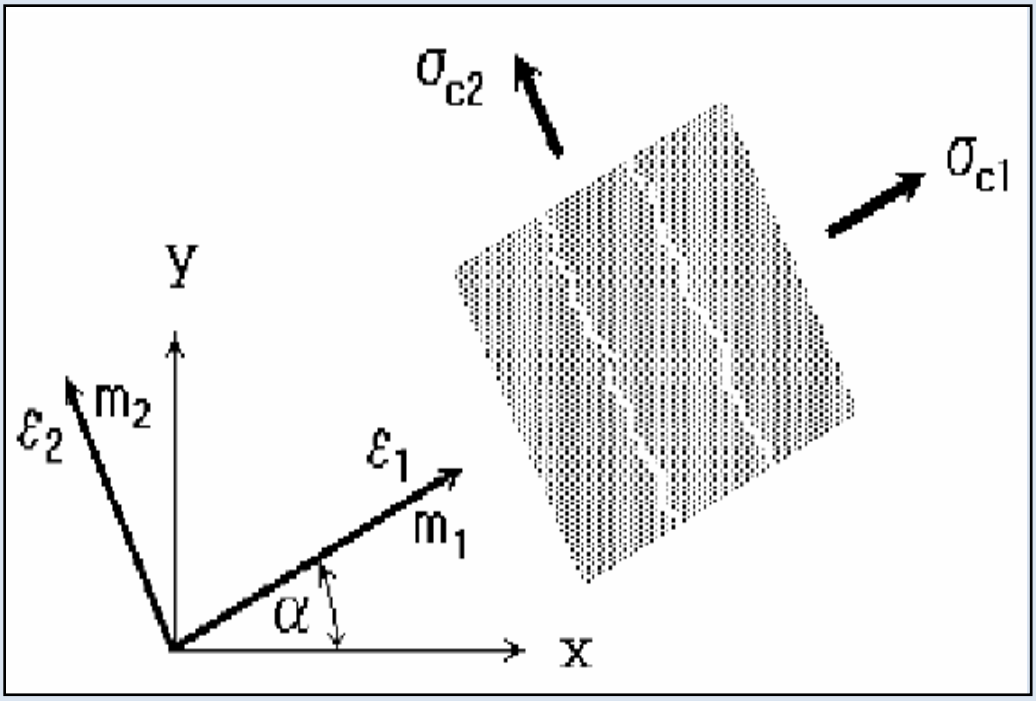

Figure 3.13 Rotated crack model. Stress and strain state [5]

If the principal strain axes rotate during the loading the direction of the cracks rotates, too. In order to ensure the co-axiality of the principal strain axes with the material axes the tangent shear modulus *Gt* is calculated according to CRISFIELD 1989 as

$$G_t = (\sigma_{c1} - \sigma_{c2})/ 2\ (\varepsilon_1 - \varepsilon_2)$$

3.9 STRESS-STRAIN LAWS FOR REINFORCEMENT [5]

3.9.1 INTRODUCTION

Reinforcement can be modelled in two distinct forms: discrete and smeared. Discrete reinforcement is in form of reinforcing bars and is modelled by truss elements. The smeared reinforcement is a component of composite material and can be considered either as a single (only one-constituent) material in the element under consideration or as one of the more such constituents. The former case can be a special mesh element (layer), while the later can be an element with concrete containing one or more reinforcements. In both cases the state of uniaxial stress is assumed and the same formulation of stress-strain law is used in all types of reinforcement.

3.9.2 BILINEAR LAW

The bilinear law, elastic-perfectly plastic, is assumed as shown in Figure 3.14

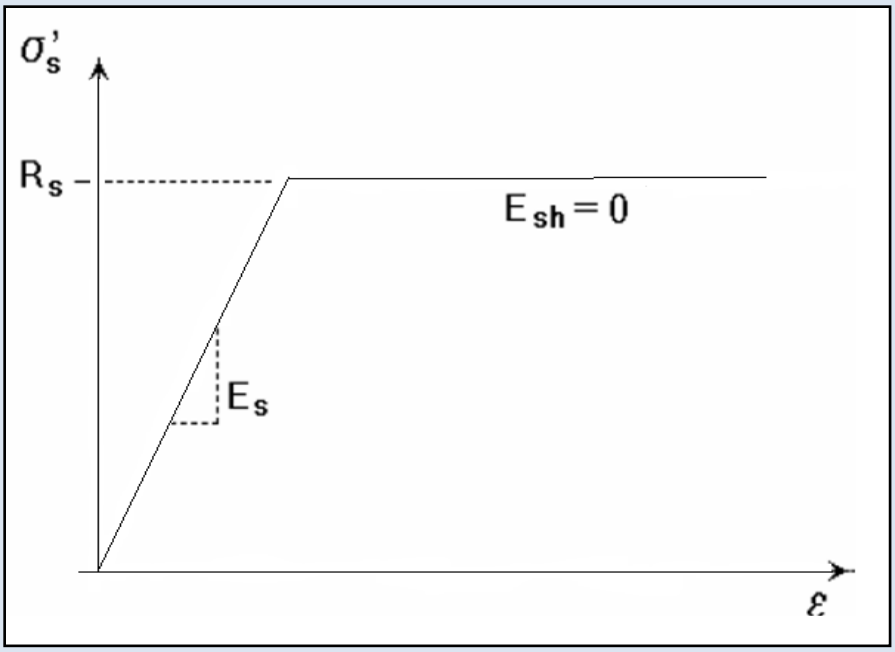

Figure 3.14 the bilinear stress-strain law for reinforcement [5]

The initial elastic part has the elastic modulus of steel E_s. The second line represents the plasticity of the steel with hardening and its slope is the hardening modulus E_{sh}. In case of perfect plasticity E_{sh} =0. Limit strain ε_L represents limited ductility of steel.

3.9.3 MULTI-LINEAR LAW

The multi-linear law consists of four lines as shown in **Figure 3.15.** This law allows modelling of all four stages of steel behaviour: elastic state, yield plateau, hardening and fracture. The multi-line is defined by four points, which can be specified by input.

The above described stress-strain laws can be used for the discrete as well as the smeared reinforcement. The smeared reinforcement requires two additional parameters: the reinforcing ratio *p* and the direction angle β as shown in **Figure. 3.16.**

Where ρ = (Area of steel/ Area of concrete)

The spacing *s* of the smeared reinforcement is assumed infinitely small. The stress in the smeared reinforcement is evaluated in the cracks; therefore it should include also a part of stress due to tension stiffening. $\sigma_{scr} = \sigma_s + \sigma_{ts}$

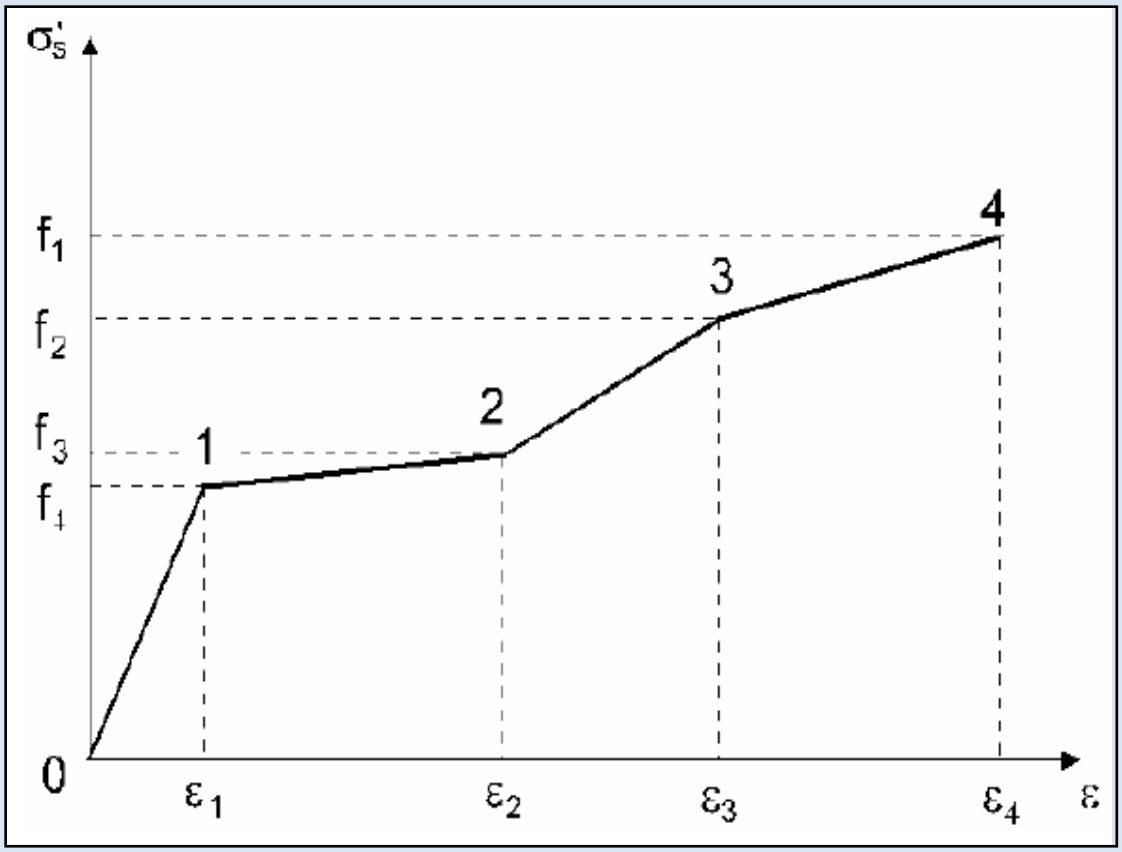

Figure 3.15 the multi-linear stress-strain law for reinforcement [5]

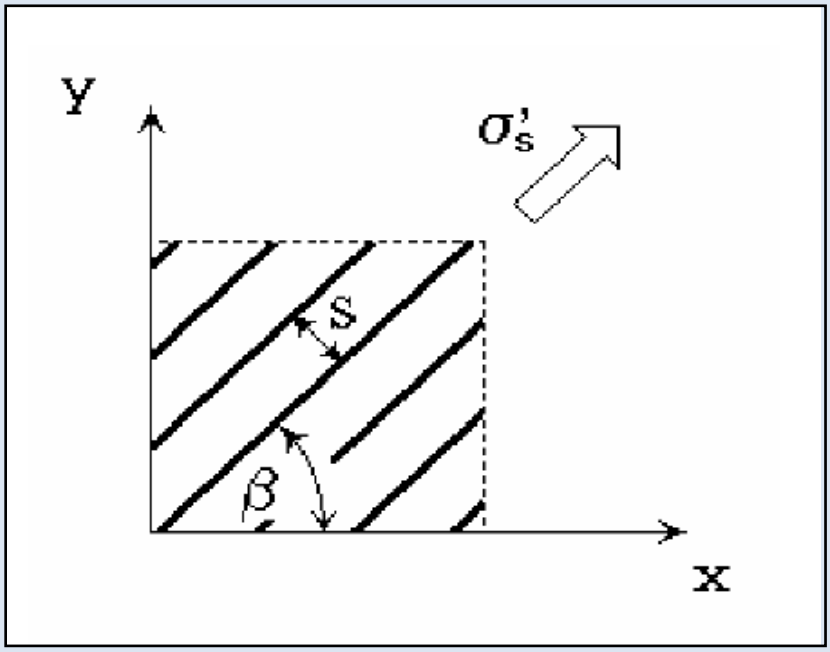

Figure 3.16 Smeared reinforcement [5]

where σ_s is the steel stress between the cracks (the steel stress in smeared reinforcement),

σ_{scr} is the steel stress in a crack. If no tension stiffening is specified $\sigma_{ts} = 0$ and $\sigma_{scr} = \sigma_s$. In case of the discrete reinforcement the steel stress is always σ_s.

Once we understand the finite element modelling, the next step is the analytical programming. The main objective of this analytical program is to get the result of under reinforced concrete frame and compare with the experimental results. In the analytical programming, first we select the materials and its properties and create geometry of the frame.

The frame is tested up to its failure point and the ultimate load deflection values are plotted as graphs. For modelling the control and retrofitted members in ATENA, concrete, reinforcement bars of different diameters, steel plates, epoxy and GFRP is used as materials.

3.10 MATERIAL PROPERTIES

Concrete, reinforcement steel, steel plates, Epoxy and GFRP (discussed in chapter 4) have been used to model the RCC frame. The specification and the properties of these materials are as under:

1) Concrete

In ATENA, concrete material is modelled as a 3D nonlinear cementitious2. The physical properties of 3D nonlinear cementitious2 material are given in **Table 3.2**. The values are calculated as per IS code 456:2000 and remaining are the default values.

2) Reinforcement Bars

HYSD steel of grade Fe-415 of 28mm, 25mm, 20mm, 16mm and 12mm diameter are used as main steel while 8mm and 10mm diameter bars are used as shear reinforcement. The properties of these bars are shown in **Table 3.3**.

Table 3.2 Material Properties of Concrete

Properties	Values
Elastic Modulus (Fresh concrete)	22,360 MPa
Poisson Ratio	0.2
Tensile Strength	3.130 MPa
Compressive Strength	20 MPa
Specific Fracture Energy	4.421E-05 MN/m
Critical Compressive Displacement	5E-04

Plastic Strain at Compressive Strength	6.681E-04
Reduction of Compressive Strength	0.8
Fail Surface Eccentricity	0.52
Specific Material weight	0.024 MN/mE+3
Coefficient of Thermal Expansion	1E-05 1/K
Fixed Crack Model Coefficient	1

Table 3.3 Material Properties of Reinforcement

Properties	Values
Elastic modulus	200000 MPa
Yield Strength	415 MPa
Specific Material weight	0.0785 MN/mE+3
Coefficient of Thermal Expansion	1.2E-05 1/K

3) Steel Plate

The function of the steel plate in the ATENA is for support and for loading. Here, the property of steel plate is same as the reinforcement bar except its yield strength. The HYSD steel of grade Fe-415 was used for steel plate.

3.11 FE MODELLING OF RCC FRAME IN ATENA

Procedure: In pre-processing window following steps are performed:-

Step1: Geometry of FE model is created .It has been presented in **Figure 3.20**.

Step2: Material properties are assigned to the various elements of the frame.

Step3: Supports and various supports, loadings and monitoring points are defined. **(Figure 3.20 & 3.21)**

Step4: Finite element meshing parameters are given and meshing of the model is generated accordingly. **(Figure 3.20)**

Step5: Various analysis steps are defined. The FE non-linear analysis is done in Run window. The FE non-linear static analysis calculates the effects of steady loading conditions on a structure, while ignoring inertia and damping effects, such as those caused by time-varying loads. A static analysis can, however, include steady inertia loads (such as gravity and rotational velocity), and time-varying loads that can be approximated as static equivalent loads (such as the static equivalent wind and seismic loads commonly defined in many building codes).

Static analysis is used to determine the displacements, stresses, strains, and forces in structures or components by loads that do not induce significant inertia and damping effects.

Step6: When the FE non linear static analysis is completed the, the results are shown in third part of the ATENA i.e. Post processing. The stress- strain values at every step, crack pattern and cracks propagation at every step shown help in to analyze the behaviour of the elements at every step of load deflection.

3.12 METHODS FOR NON-LINEAR SOLUTION [5]

The best part of the ATENA is the simpler way of solving the non-linear structural behaviour through finite element method and its incremental loading criteria. Different methods are available in ATENA for solving non-linear equations such as, linear method, Newton-Raphson Method, Modified Newton-Raphson method, Arc Length methods are used in ATENA.

Among these the Newton-Raphson Method and Modified Newton-Raphson Method are more commonly used methods. In our present study, Newton-Raphson method is used for solving the simultaneous equations. It is an iterative process of solving the non-linear equations.

One approach to non-linear solutions is to break the load into a series of load increments. The load increments can be applied either over several load steps or over several sub steps within a load step. At the completion of each incremental solution, the program adjusts the stiffness matrix to reflect the nonlinear changes in structural stiffness before proceeding to the next load increment. .

The ATENA program overcomes this difficulty by using Full Newton-Raphson method, or Modified Newton-Raphson method, which drive the solution to equilibrium convergence (within some tolerance limit) at the end of each load increment. In Full Newton-Raphson method, it obtains the following set of non-linear equations:

$$K(p)\,\Delta p = q - f(p)$$

where: q is the vector of total applied joint loads,

$f(p)$is the vector of internal joint forces,

Δp is the deformation increment due to loading increment,

p are the deformations of structure prior to load increment,

$\boldsymbol{K}(p)$ is the stiffness matrix, relating loading increments to deformation increments.

Figure 3.19 illustrates the use of Newton-Raphson equilibrium iterations in nonlinear analysis. Before each solution, the Newton-Raphson method evaluates the out-of -balance load vector, which is the difference between the restoring, forces (the loads corresponding to the element stresses) and the applied loads. The program then performs a linear solution, using the out-of -balance loads, and checks for convergence. If convergence criteria are not satisfied, the out-of-balance load vector is re-evaluated, the stiffness matrix is updated, and a new solution is obtained. This iterative procedure continues until the

problem converges.

But sometimes, the most time consuming part of the Full Newton-Raphson method solution is the re-calculation of the stiffness matrix $\boldsymbol{K}$ ($pi-1$) at each iteration. In many cases this is not necessary and we can use matrix $\boldsymbol{K}$ ($p0$) from the first iteration of the step. This is the basic idea of the so-called Modified Newton-Raphson method. It produces very significant time saving, but on the other hand, it also exhibits worse convergence of the solution procedure. The simplification adopted in the Modified Newton-Raphson method can be mathematically expressed by:

$$K\,(p_i-1) = K\,(p_0)$$

The modified Newton-Raphson method is shown in **Figure 3.18**. Comparing **Figure3.17** and **Figure3.18**, it is apparent that the Modified Newton-Raphson method converges more slowly than the original Full Newton-Raphson method. On the other hand a single iteration costs less computing time, because it is necessary to assemble and eliminate the stiffness matrix only once. In practice a careful balance of the two methods is usually adopted in order to produce the best performance for a particular case. Usually, it is recommended to start a solution with the original Newton-Raphson method and later, i.e. near extreme points, switch to the modified procedure to avoid divergence.

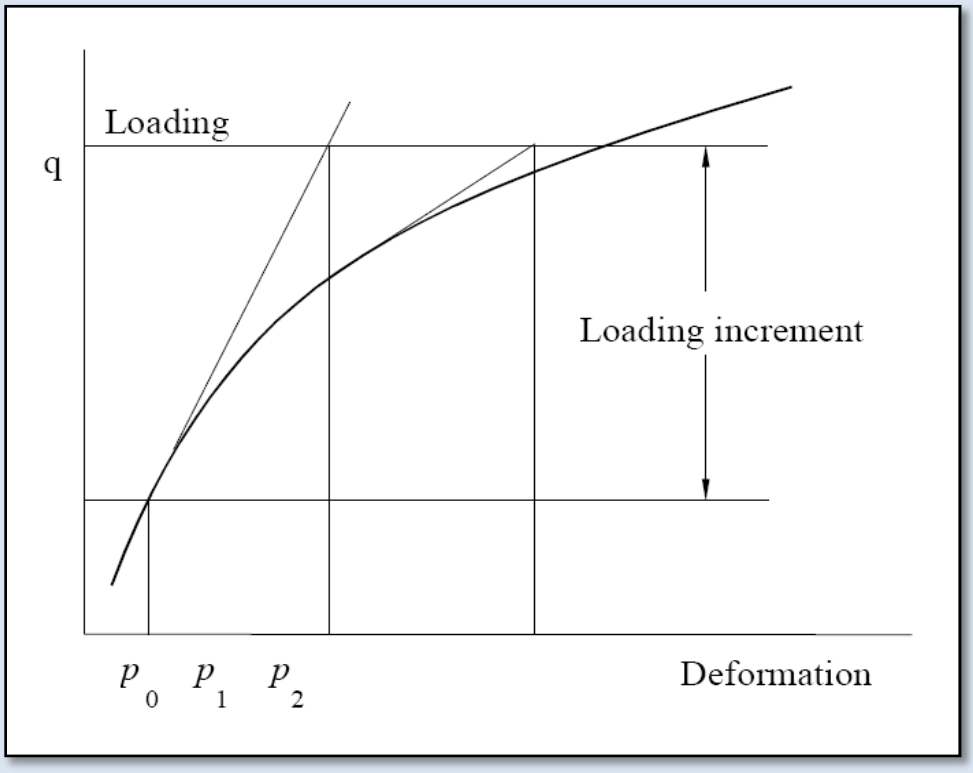

Figure 3.17 Full Newton-Raphson Method [5]

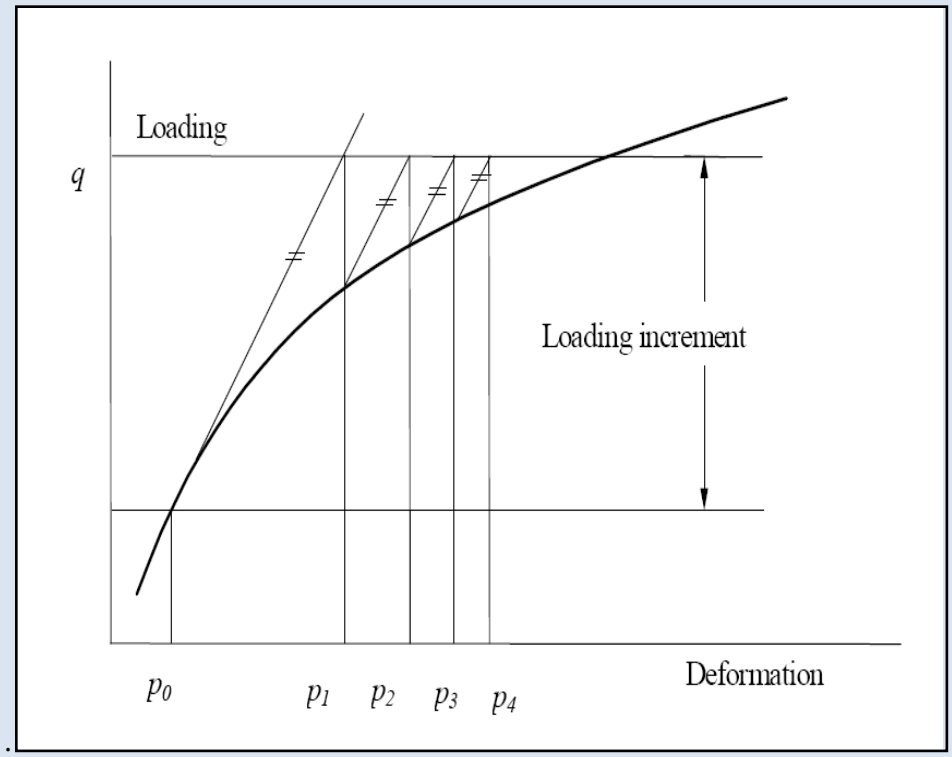

Figure 3.18 Modified Newton-Raphson Method [5]

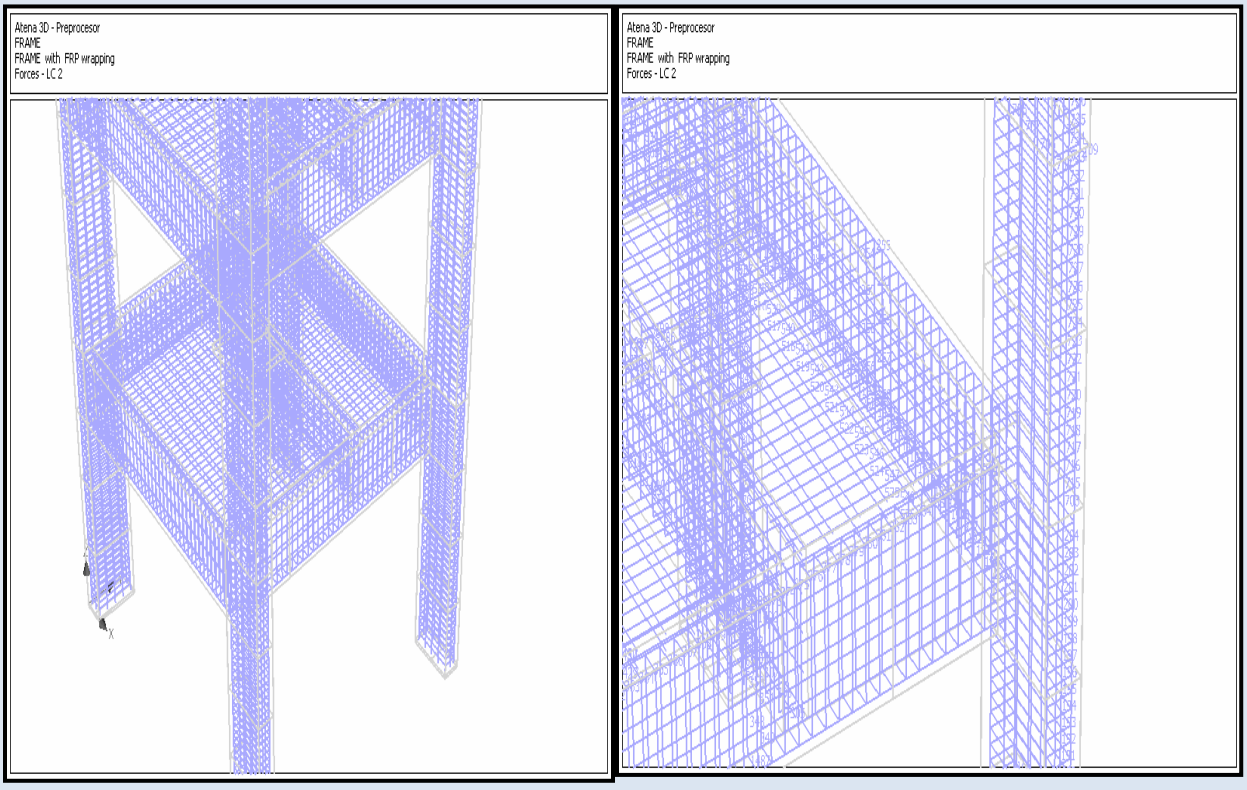

Figure 3.19 Modelling of Reinforcement in ATENA

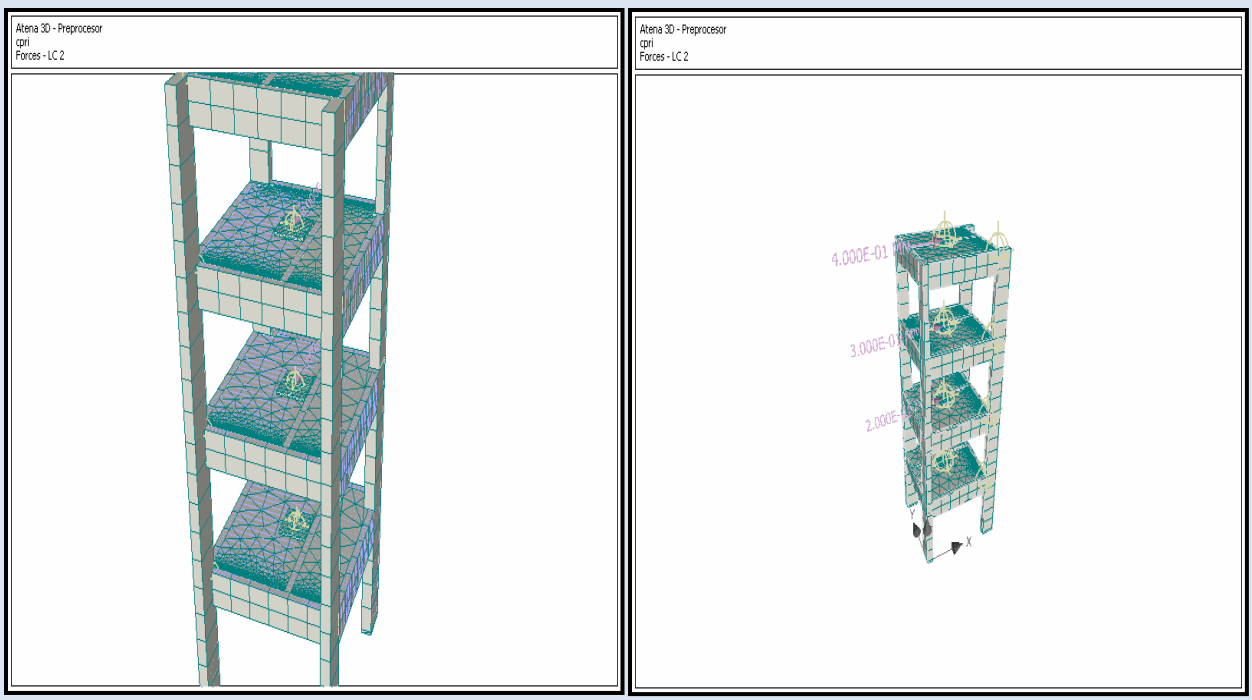

Figure 3.20 Definitions of Meshing, Loading & Monitoring Points

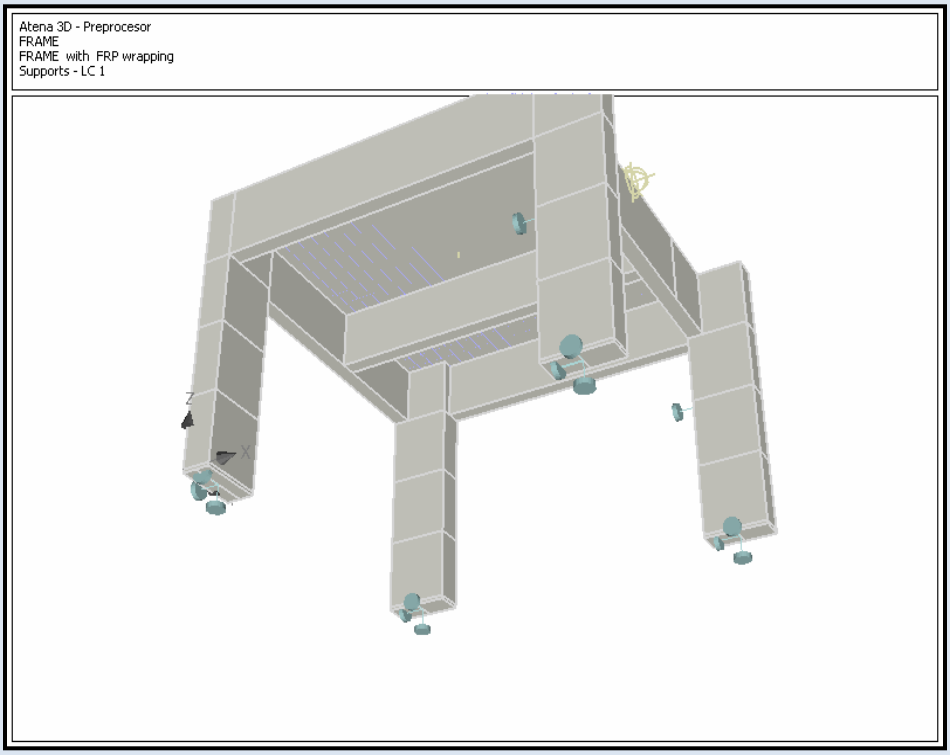

Figure 3.21 Definition of Steel plates and Supports in ATENA

CHAPTER 4

FE MODELLING OF RETROFITTED RC FRAME

4.1GENERAL

FRP is a composite material consisting of numerous high-strength fibers impregnated in resin. It is gaining popularity for structural strengthening because of its high tensile strength, for weight and high durability (no corrosion) **[**14].

A concrete structure may need strengthening for many reasons [7]

- To increase live-load capacity, e.g. of a bridge subject to increased vehicle loads or a building the use of which is to change from residential to commercial.
- To add reinforcement to a member that has been under designed or wrongly constructed.
- To improve seismic resistance, either by providing more confinement to increase the strain capacity of the concrete, or by improving continuity between members.
- To replace or supplement reinforcement, e.g. damaged by impact or lost due to corrosion.
- To improve continuity, e.g. across joints between precast members.

In most cases it is only practical to increase the live-load, capacity of a structure. However, in some situations it may be possible to relieve dead load, by jacking and propping, prior to the application of the additional reinforcement. In these cases, the additional reinforcement will play its part in carrying the structures dead load. Three basic principles underlie the strengthening of concrete structures using fiber composite materials, which are the same irrespective of the type of structure:

- Increase the bending moment capacity of beams and slabs by adding fiber composite materials to the tensile face.
- Increase the shear capacity of beams by adding fiber composite materials to the sides in the shear tensile zone.
- Increase eh axial and shear capacity of columns by wrapping fiber composite materials around the perimeter.

The need to increase the capacity of the existing structures has recently become one of the most active areas in civil engineering. Several strengthening methods have been used in the past with varying degree of success. These include:

- Enlargement of the cross section,
- Addition of new steel members,
- Steel plate bonding,
- External post-tensioning,
- Reducing of span length, and recently
- External bonding with FRP plate

FRP has been successfully used to increase the flexural and shear capacities of RC beams. Externally bonded FRP laminates and fabrics can be used to increase the shear strength of reinforced concrete beams and columns. It can be seen that the shear strength of columns can be easily improved by wrapping with a continuous sheet of FRP form a complete ring around the member. Shear strengthening of beams, however, is likely to be more problematic when they are cast monolithically with slabs. This increases the difficulty of anchoring the FRP at the beam/slab junction and increases the risk of debonding failure. Nevertheless, bonding FRP on either the side faces, or the side faces and soffit, will provide some shear strengthening fro such members. In both cases, it is recommended that the FRP is placed such that the principal fiber orientation is either 45^0 or 90^0 to the longitudinal axis of the member. There is some evidence that the shear resistance of beams can be further improved by bonding additional sheets with their fibers orientated at right angles to the principal fiber direction. In Finite Element Modelling of Reinforced Concrete Beams Strengthened with FRP Laminates FRP-strengthened beams failure may occur due to beam shear, flexural compression, FRP rupture, FRPdebonding or concrete cover ripping.

4.1.1TECHNIQUES OF SEISMIC RETROFITTING

Various techniques of seismic retrofitting have been developed and used in practice. The basic concept of these techniques of retrofitting is aimed as:

- Upgrading of lateral strength of the structure
- Increasing the ductility of structure
- Increasing the strength and ductility

The decision to repair and strengthen a structure depends not only on the technical considerations as mentioned above but also on a cost/benefit analysis of the different possible alternatives. It is suggested that the cost of retrofitting of a structure should remain below 25% of the replacement as major justification of retrofitting.[23]

4.1.2 CLASSIFICATION OF RETROFITTING-TECHNIQUES

There are two ways to enhance the seismic capacity of existing structures:

- Global Techniques
- Local Techniques

The first is a structural level approach of retrofitting which involves global modification to the structural system**.** These include:

- Adding Shear wall
- Adding Infill wall
- Adding Bracing
- Adding wing wall/ buttresses
- Mass reduction
- Supplemental Damping and Base Isolation

The second is member level approach of retro-fitting known as local retrofitting which deals with an increase of ductility of components with adequate capacities to satisfy their specific limit state. The member level retrofit approach is to upgrade the strength of the members which are seismically deficient. This approach is more cost effective as compared to structural level retrofit. The most common method of enhancing the individual member strength is jacketing. It includes the addition of concrete, steel or fibre reinforced polymer (FRP) jackets for use of confining RCC columns, beams, joints and foundations.

Many terms have been used to define FRP composites. Modifiers have been used to identify a specific fibre such as:

- Glass Fibre Reinforcement Polymer (GFRP)
- Carbon Fibre Reinforcement Polymer (CFRP)
- Aramid Carbon Fibre Reinforcement Polymer (AFRP)

Another familiar term used is Fibre Reinforced Plastics. In addition other acronyms developed over the years are Fibre Reinforced Composites, Glass Reinforced Plastics and the Polymer Matrix Composites (PMC) can be found in many references.[23]

4.1.3 COMPOSITION OF FRP

FRP composites are materials that consist of two constituents. The constituents are combined at a macroscopic level and are not soluble in each other. One constituent is the reinforcement, which is embedded in the second constituent, a continuous polymer called the matrix. The reinforcing material is in the form of fibers, i.e., carbon and glass, which are typically stiffer and stronger than the matrix. The FRP composites are anisotropic materials; that is, their properties are not the same in all directions. [3]

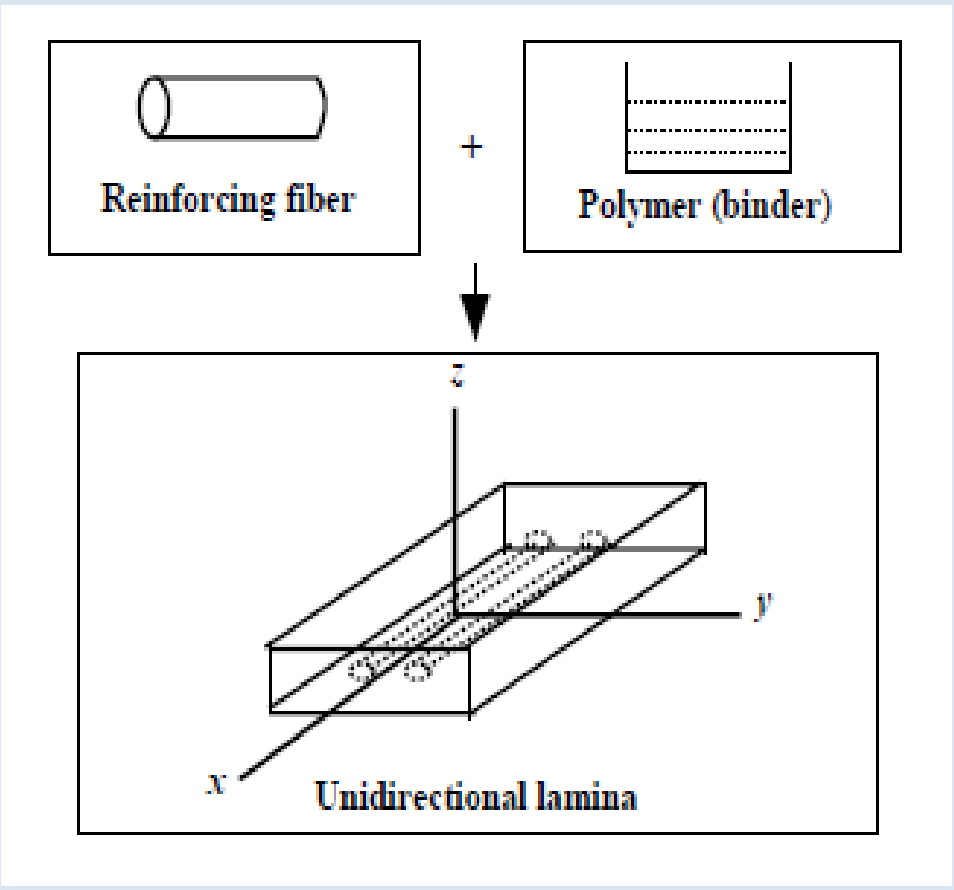

Figure 4.1 A schematic diagram of FRP composites. [3]

4.1.4 VARIOUS FAILURE MODES

M. Barbato 2009 has experimentally identified the failure modes and grouped them as under::

- Flexural failure by concrete crushing or by steel yielding followed by concrete crushing (flexure failure mode which is similar to the failure mode of conventional/non-retrofitted RC beams),
- Flexural failure due to FRP rupture (FRP rupture failure mode),

- Flexural failure due to plate end interfacial debonding, to concrete cover separation or to intermediate crack induced debonding (debonding failure mode), and

It is noteworthy that all the failure modes typical of FRP-retrofitted beams (i.e., FRP rupture and debonding) are brittle in nature. In addition, the debonding failure modes correspond to a less than optimal use of the strength capabilities of the FRP material. In order to increase the efficiency of the FRP-retrofit reducing the impact of debonding failure modes, mechanical anchorage techniques have been devised and employed, e.g., use of mechanical devices at the FRP plate/sheet ends, FRP sheets wrapped around the RC member at the FRP plate/sheet ends (U-wrap), and U-shaped FRP plates/ sheets along the entire length of the RC beam (U-shape) [7].

Researchers have observed new types of failures that can reduce the performance of CFRP when used in retrofitting structures. These failures are often brittle, and include debonding of concrete layers, delamination of CFRP and shear collapse, brittle debonding has particularly been observed at laminate ends, due to high concentration of shear stresses at discontinuities. Where shear cracks in the concrete are likely to develop. Thus, it is necessary to study and understand the behaviour of CFRP strengthened reinforced concrete members, including those failures [21].

These failures are highly undesirable due to their brittleness. In order to ensure the safe design of structures, the load capacity associated with these failures must be accurately evaluated. However, presently there are no commonly acceptable design methods of predict the peeling failure load yet. In this paper, the authors employ the nonlinear finite element method to predict the peeling failure load [21].

4.2 FIBER REINFORCED POLYMER MODELLING

In general case of RC structure, the element geometric modelling of concrete has been done using 3D solid brick element with 8 up to 20 nodes in ATENA as shown in Figure 4.2. The 3D solid brick element having three degree of freedom at each node: translations in the nodal x, y and z directions. This is an isoparametric elements integrated by Gauss integration at integration points. This element is capable of plastic deformation, cracking in three orthogonal directions, and crushing. The most important aspect of this element is the treatment of nonlinear material properties.

4.2.1 MODELLING OF FRP

The FRP modelling can be done as a 3D shell element in ATENA. The Ahmad shell element implemented in ATENA (Ahmad et al., 1970), described in ATENA theory manual. The present Ahmad element belongs to group of shell element formulation that is based on 3D elements concept. It can be used to model thin as well as thick shell or plate structures.

4.2.2 GEOMETRY OF THE FRP

The FRP can be modeled as a shell element in ATENA. The Ahmad shell element used the 20 nodes isoparametric brick element as shown in Figure 4.2. This is needed, in order to be able to use the same pre and post-processors support for the shell and native 3D brick element. After the 1st step of the analysis, the input geometry will automatically change to the external geometry as shown in Figure 4.3. As nodes 17 and 18 contain only so called bubble function, the element is post-processed in the same way is it would be the iso-parametric brick element [5].

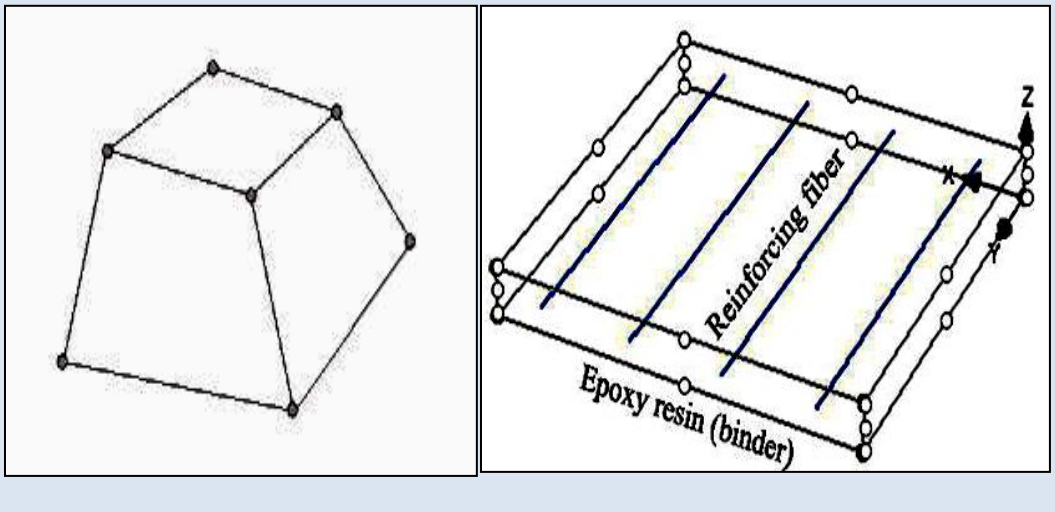

Figure 4.2Eight Noded brick element model for concrete and 20 nodes shell element model for FRP composite [3].

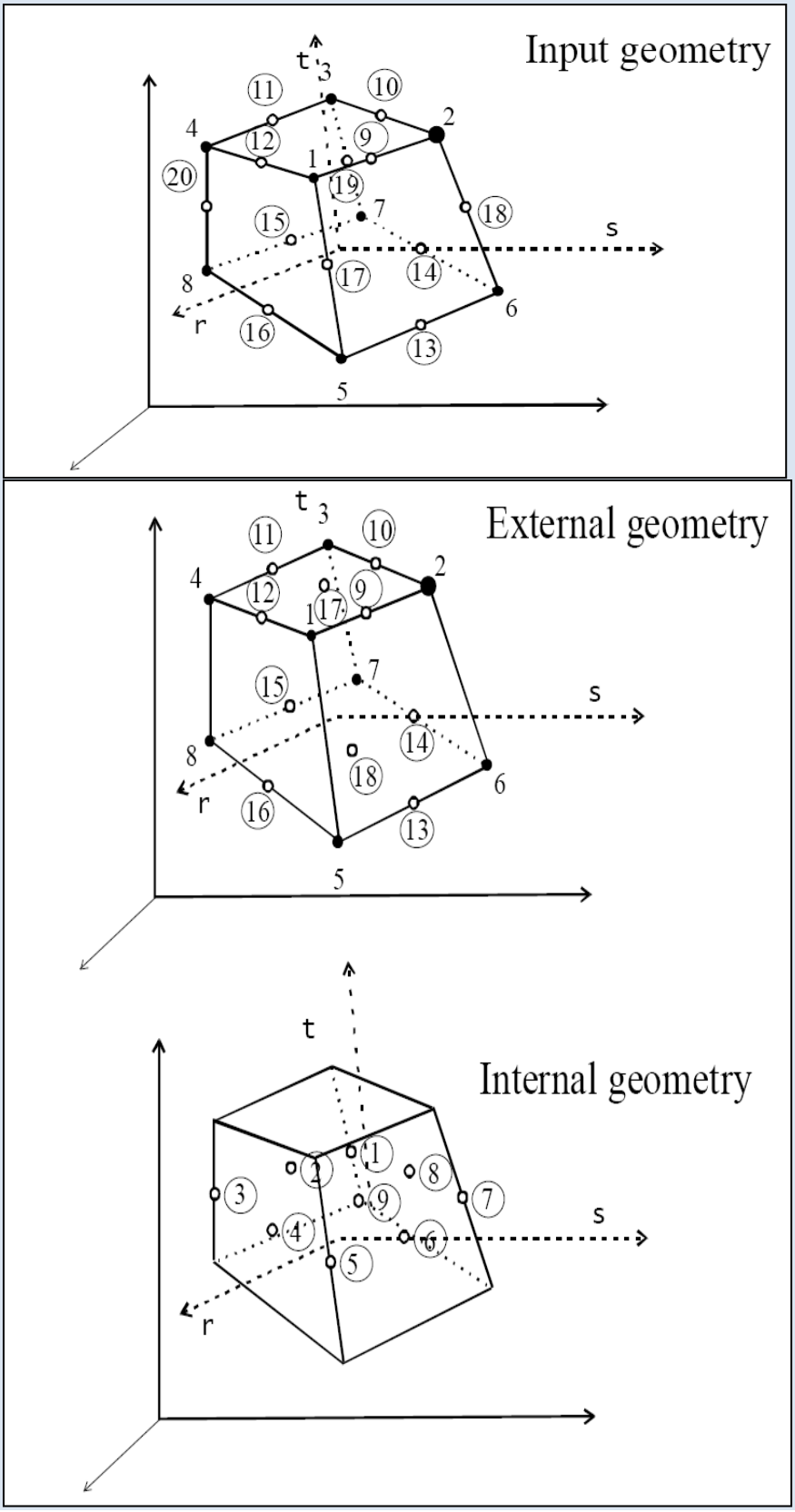

Figure 4.3 Geometry of the FRP [5]

4.2.3 ELEMENT PROPERTY OF THE FRP

FRP is an Ahmad shell element. In the following general shell element theory concept, every node of element has five degree of freedom, e.g. three displacements and two rotations in planes normal to mid surface of element. In order to facilitate a simple connection of this element with other true 3D elements, the five degrees of freedom are transformed into x, y, z displacement of a top node and x, y displacement of a bottom node degrees of freedom. The two nodes are located on the normal to mid-surface passing through the original mid-surface element's node.

4.3 MATERIAL PROPERTIES

Concrete, reinforcement steel, steel plates (discussed in detail in chapter 3), Epoxy and GFRP have been used to model the RCC frame. The specification and the properties of Epoxy and GFRP materials are as under:

4.3.1 CONCRETE

Concrete is modeled as 3D Nonlinear Cementitious- 2 material. It is assumed that damage index is 0.6 at final stage. Even after the repair Elastic modulus is assumed to be 0.4 of initial value. The other values of concrete are incorporated corresponding to 0.4E in the retro-fitted model.

4.3.2 STEEL PLATE

The steel plate used for fixing the supports are modeled in the same way as done in case of control frame in previous chapter.

4.3.3 STEEL REINFORCEMENT

The steel reinforcement is also modeled in the same way as done in case of control frame in previous chapter with one major difference. As the steel has yielded to its yield point, the value of yield stress is taken 210 MPa instead of 415 MPa.

4.3.4 MODELLING OF EPOXY

Mbrace Saturant was used as an epoxy in the analysis. The material properties are taken from the "Watson Bowman Acme corp." company paper.

The material properties of epoxy are shown in table 4.1.

Table 4.1 Material Properties of Epoxy [8]

Properties	Values
Elastic Modulus	3035 MPa
Poisson Ratio	0.4
Yield Strength	54 MPa
Specific Material Weight	0.00983 MN/mE+3
Coefficient of Thermal Expansion	5.75E-05 1/K

4.3.5 GLASS FIBRE REINFORCEMENT POLYMER

Mbrace G-sheet EU-900 unidirectional Glass fibre sheet is used in retrofitting. The properties which are used in the modelling are taken from the Mbrace Product Data, shown in the **Table 4.2.**

Table 4.2 Material Properties of GFRP [8]

Properties	Values
Strain, stress	(0,0); (0.005,390); (0.01,690) MPa
Specific Material Weight	0.026 MN/mE+3
Coefficient of Thermal Expansion	5.E-06 1/K
Elastic Modulus	70 GPa

4.4 MODELLING OF FRP RETROFITTING IN ATENA

In ATENA it can be done in two ways. First method is by making two construction cases. The material properties of FRP are taken as negligible when the 1st case is activated. The analysis is done in the same way as done in case of control frame. After attaining the required load/stress level construction case 2 is activated in which the full values of FRP material are incorporated for strengthening and analysis is done as explained earlier. In the second method properties of material corresponding to particular value of Damage-Index are assigned to the elements and structure is analyzed.

In the present study second method is opted due to the complexity of model and limitation of the software as the memory required in former case is almost double as compared to the latter one. The properties of Epoxy and GFRP used in the model have already been discussed in detail.The retrofitting scheme adopted

has been presented in the **Figure 4.3**. But due to the limitation of the software and to make the analysis feasible only vertical elements are modeled to be retrofitted.

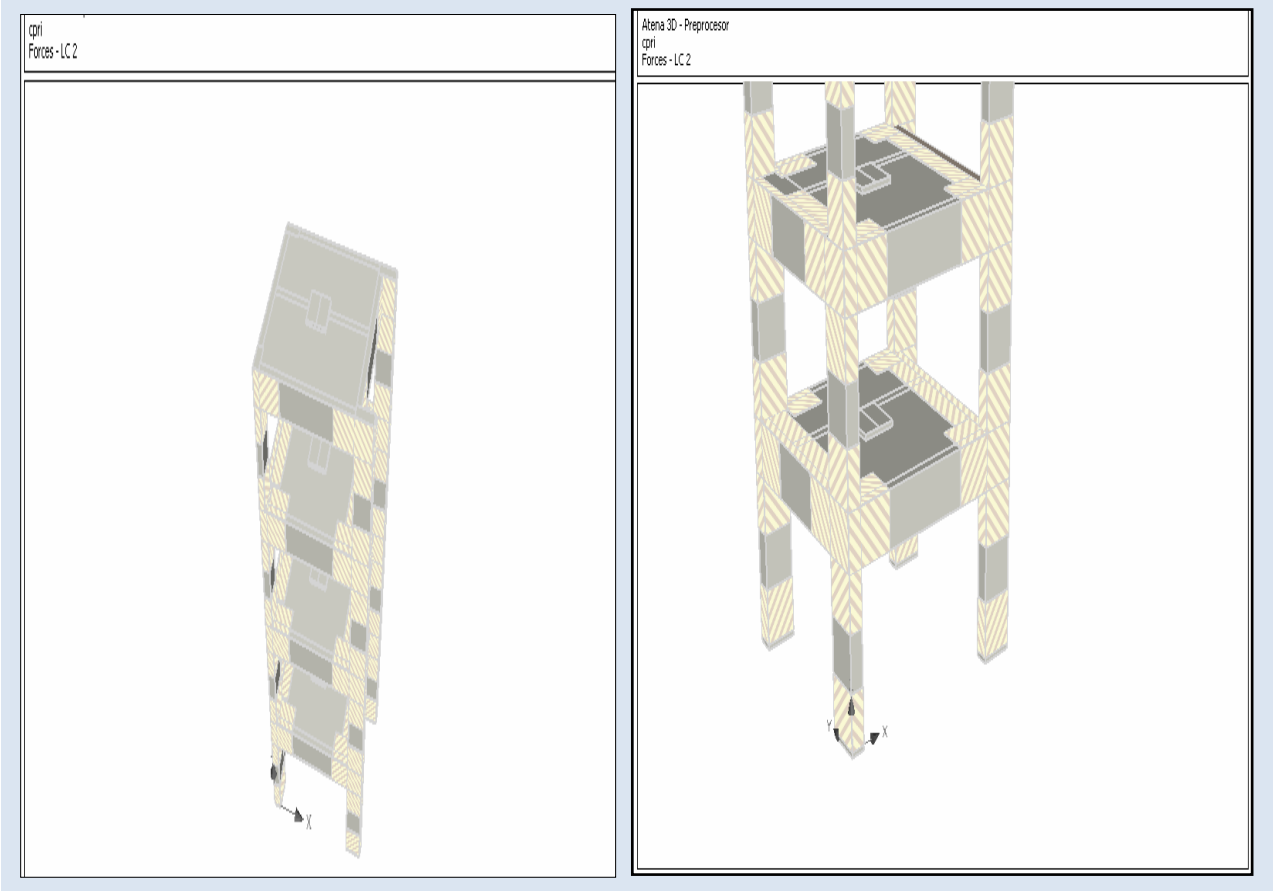

Figure 4.4 Scheme of FRP retrofitting

Closure

After performing complete steps of finite element modelling of FRP retrofitted frame in ATENA, analysis has been carried out and post-processed data has been extracted to obtain the results which have been discussed in **Chapter 5** in detail.

CHAPTER 5

RESULTS AND DISCUSSIONS

This chapter presents the results of Finite Element analysis of RCC frame. Finite element analysis of RCC frame under the static incremental loads has been performed using ATENA software. Subsequently these results are compared with experimental results of 'Round Robin Exercise on Experiment and Analysis of Four Storey Full Scale Reinforced concrete Structure under Monotonic Push-over Loads'. This is followed by load deflection curve and the cracking behaviour obtained from the analysis. In the end results obtained from the retrofitted frame have been discussed.

5.1 FE MODEL RESULTS OF CONTROL FRAME

In the present study, non-linear response of RCC control frame modelled as per details discussed in Chapter 3 (3.2 General Description of Structure) using FE Modelling under the incremental loading has been carried out. The objective of this study is to see the variation of load- displacement graph, the crack patterns, propagation of the cracks and the crack width at different values of the base shear.

5.1.1 BASE-SHEAR V/S DEFORMATIONS AT VARIOUS FLOOR LEVELS

In FE Model Pushover loads have been applied in inverse triangular fashion as done in case of experiment. The ratio of force at "1st floor: 2nd floor: 3rd floor: 4th floor" has been kept as "1:2:3:4" as shown in **Figure 3.6**.Due to this loading pattern, if P is the load on the first floor then the base shear would be equal to P+2P+3P+4P = 10P. The value of P is taken as 100KN in FE Model.

The load on the structure has been gradually increased in the steps till failure. When the FE non linear analysis is completed, the results are shown in third part of the ATENA i.e. Post processing. The load-deflection values at every step have been recorded, further the crack pattern and cracks propagation at every step has been studied. The base-shear v/s deflection curves at various floor levels have been plotted and are presented in **Figure 5.1 to 5.4.**

Deflection at the floor level-4 has been plotted in **Figure 5.4**. It can be seen from that the structure behaved linearly elastic up to the value of base shear around 360 KN. At this point the minor cracks started to get generated at top floor level. After this point there is a slight curvature in the plot and deflection started increasing with the load increments. When the base-shear reached to the value of 500 KN, the graph depicted non-linearity in its behaviour. It is clear from the **Figure 5.4** that at base shear 750

KN, increase in deflection is more with load increments. At 840 KN base shear deflection has been observed to be 125mm and a rapid increase in displacement is observed. It has reached to the value of 175mm when base shear is 880 KN. After this point there is constant increase in deflections and plot has become almost flat after the value of base-shear 927 KN. Subsequently deflection started increasing without any significant increment in load; it has reached to the value of 345mm with the base-shear value 952 KN.

Deflection at the floor level-3 has been depicted through **Figure 5.3**. It can be observed from this plot that the load-deformation behaviour is same as of fourth floor level. The maximum value of deflection has been observed to be 331mm at the base shear of 952KN. Further, the deflection has been found to be 488mm at the base shear of 962 KN

Deflection at the floor level-2 has been depicted through **Figure 5.2**. It can be observed from this plot that there was decrease in the value of displacement at same value of base shear, the structure showed the same behaviour as that of third and fourth floor level. The maximum deflection at base shear 952 KN has been observed to be 331mm. It has reached to the value of 391mm when base shear is 962 KN, after this it started increasing without any increment in load; it has reached to the value 725 mm.

Deflection at floor level-1 has been depicted through **Figure 5.1**. It can be seen from the Figure5.1 that floor level-1 has experienced the minimum deflection even though the damage experienced by this floor is maximum. The variation of load-deflection curve is same as per other floor levels. The maximum deflection as base shear 952 KN has been found to be 230mm which increases up to 425mm, even after without any application of load.

The displacements at various floor levels for different base shear have been tabulated in Table 5.1:

Table 5.1 Comparison of Displacements at different Base shear at various floor levels

Sr. No.	Base Shear In (KN)	Deflection at 1^{ST} Floor (mm)	Deflection at 2^{ND} Floor (mm)	Deflection at 3^{RD} Floor (mm)	Deflection at 4^{th} Floor (mm)
1.	2	0.0073	0.0116	0.0156	0.019
2.	100	0.837	1.32	1.74	2.08
3.	150	1.29	2.02	2.67	3.18
4.	200	1.8	2.8	3.68	4.5
5.	250	2.5	3.83	4.94	5.81
6.	300	3.06	4.7	6.05	7.0
7.	350	4.06	6.25	7.91	9.15

8.	402	5.34	8.1	10.1	11.6
9.	452	6.66	9.99	12.6	14.1
10.	497	9.2	14.1	17.7	20.2
11.	507	11.1	15.9	19.4	21.7
12.	547	13.2	19.1	23.1	25.9
13.	601	15.2	22.5	27.3	30.6
14.	652	20.6	31.6	38.8	43.1
15.	702	23.8	37.1	45.5	50.6
16.	752	26.4	41	50.2	55.8
17.	802	43.4	69.2	86.4	93.4
18.	850	74.7	119	142	151
19.	882	87.4	139	165	177
20.	901	96.3	155	183	192
21.	927	106	172	203	213
22.	947	136	231	285	299
23.	952	158	267	331	345
24.	962	230	391	488	502
25.	947	346	598	766	787

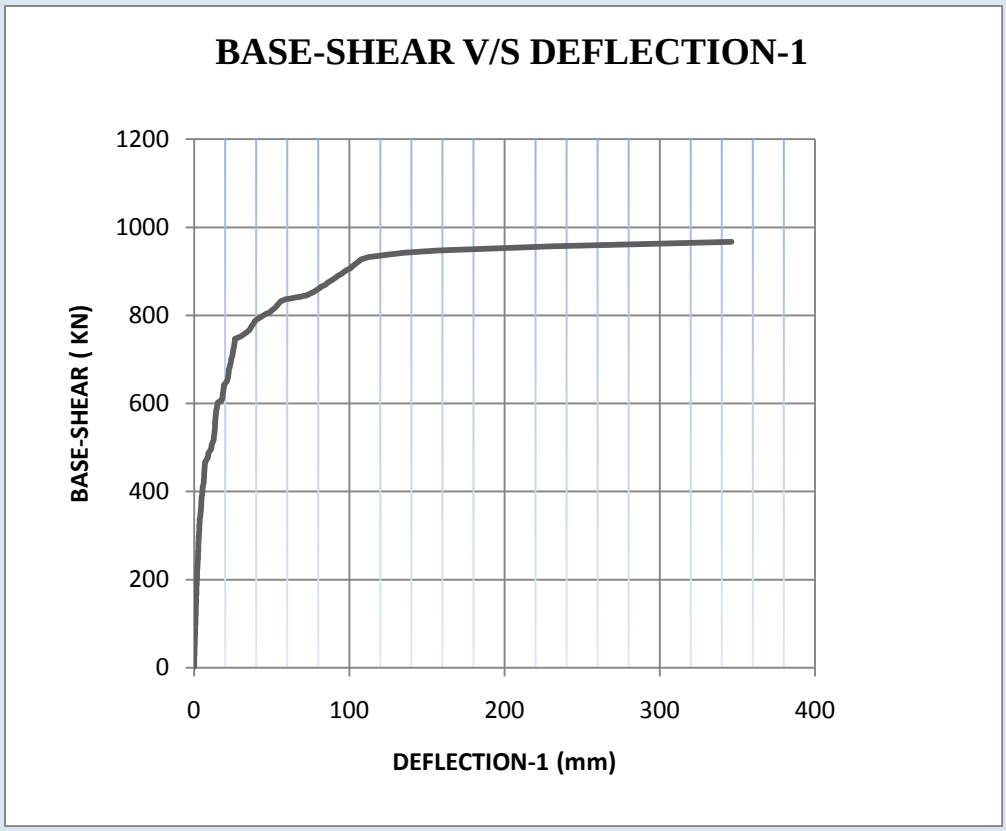

Figure5.1 Base shear v/s Displacement at Floor level-1

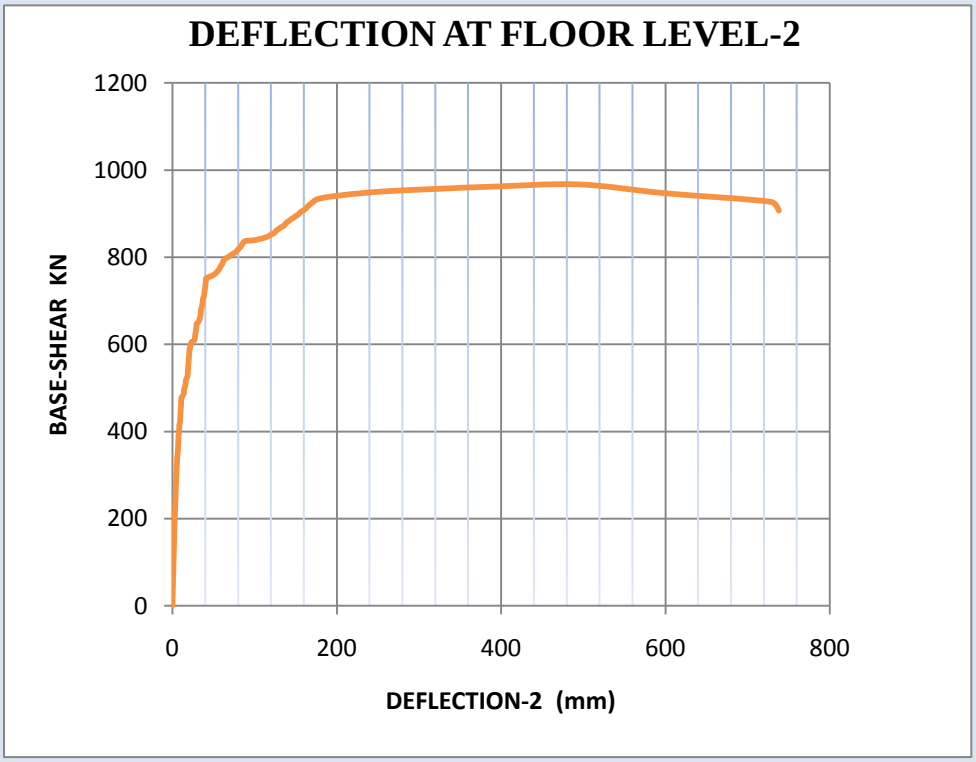

Figure5.2 Base Shear v/s Displacement at Floor level-2

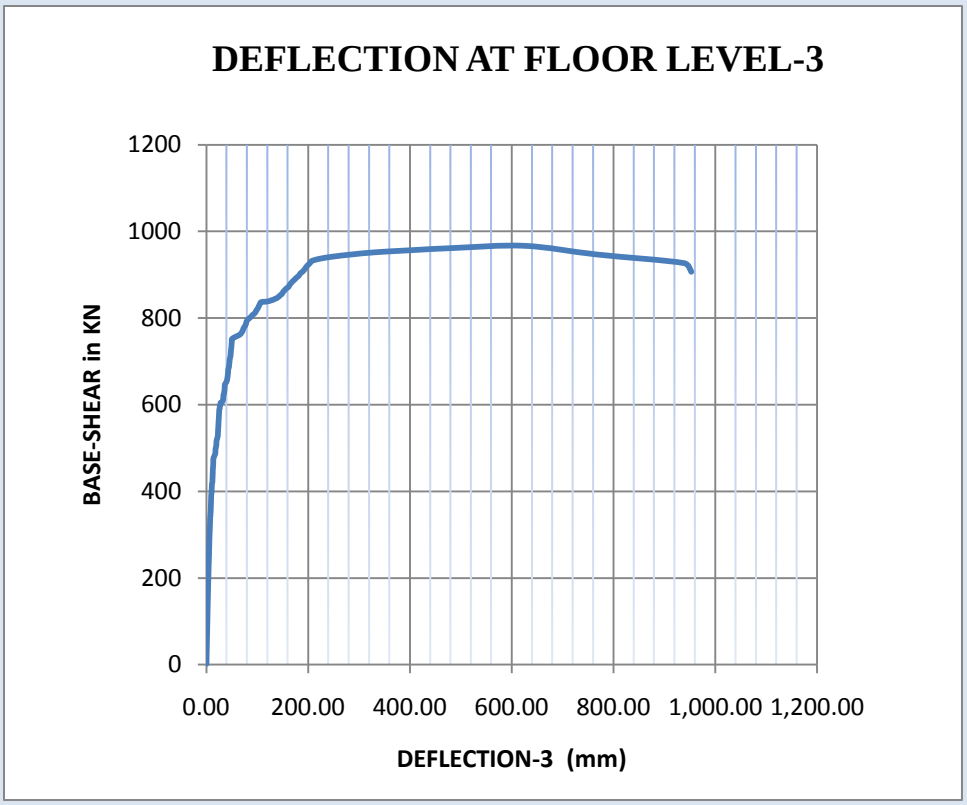

Figure 5.3Base shear v/s Displacement at Floor Level-3

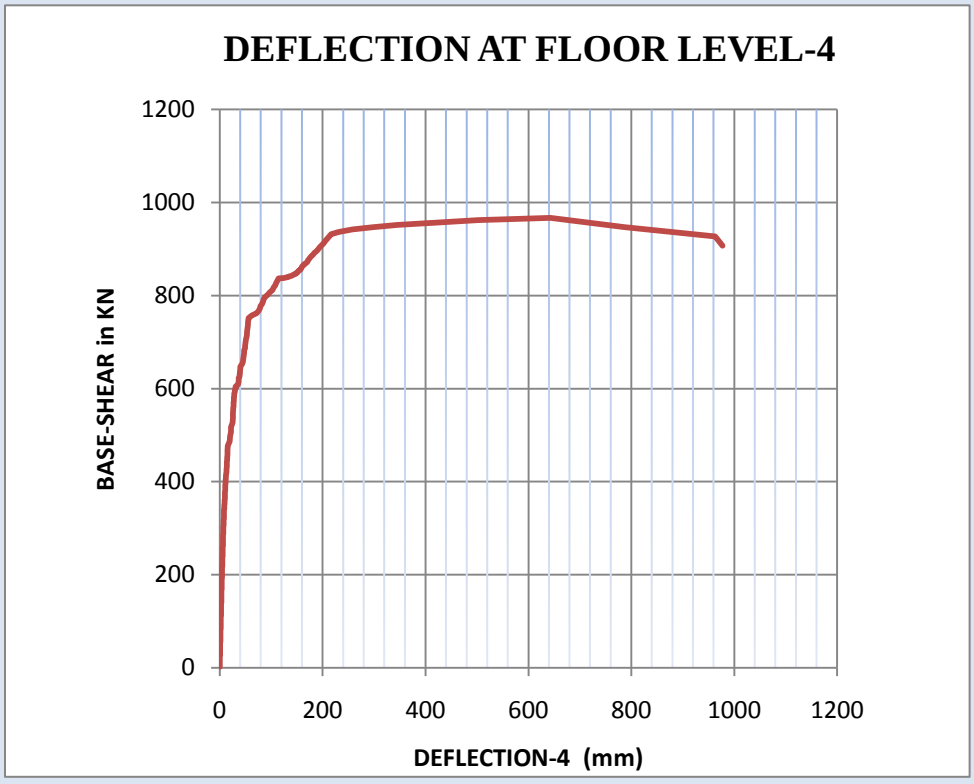

Figure 5.4 Base shear v/s Displacement at Floor Level-4

5.1.2 CRACK PATTERNS

The variation of crack pattern has been taken out from the post processer of ATENA and are plotted in **Figure 5.5** to **5.16**. A discussion on crack pattern plotted here has been presented here.

The shape of un-deformed and deformed structure has been shown in Figure 5.5. In the deformed shape storey drift in the X direction (direction of loading) at upper levels is clearly visible.

CRACK PATTERNS AT STEP-150

It can be observed from Figure 5.6 that micro-cracks appeared in the structure when frame is in linear zone. The first crack has been observed at 150^{th} step at value of base shear 300 KN in the shape of shear crack, when the value of base shear is exactly 300KN. This very small sized (actually invisible) crack appeared at left side beam-column joint of first storey.

CRACK PATTERNS AT STEP-175

The crack pattern at 175th step of the analysis at value of base shear 350 KN is presented in **Figure 5.7**. At 1^{st} and 2^{nd} floor level shear cracks have been observed near beam column joints. Cracks of very small size have been observed in the floor slab near right side columns. No visible flexural or beam-column failure have been observed in linear zone, crack at the base of beam-column joints, joined with the shear cracks at first floor level have been observed as seen in Figure .

CRACK PATTERNS AT STEP-200

The various views of crack pattern at 200^{th} load step at value of base shear 450 KN are presented in **Figure 5.8**. Side elevations show the beam- column joint failures at 1^{st} floor level only along with few flexural cracks in beams. Lower level floor slab is also showing lot of cracks. Max. size of crack at this load step has been found to be 0.9 mm. Very few cracks at 3^{rd} floor level and no crack was found at top level.

CRACK PATTERNS AT STEP-250

The crack pattern at 250^{th} load step at value of base shear 625 KN are presented in **Figure 5.9** & **Figure 5.10**. The beam- column joint failures can be observed in side elevations of the frame at 1^{st}, 2^{nd} and at some points of 3^{rd} floor level along with some flexural cracks in beams. Lower level floor slab is also showing lot of cracks. Max. size of crack at this load step was found to be 1.95mm. Very few cracks at 3^{rd} floor level and no crack was found at top level. Major damage was noticed in CL 15.

After reaching the value of base shear 680 KN, cracks have been observed on lower two floor levels and have been propagating towards upper storeys. Maximum crack size at this level has been observed of 2.1mm width.

CRACK PATTERNS AT STEP-300

The crack pattern from all views along with the perspective view of the frame at 300^{th} load step of the FE analysis at value of base shear 850 KN has been presented in **Figure 5.11** & **Figure 5.12**. From side views it can be seen that 1^{st}, 2^{nd} ,3^{rd} floor level and few points of 4^{th} floor level have experienced the beam- column joint failures along with flexural cracks in beams. Lot of cracks can be seen in the lower level floor slabs. Max. size of crack at this load step is found to be 13.5 mm. Some cracks at 3^{rd} floor level and very few crack can be seen at top level. The elements of lower two storeys have experienced moderate damage whereas upper storeys experienced minor damage.

The crack pattern along with iso-areas at 344^{th} load step has been presented in **Figure 5.13**. This is the ultimate load level of the frame. Red color is depicting maximum stresses in tension while the members in yellow are under compression.

CRACK PATTERNS AT STEP-344

All the views showing the crack pattern at 344^{th} load step of the FE analysis at value of base shear 962 KN are presented in **Figure 5.14** & **Figure 5.15**. The beam- column joint failures at 1^{st}, 2^{nd} ,3^{rd} and at few points of 4^{th} floor level along with flexural cracks in almost all the flexural members can be visualised from different side views All floor slabs except top level floor slab are showing cracks. Max. size of crack at this load step is found to be 78.1 mm. Some cracks at 3^{rd} floor level and very few crack have been seen at top level. Major damage has been noticed in elements of lower two storeys whereas 3^{rd} storey experienced moderate damage. The top storey experienced minor damage.

Zoomed view of crack patterns at upper (3rd and 4th)and lower floor levels (1st and 2nd) is presented in

Figure 5.16.

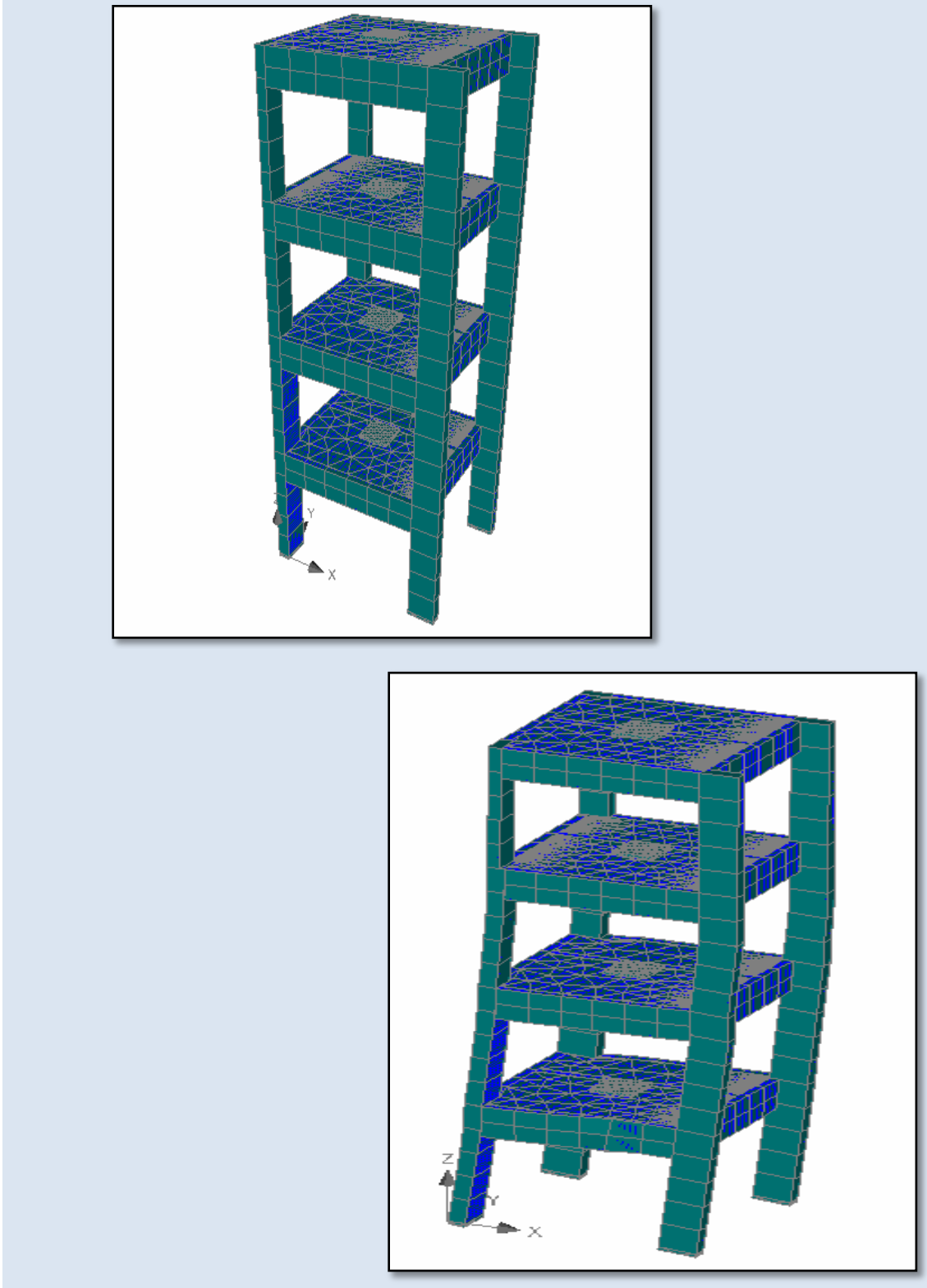

Fig5.5 Undeformed and Deformed Shape of RC Frame

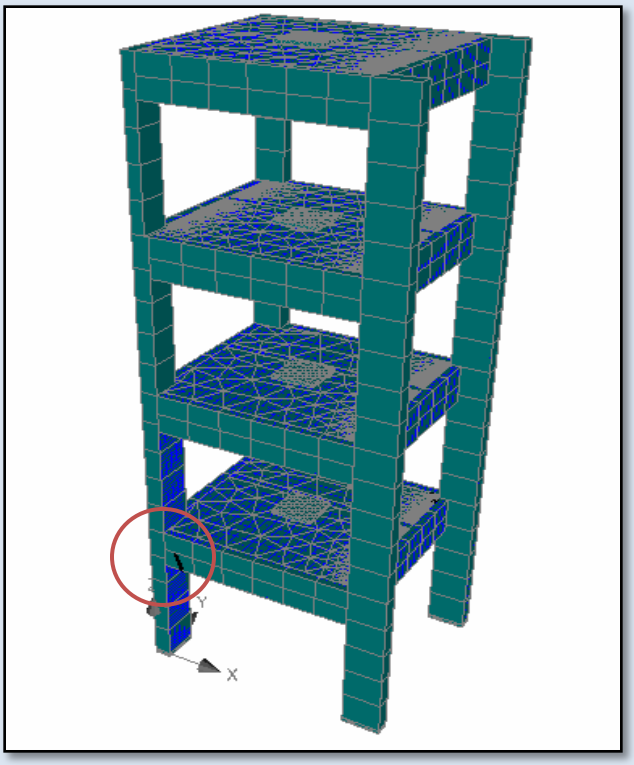

Fig5.6 Crack Pattern at Step-150 at Base Shear-300KN

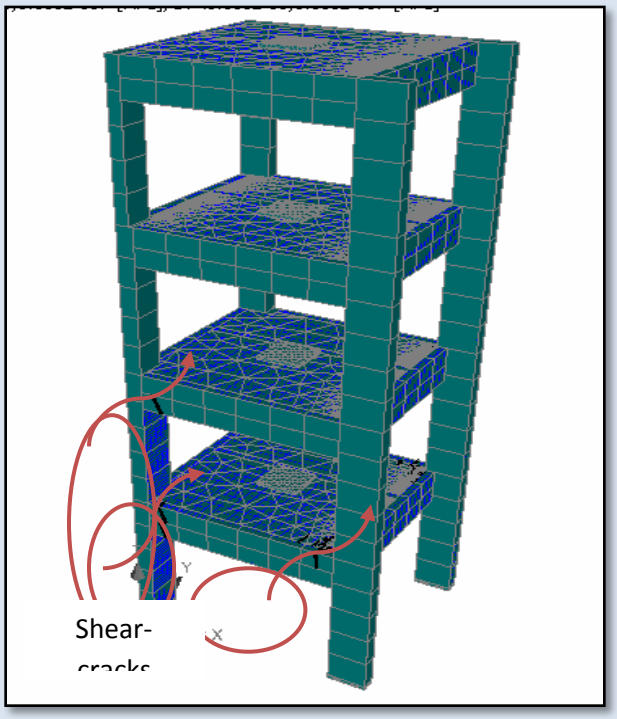

Fig5.7 Crack Pattern at Step-175 at Base-Shear-350KN

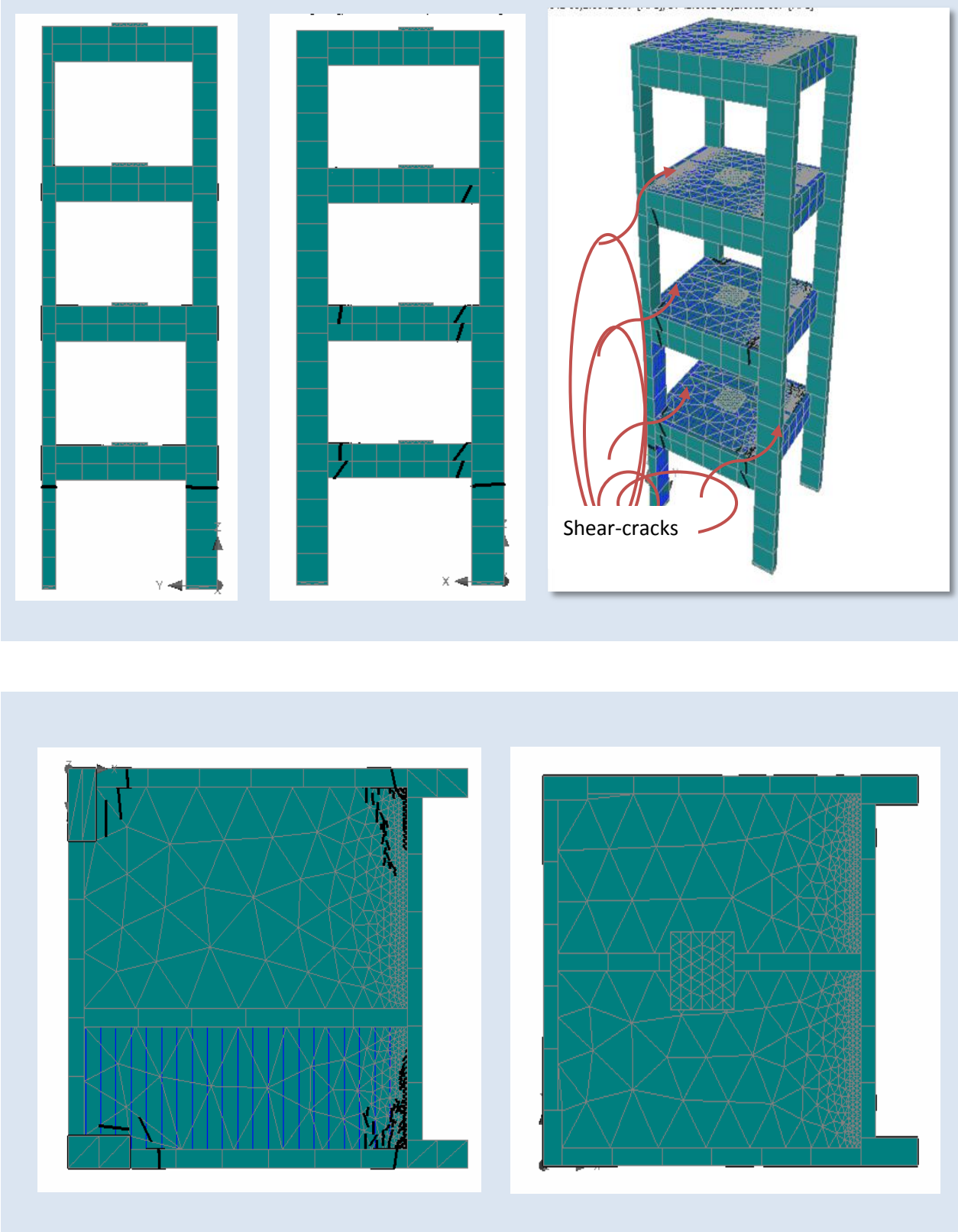

Fig5.8 Crack Pattern at Step-200 at Base-Shear-450KN

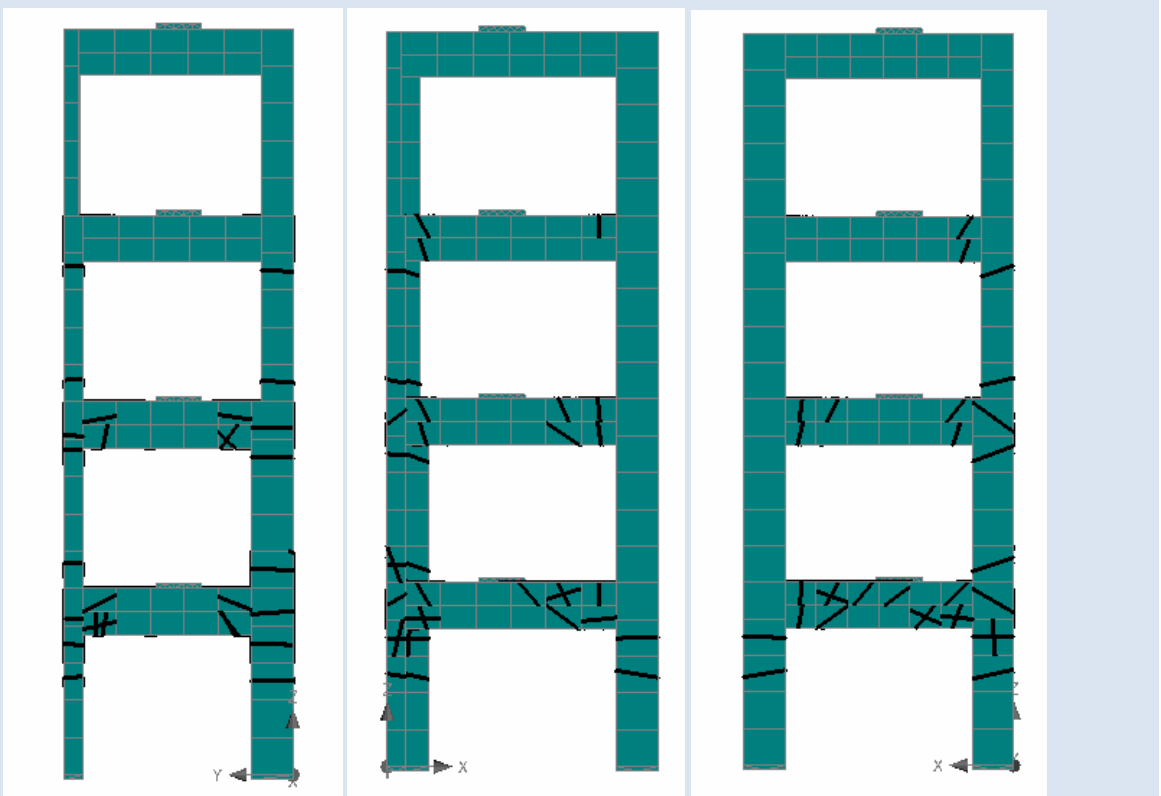

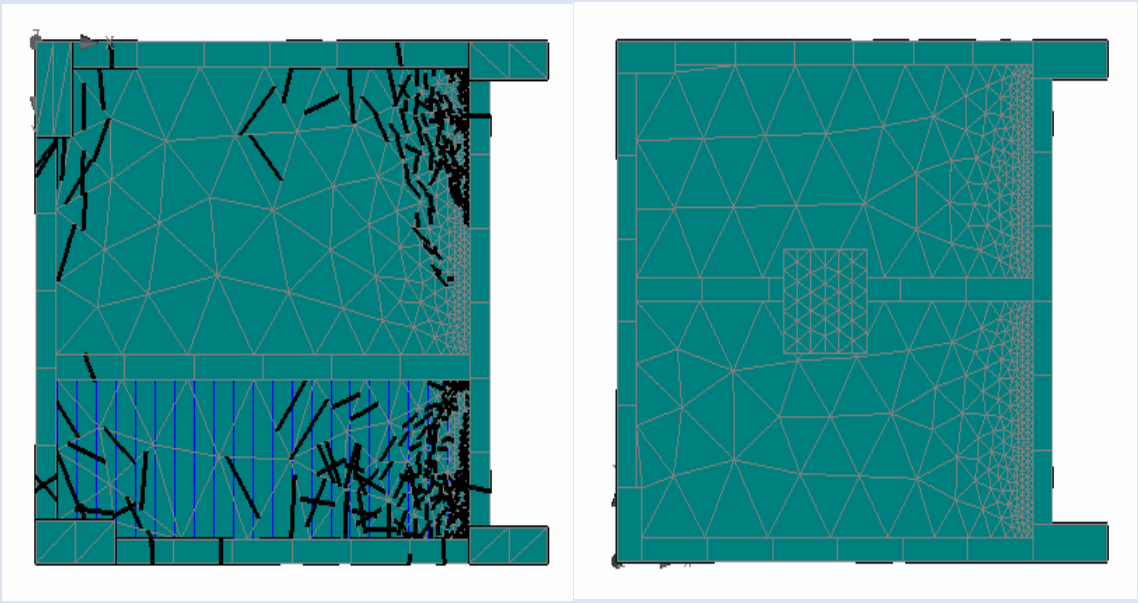

Fig5.9 Crack Pattern at Step-250 at Base-Shear-625KN

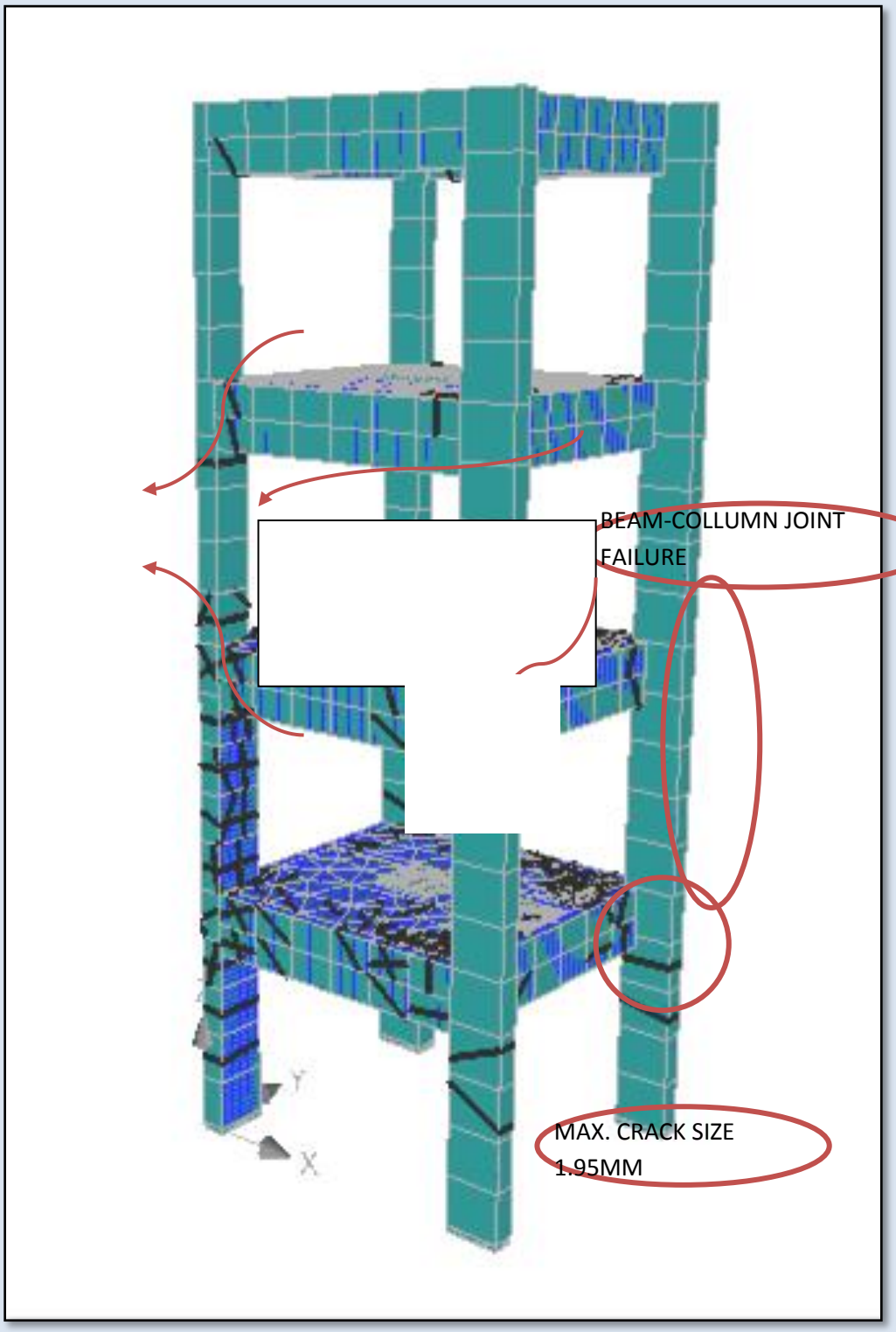

Fig 5.10 Crack Pattern at Step-250 (Perspective View)

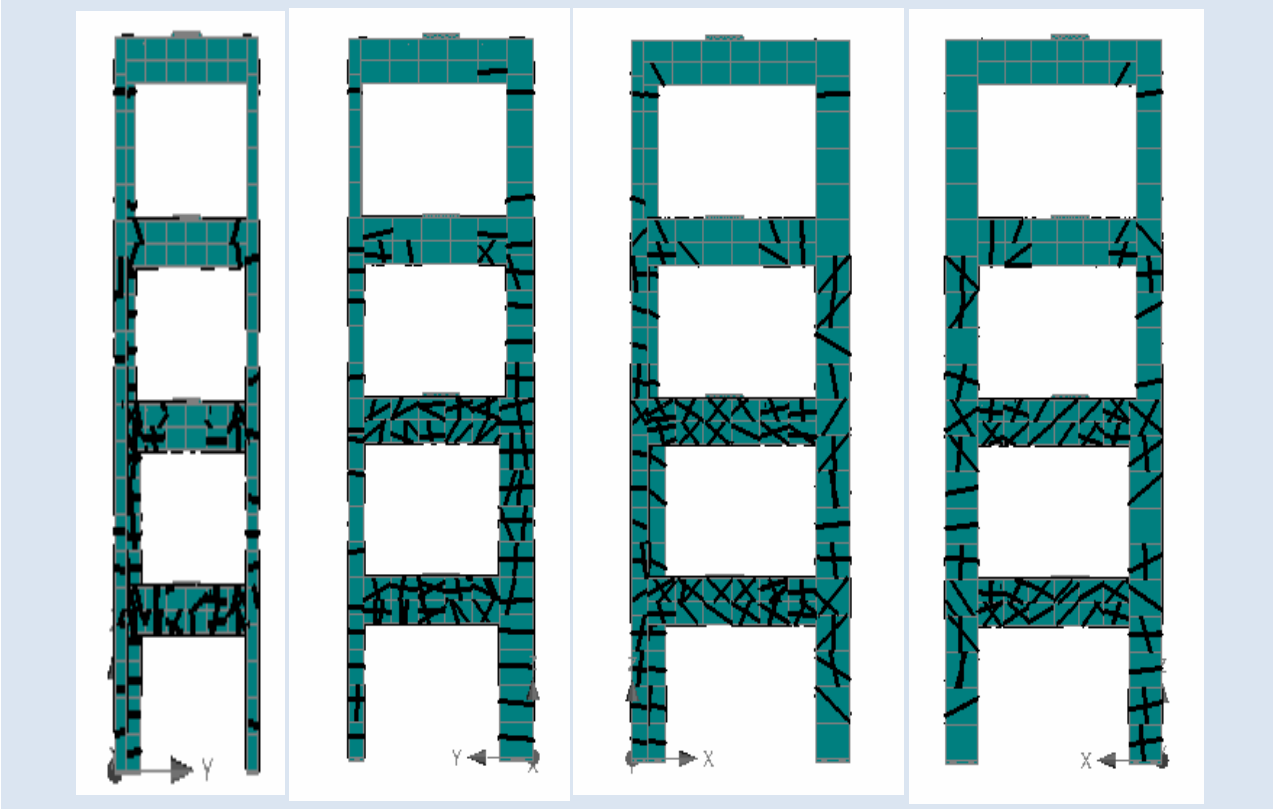

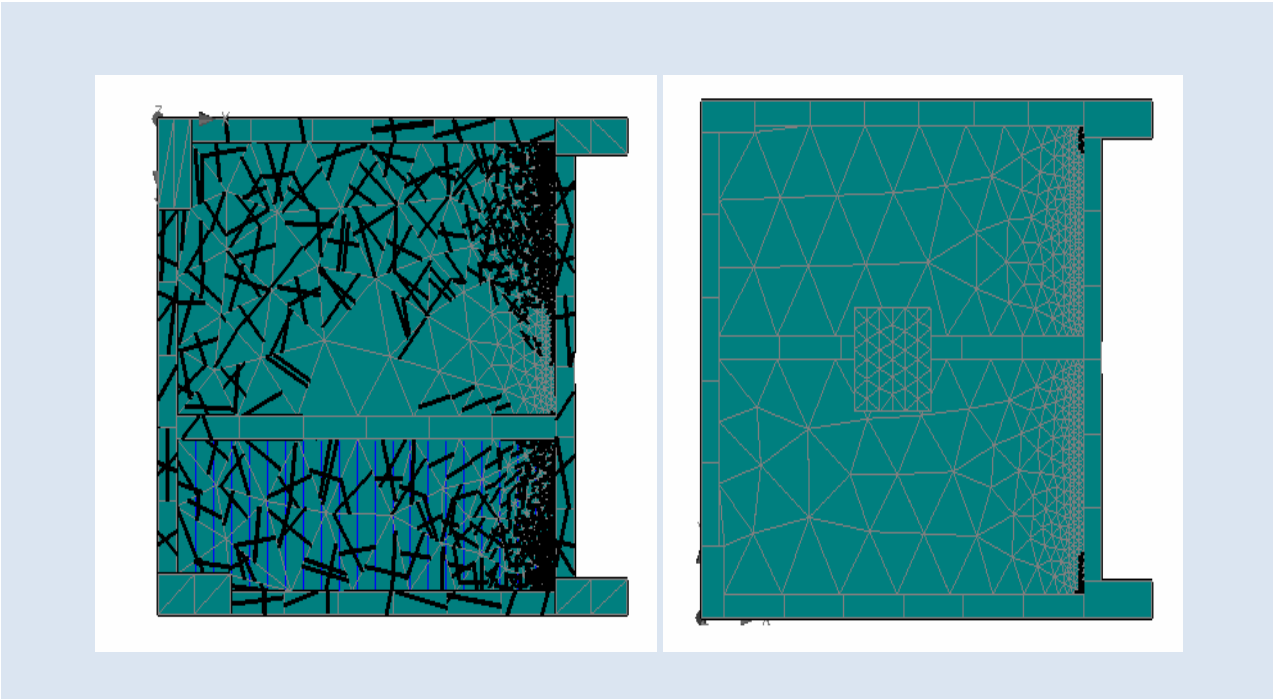

Fig5.11 Crack Pattern at Step-300 at Base-Shear-850KN

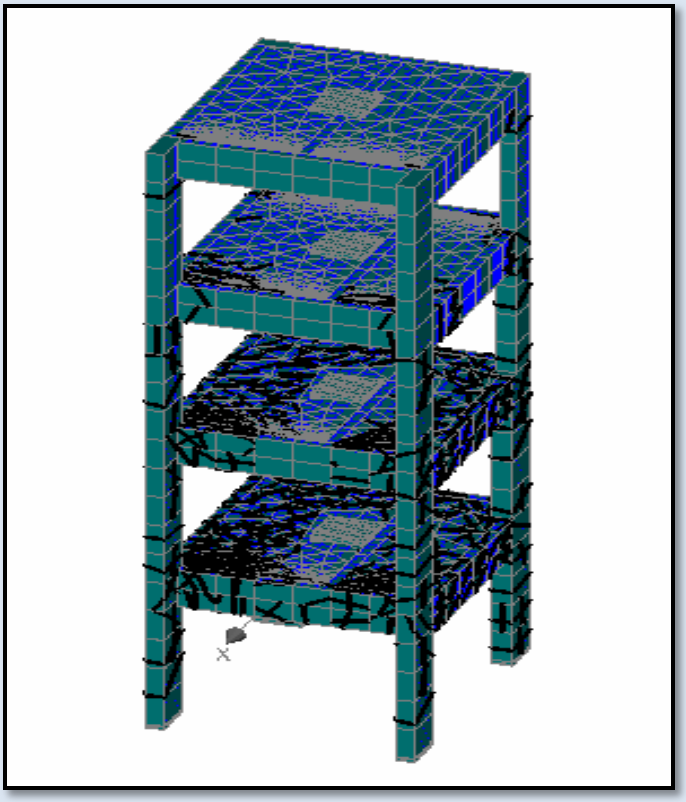

Fig5.12 Crack Pattern at Step-300 (Perspective View)

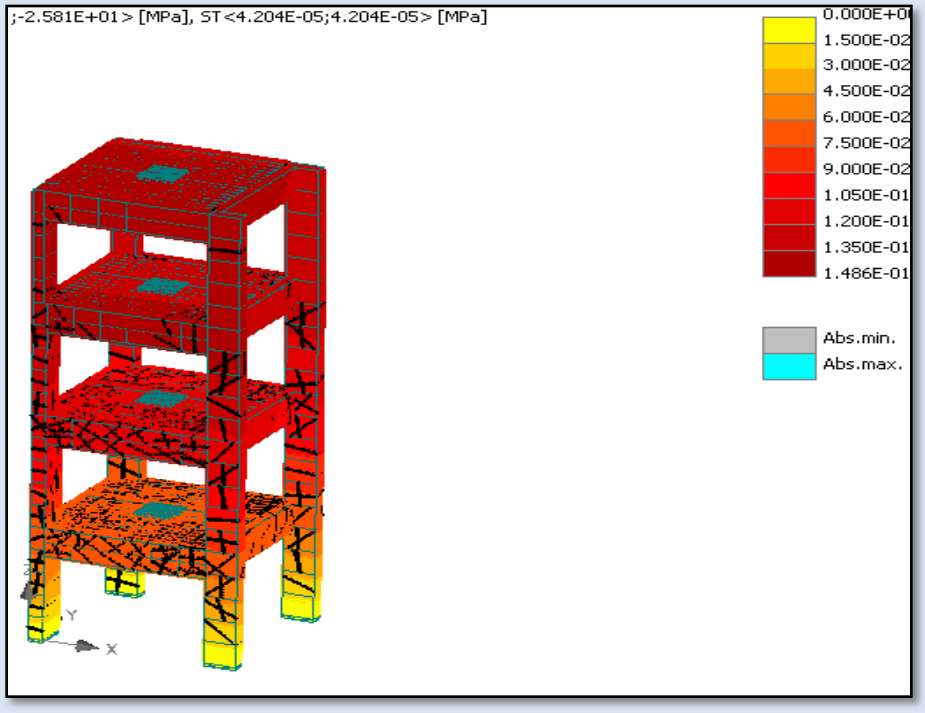

Fig5.13 Crack Pattern and Iso-areas at Step-344

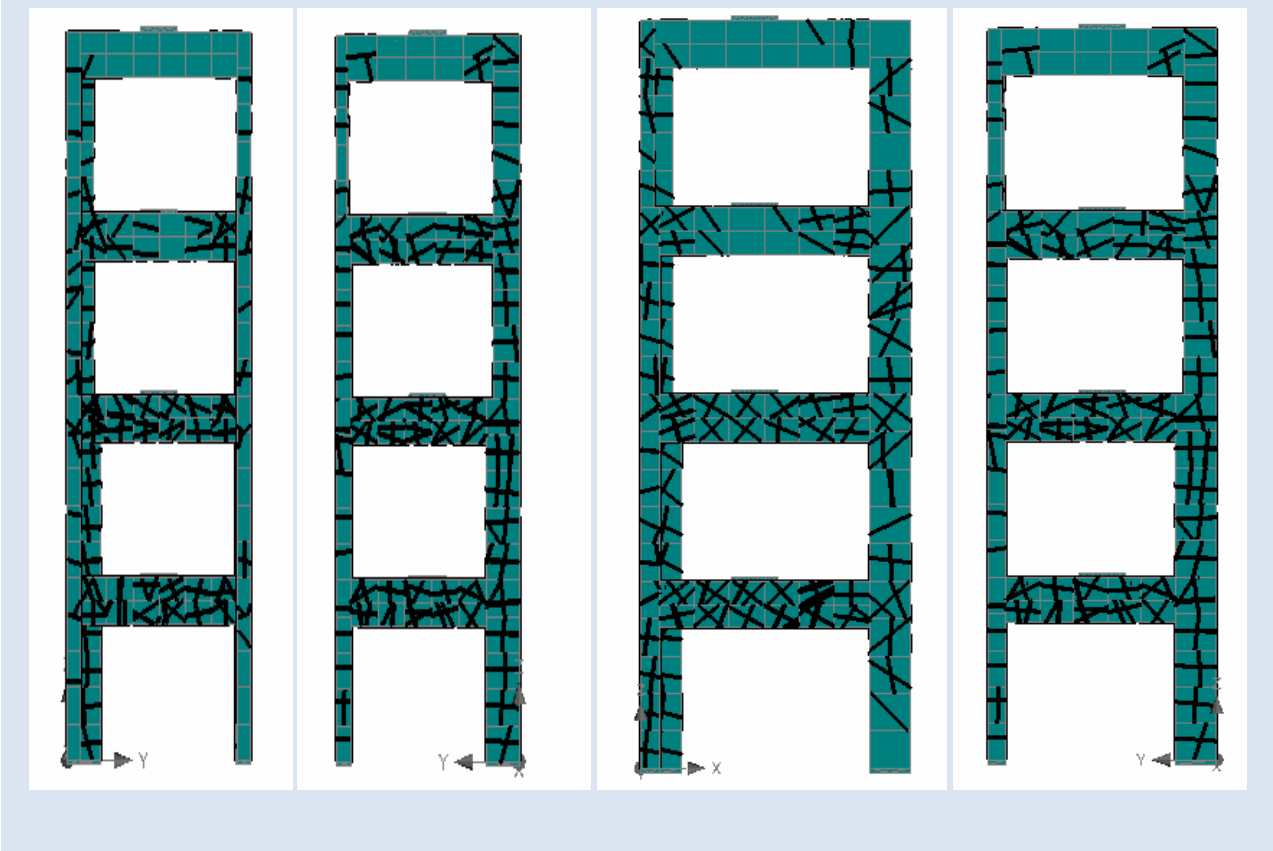

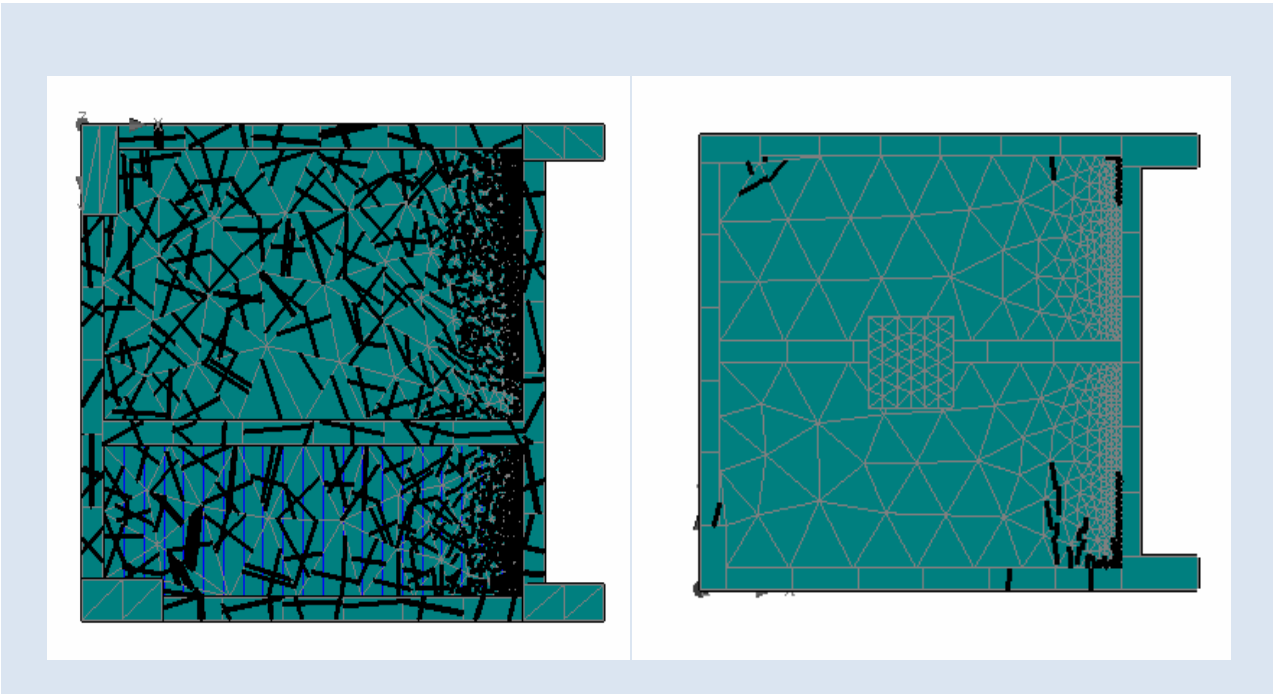

Fig5.14 Crack Patterns at Step-344 at Base-Shear-962KN

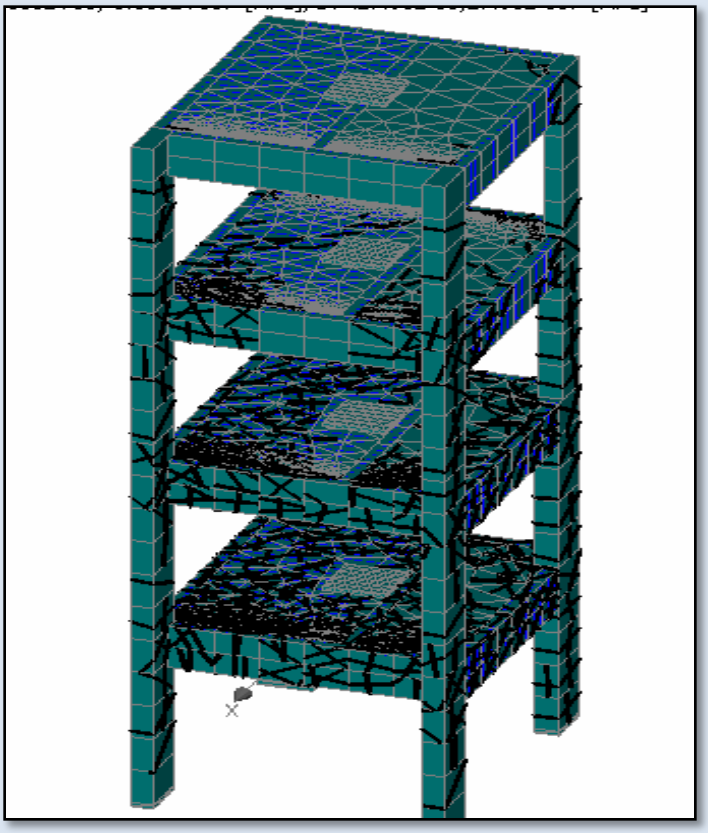

Fig5.15 Crack Pattern at Step-344 (Perspective view)

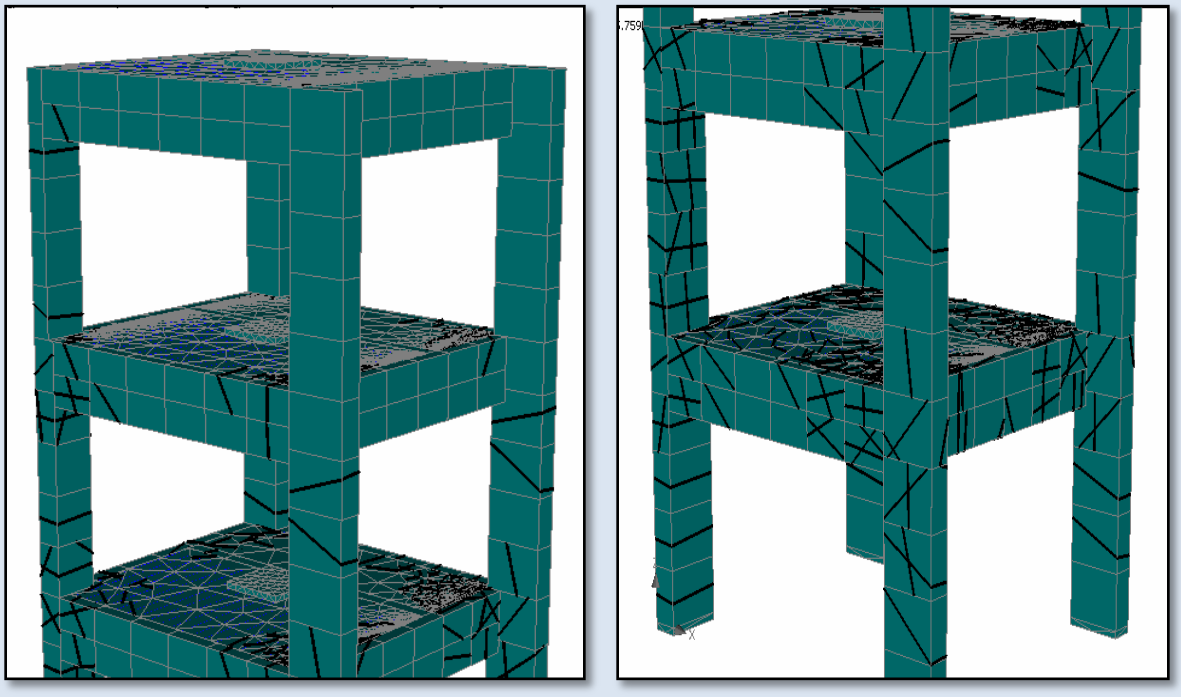

Fig5.16 Crack Pattern at Different Floor Levels (Zoomed View)

5.2COMPARISON BETWEEN THE FE MODEL AND THE EXPERIMENTAL RESULTS OF THE CONTROL FRAME

5.2.1 Experimental Results of Control Frame [4]

Base shear v/s Floor Displacement (Pushover Curves) the pushover curves as obtained for extreme right side column (CL20) side are plotted in **Figure 5.17**. As can be seen from the **Figure5.17**, the maximum displacement for CL 20 has been obtained as 765mm. The average top drift is therefore equal to round 4% of the total height of the building.

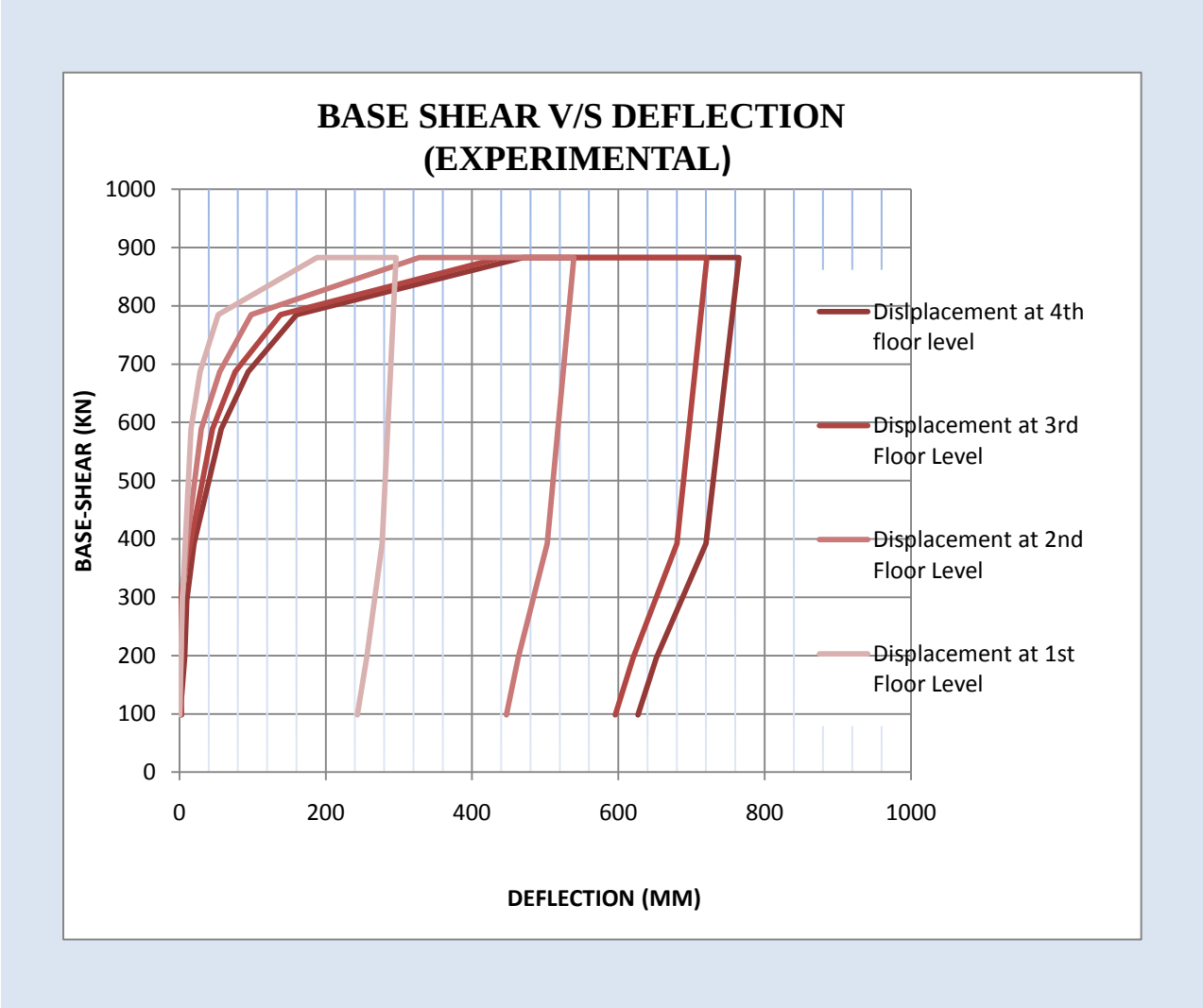

Figure5.17 Combined Pushover Curve from Experimental Data [4]

5.2.2 COMPARISON BETWEEN THE FE MODEL AND THE EXPERIMENTAL RESULTS OF THE CONTROL FRAME

- The behaviour of the frame has been observed to be linear up to the value of base shear around 360 KN and the first crack has been observed at 150^{th} step, whereas the structure has been found to be linear up to the value of base shear 300 KN in case of experiment. At this point the flexural tension cracks at the base of the columns depicting reduction in stiffness have been observed.
- After reaching a base shear value of approximately 500 KN, the cracks at the base of the columns have been found to open wider and failures at other location like beams and beam – column joints started. The maximum size of the crack at this level has been found to be 0.1mm width. Whereas in case of experiment at a base shear value of approximately 500 KN, the cracks at the base of the columns have been observed and failures at beam – column joints start to show up. As a result the stiffness of the frame further goes down, as can be seen from the pushover curve.
- After reaching the base shear values of 750 KN, displacements have found to be increasing at fast rate whereas in case of experiment at the base shear values of 700 KN, the joints of the frame have found to be displaying rapid degradation and the inter storey drift increasing rapidly.
- After this stage, at further increase in the lateral load (880 KN), the FE model has been observed to display soft behavior and displacement increased for the same increase in the base shear but experimentally after reaching a base shear of 800 KN, the frame has been found undergoing increasing displacement at almost constant load. After reaching a base shear of 90t (882.90 KN), i.e. 9t load at first floor 18t at second floor, 27t at third floor and 36t at fourth floor, the structure has been observed undergoing increasing displacement at constant load .
- Maximum deflection has been found to be more than 900mm at 950 KN. Maximum Crack size at this level is observed 75mm in the FE model. Maximum deflection at fourth level at 880KN is 770mm experimentally which is 173mm in case of FE model.
- Variety of failures like beam-column joint failure, flexural failures and shear failures have been observed almost in the same way as seen in the case of experiment.

- Prominent failures shown by both models have been the joint failures. Also the severe damages have been observed at joints of lower floors whereas moderate damages have been observed in first and second floors. Minor damage is seen at floor level in both the cases.

Table 5.2 Comparison of Experimental and FE Model Results of Control RC Frame at Fourth Floor Level

SR.NO.	EXPERIMENTAL RESULTS		FE MODEL RESULTS	
	Base Shear(KN)	Deflection(mm)	Base Shear(KN)	Deflection(mm)
1.	98.1	1	98	2.03
2.	196.2	7	196	4.32
3.	294.3	10	294	6.86
4.	392.4	20	392	10.6
5.	588.6	57	588	28.1
6.	686.7	94	687	49.1
7.	784.8	160	787	84.3
8.	882.9	470	883	177
9.	882.9	765	922	208
10.	392.2	720	952	345
11.	--	--	947	787
12.	--	-	927	963

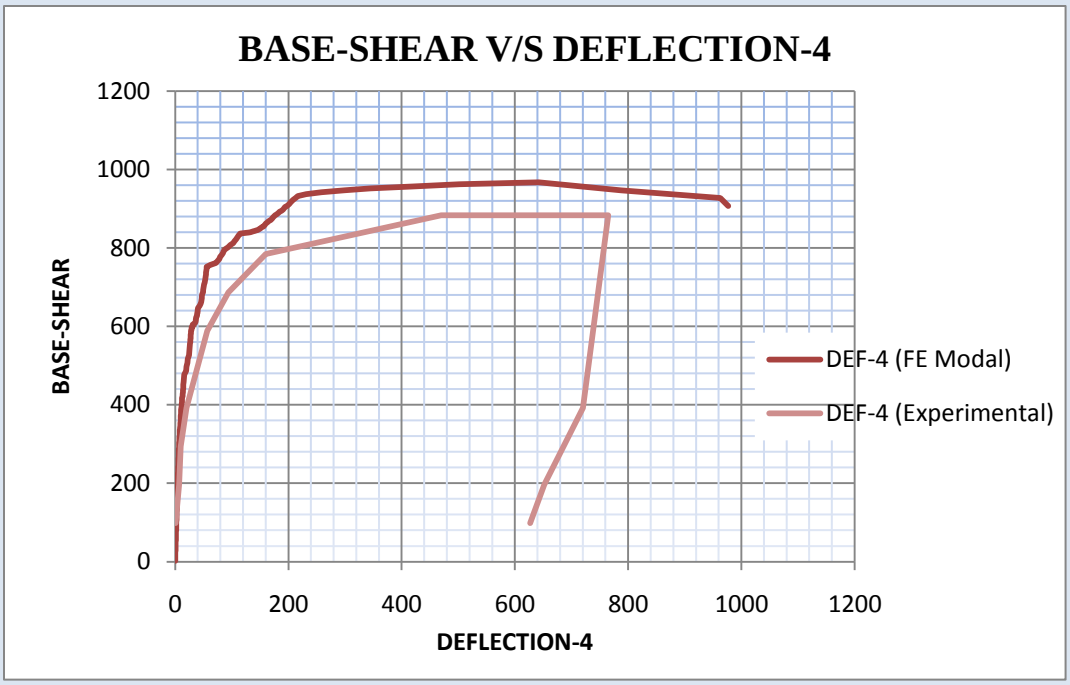

Figure 5.18 Variation of Base shear v/s Displacement at Floor -4 Level

(Experimental & FE Model)

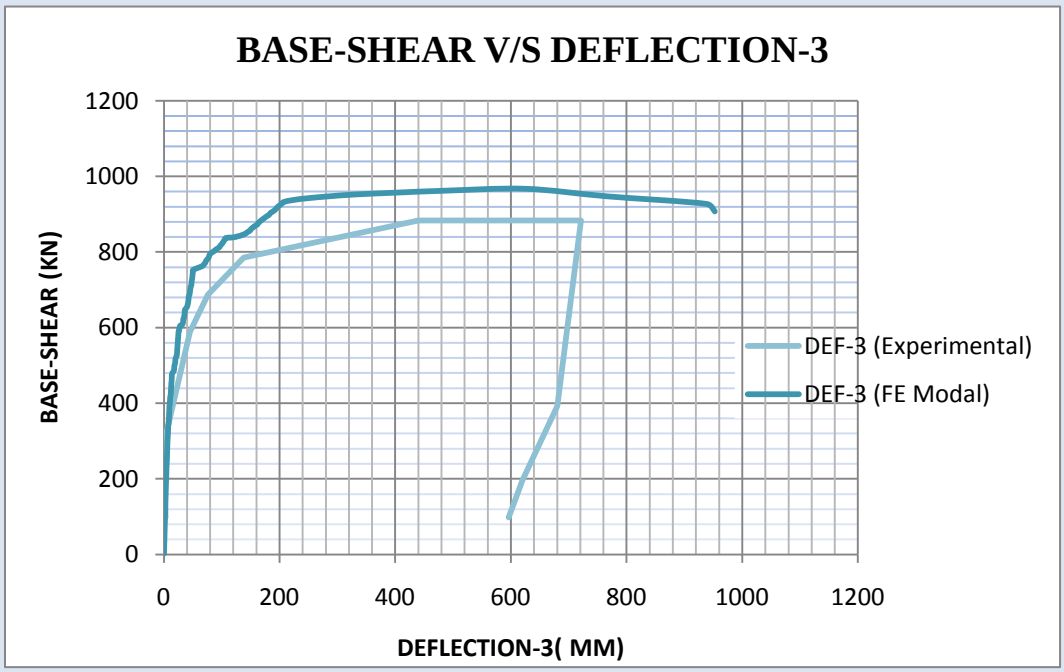

Figure 5.19 Variation of Base shear v/s Displacement at Floor Level-3

(Experimental & FE Model)

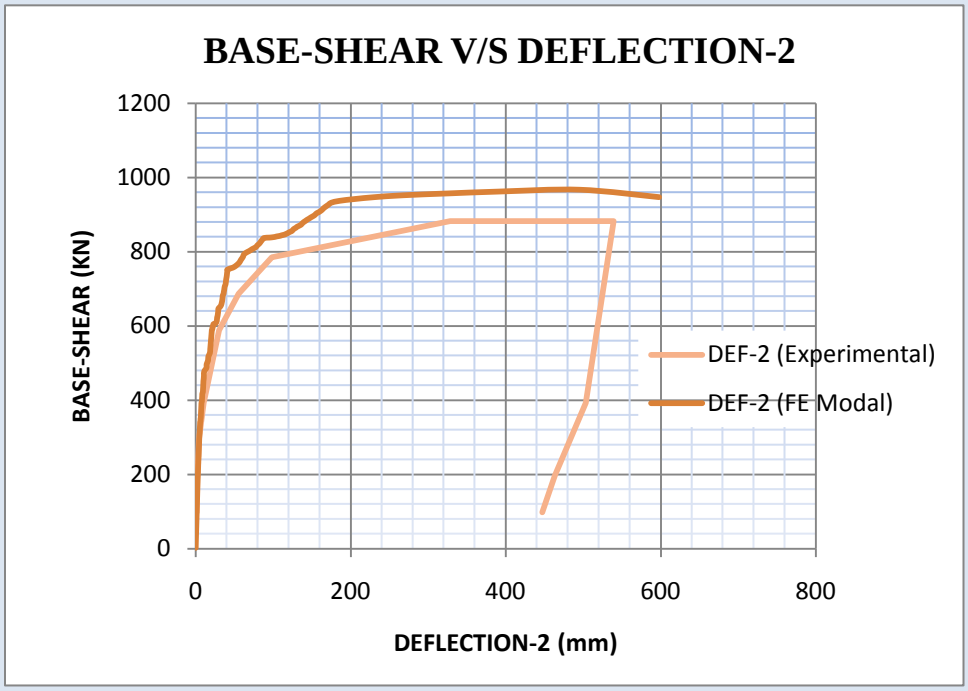

Figure 5.20 Variation of Base shear v/s Displacement at Floor Level-2

(Experimental & FE Model)

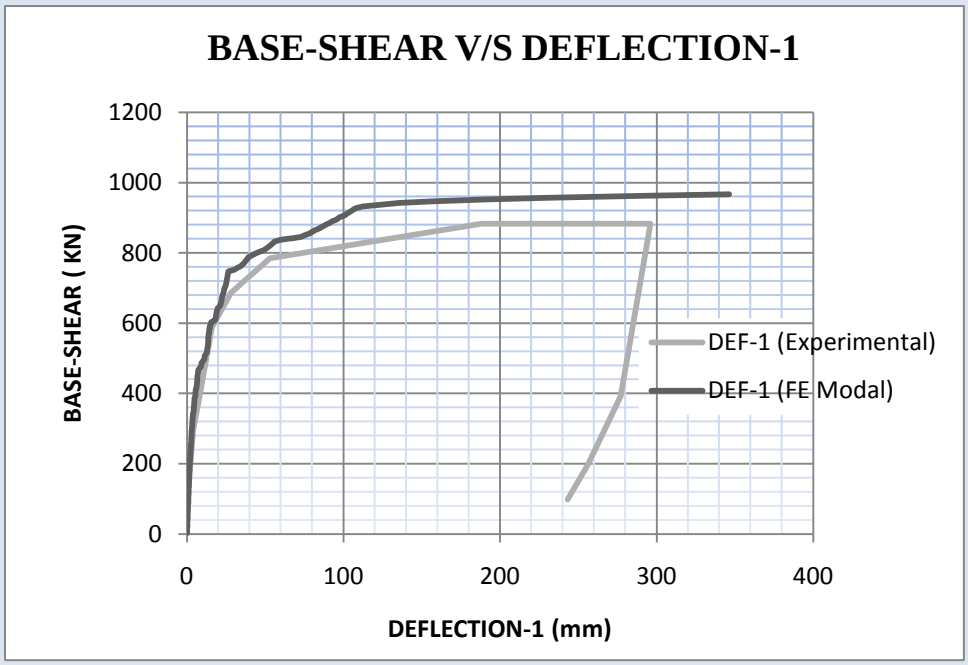

Figure 5.21 Variation of Base shear v/s Displacement at Floor Level-1

(Experimental & FE Model)

5.3 RESULTS OF RETROFITTED FRAME

In the present study, non-linear response of RC retrofitted frame modelled as per details discussed in Chapter 4 using FE Modelling under the incremental loading has been carried out. The variation of load-displacement graph, the crack patterns, propagation of the cracks and the crack width at different values of the base shear has been studied.

5.3.1 FRP MODELLING AND ANALYSIS

After performing the analysis of RC frame up to the ultimate loading and maximum deflection, the next step is to model FRP retrofitted damaged frame and to analyze the same frame in ATENA. The FRP modelling has been done as a 3D shell element in ATENA. The Ahmad shell element implemented in ATENA (Ahmad et al., 1970), described in ATENA theory manual. The present Ahmad element belongs to group of shell element which can be used to model thin as well as thick shell or plate structures.

5.3.2 BASE-SHEAR V/S DEFORMATIONS AT VARIOUS FLOOR LEVELS

In FE Model Pushover loads have been applied in inverse triangular fashion as done in case of experiment. The ratio of force at "1st floor: 2nd floor: 3rd floor: 4th floor" has been kept as "1:2:3:4. Due to this loading pattern, if P is the load on the first floor then the base shear would be equal to P+2P+3P+4P = 10P. The value of P is taken as 100KN in FE Model.

The load on the structure has been applied in gradual increments till failure. The behaviour of the elements at every step of load deflection is analyzed with the help of base shear-deflection values at every step, crack pattern and cracks propagation at every step. From the post-processed data, the values of deflection at different values of base-shear have been taken and base-shear v/s deflection curves have been plotted in **Figure 5.22 to 5.25**. The behaviour of the structure has been studied at various load levels.

It can be seen from the **Figure 5.22** that the retrofitted model has been found to behave totally linearly elastic up to a value of base shear 250 KN. After this point slight curvature has been observed in the graph and deflection has been increasing very slowly with the load increments. It has found to be almost linear till a base shear value of 800 KN, after this graph has depicted non-linearity in the behaviour of retrofitted frame. After crossing the value of base shear 800 KN, fast increase in the deflection with load increments has been observed. At 850 KN base shear deflection is 10 mm and it has been increasing at fast speed, it crossing 25.4mm when base shear has reached 1300KN. After this point there is constant increase in deflections without any significant increment in load, graph is almost flat at 1350KN and deflection has crossed the value of 87.8mm.The value of ultimate load corresponding to this base shear has been found to be 540 KN. It has been observed that the top storey experienced major damages in this case opposite to the case of control frame.

Base shear v/s deflection curves at floor level-3 depict lesser deflections as compared to top storey deflections as shown in **Figure 5.23**. 1st and 2nd floor levels have experienced very lesser deflections.

At base shear of 1000KN structure has been found to suffer severe cracking at upper floor levels. Cracks in almost every floor have been observed in the FE model.

Results obtained from the analysis are plotted as base shear v/s deflection curves at different floor level are as given below:

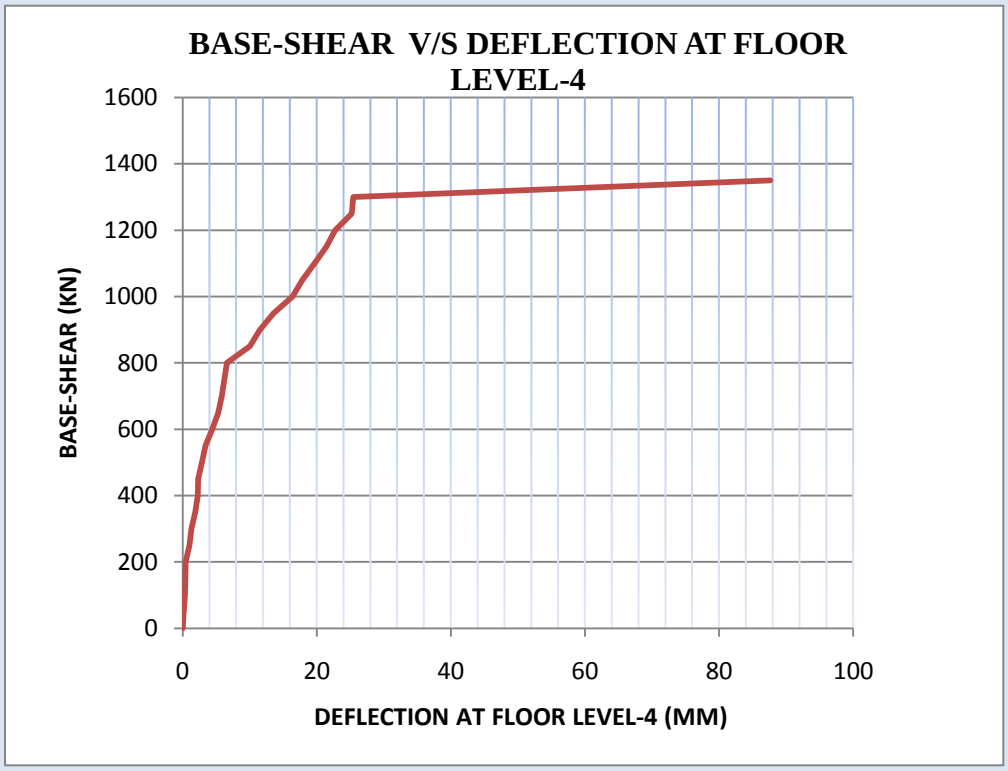

Figure 5.22 Base shear v/s Displacement at Floor Level-4 for Retrofitted Frame

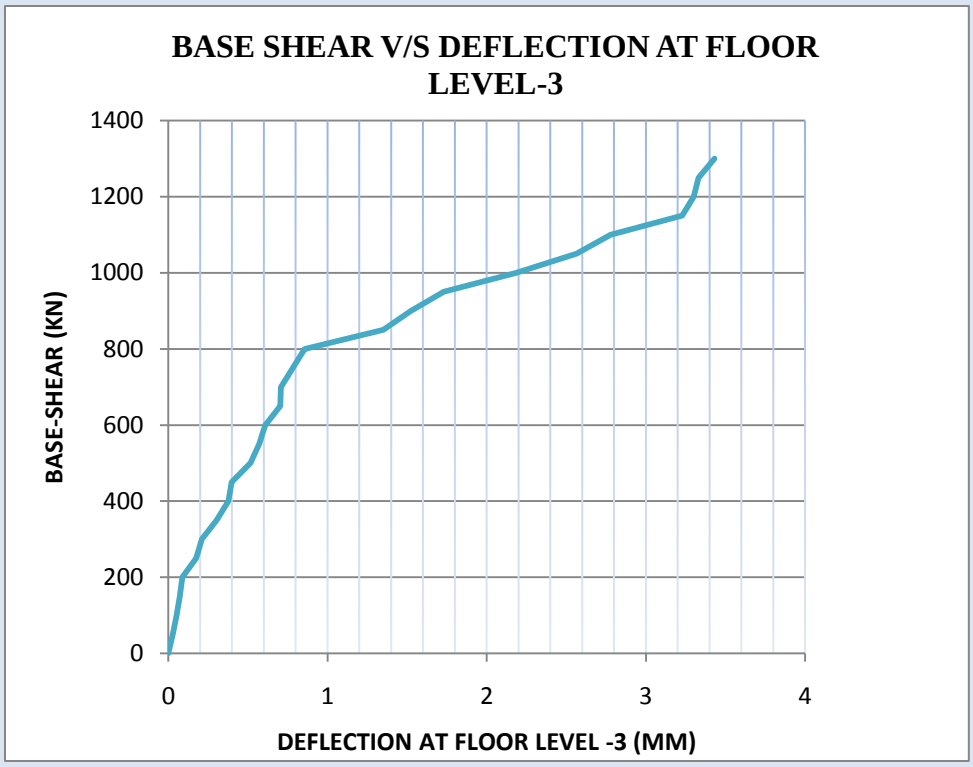

Figure 5.23 Base shear v/s Displacement at Floor Level-3 for Retrofitted Frame

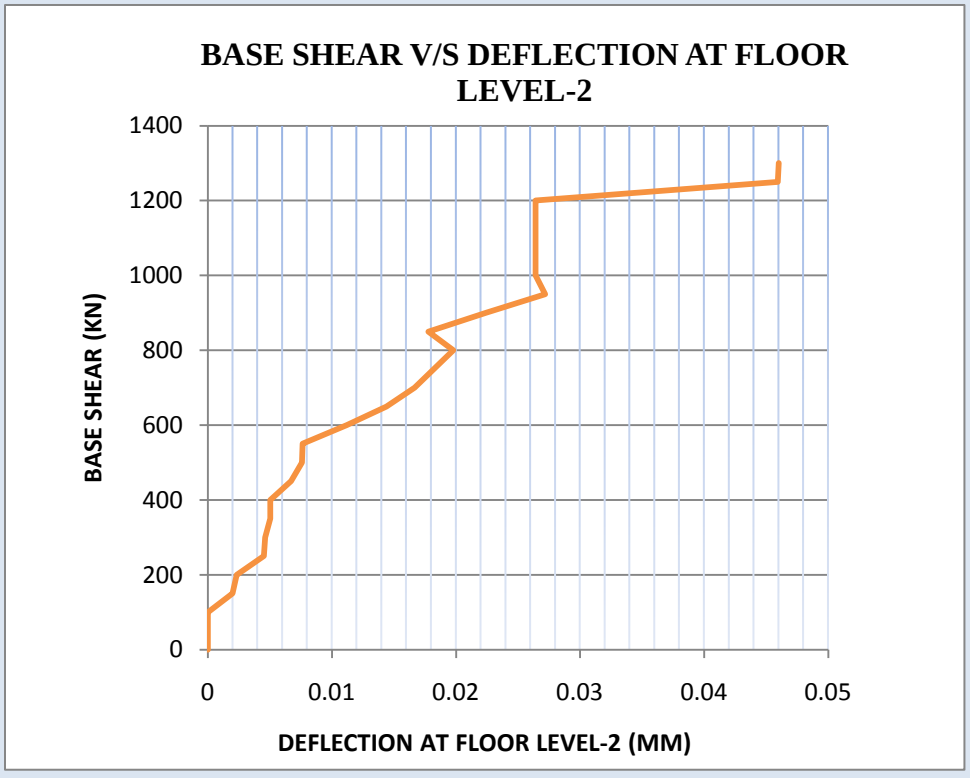

Figure 5.24 Base shear v/s Displacement at Floor Level-2 for Retrofitted Frame

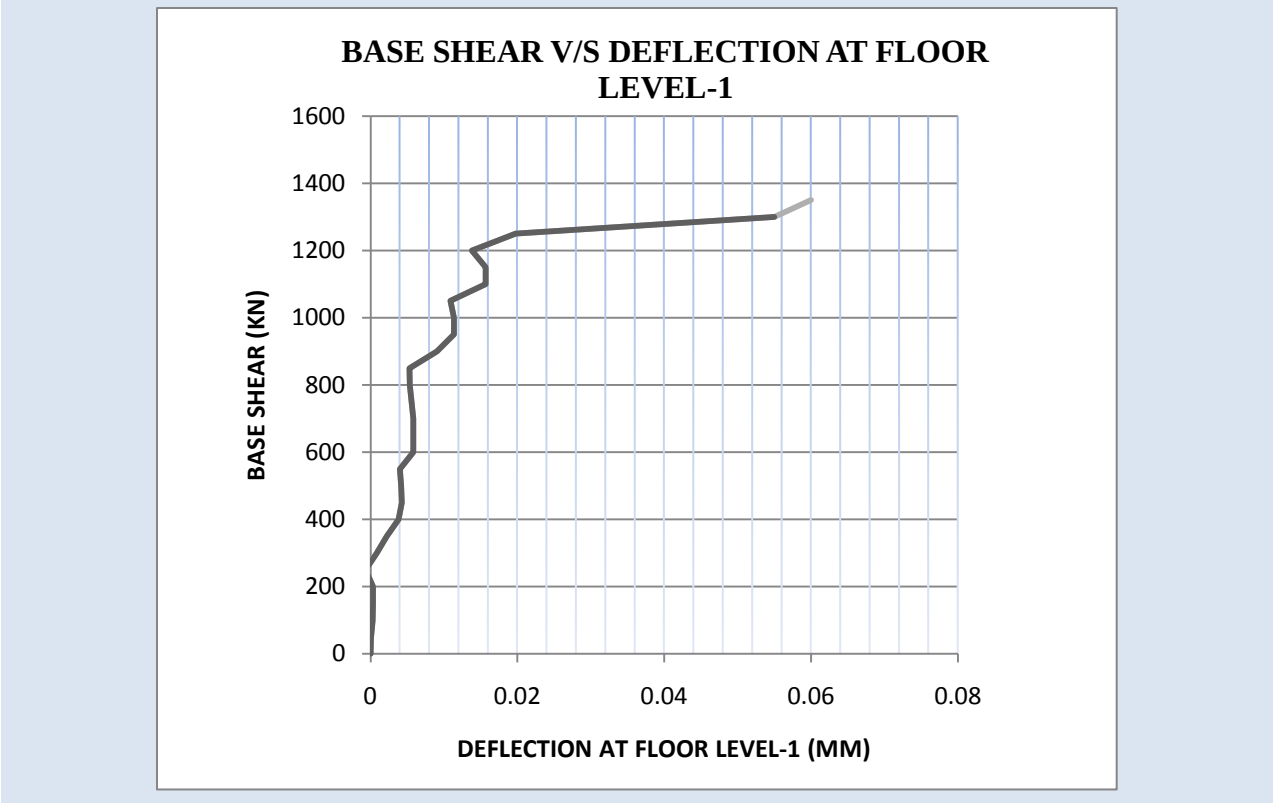

Figure 5.25 Base shear v/s Displacement at Floor Level-3 for Retrofitted Frame

5.3.3 CRACK PATTERNS

The variation of crack pattern has been taken out from the post processer of ATENA and are plotted in **Figure 5.27 to 5.32**. A discussion on crack pattern has been presented here.

CRACK PATTERNS AT STEP-15

The crack patterns in side elevation, bottom view along with perspective view of the structure at 15^{th} load step at value of base shear 800 KN has been presented in **Figure 5.26**. From the side elevations, column joint failures at 4^{st} floor level only along with few flexural cracks in beams, can be seen. Lower level floor slabs have experienced no cracks. Max. size of crack at this load step has been found to be 0.9mm. This shows that strengthened portion of the frame has experienced no cracking. **Figure 5.27** in which two perspective view are presented, presents iso-areas, which clearly show that maximum tension is being experienced by top storey of the frame wherw as lower storey is going through compressive stesses.

CRACK PATTERNS AT STEP-19

The crack patterns in side elevation, bottom view along with perspective view of the structure at 19th load step at value of base shear 1000 KN are shown in **Figure 5.28**. Side elevations show the beam- column joint failures at 3rd and 4st floor level only along with flexural cracks in beams. Lower level floor slabs have experienced no cracks. Max. size of crack at this load step has been found to be 1.48 mm. Mamimum damage has been experienced by column CL-19 at 4th floor level whereas CL-15 was the member receiving maximum damage 3rd level. Lower level floor slabs experience no cracks. This show that strengthened portion of the frame has experienced no cracking.

CRACK PATTERNS AT STEP-22

The crack patterns in side elevation, bottom view along with perspective view of the structure at 22th load step a at value of base shear 1150 KN re presented in **Figure 5.30 and 5.31**. It can be seen from side elevations that the beam- column joint failures at 3rd and 4st floor level only along with flexural cracks have occurred in beams. Lower level floor slabs experience no cracks. Max. size of crack at this load step has beeen found to be 2.40 mm. Maximum damage has been experienced by columns CL-15 and CL-19 at 4th floor level whereas CL 15 was the member receiving maximum damage at 3rd level. Lower level floor slabs experience no cracks. This shows that strengthened portion of the frame has experienced minor cracking. Severe damages have been observed at joints of upper floors whereas minor damage is observed in first and second floor level.

CRACK PATTERNS AT STEP-26

It has been observed that frame observed ultimate load at 26th load step at value of base shear 1350 KN. At this level frame has observed cracks at every level. At this ultimate value of base-shear retrofitted frame has also observed delamination of FRP wrapping at many places, showing the brittle failure of the frame.

CRACK PATTERNS AT STEP-15 MAX. CRACK SIZE-0.9 MM

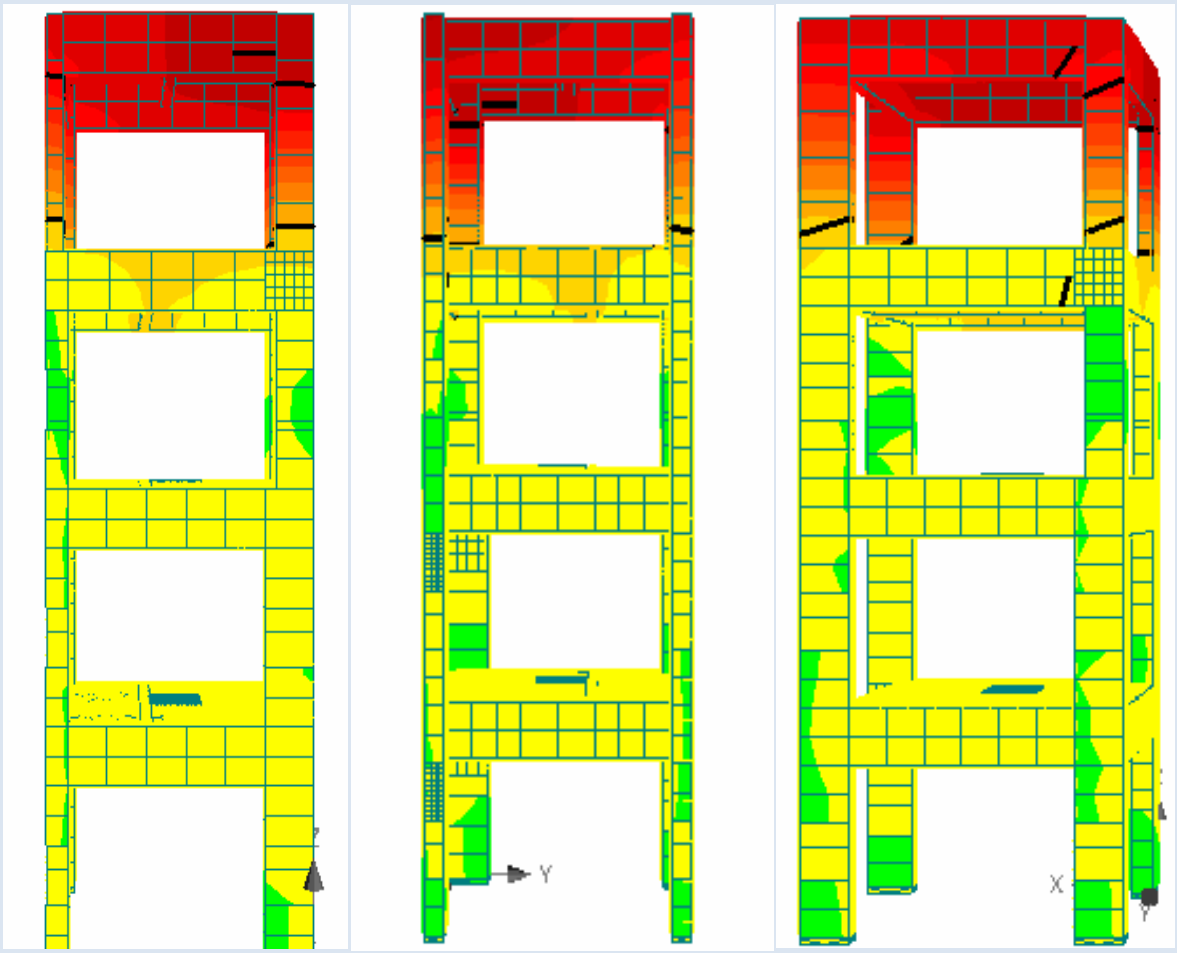

Fig5.26Crack Pattern at Step-15 at Base- shear 800 KN

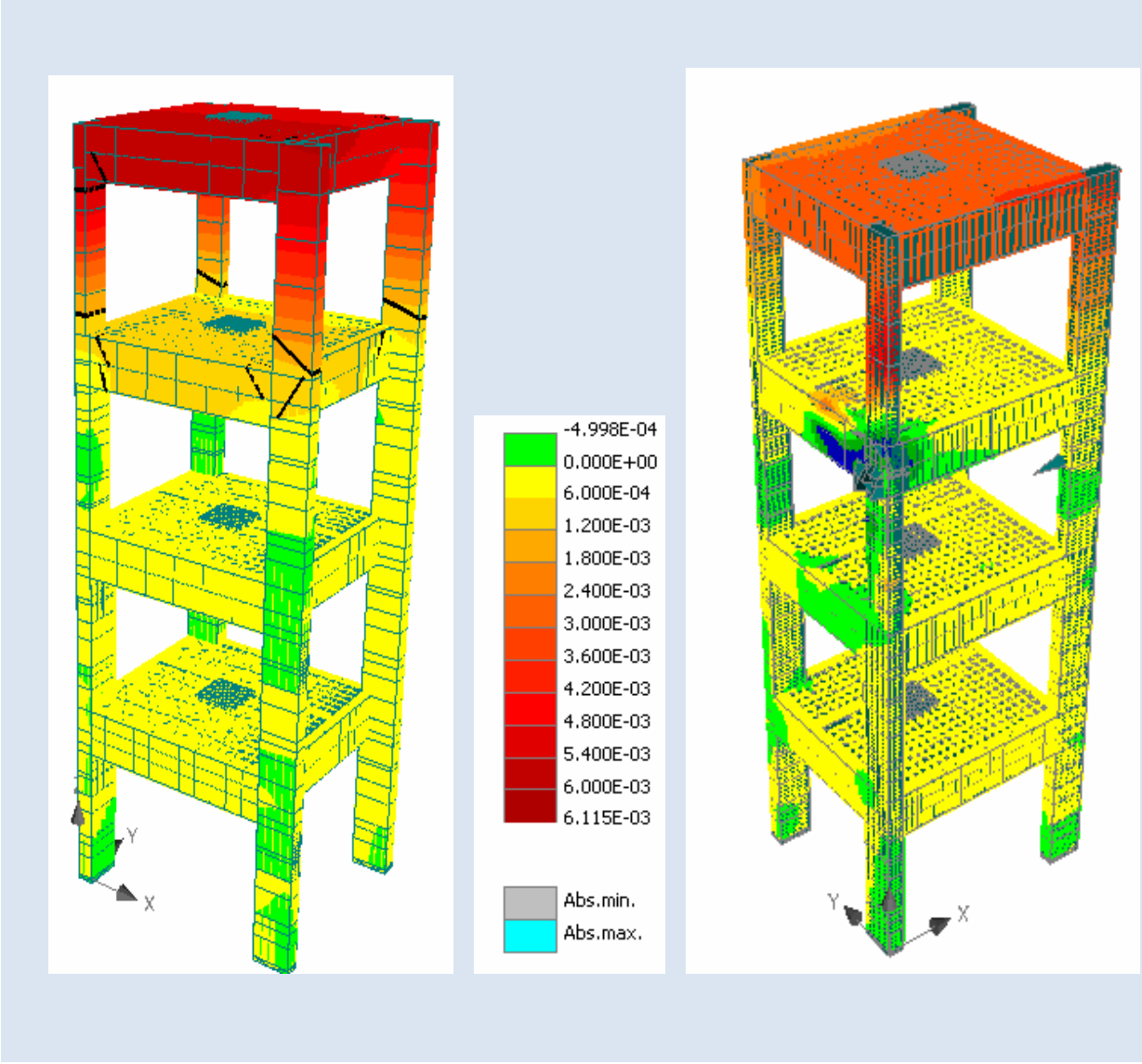

Fig5.27 Crack Pattern at Step-15 (Perspective view)

CRACK PATTERNS AT STEP-19 MAX. CRACK SIZE-1.48MM

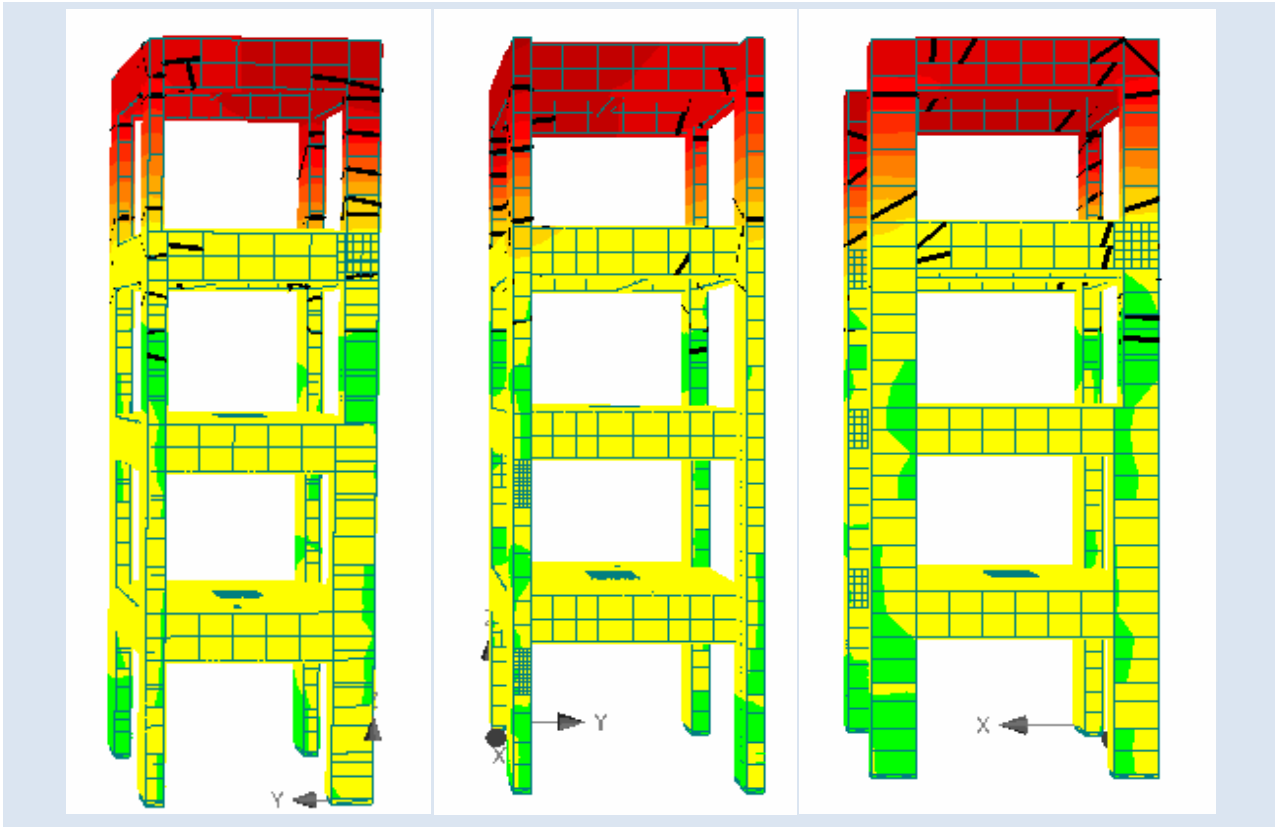

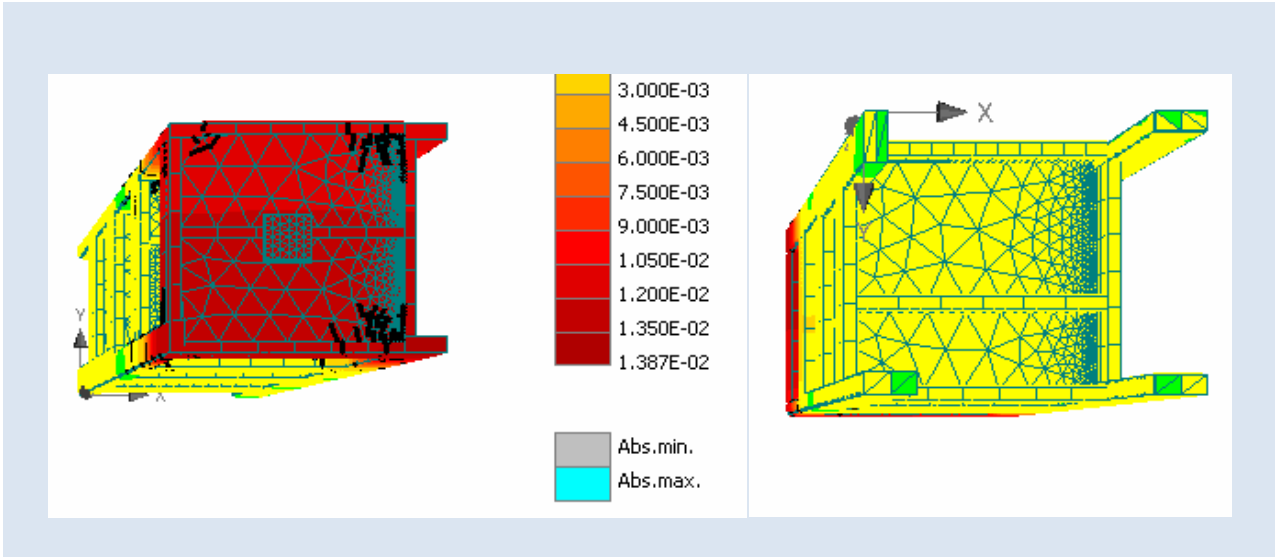

Fig5.28 Crack Pattern at Step-19 at Base-shear 1000 KN

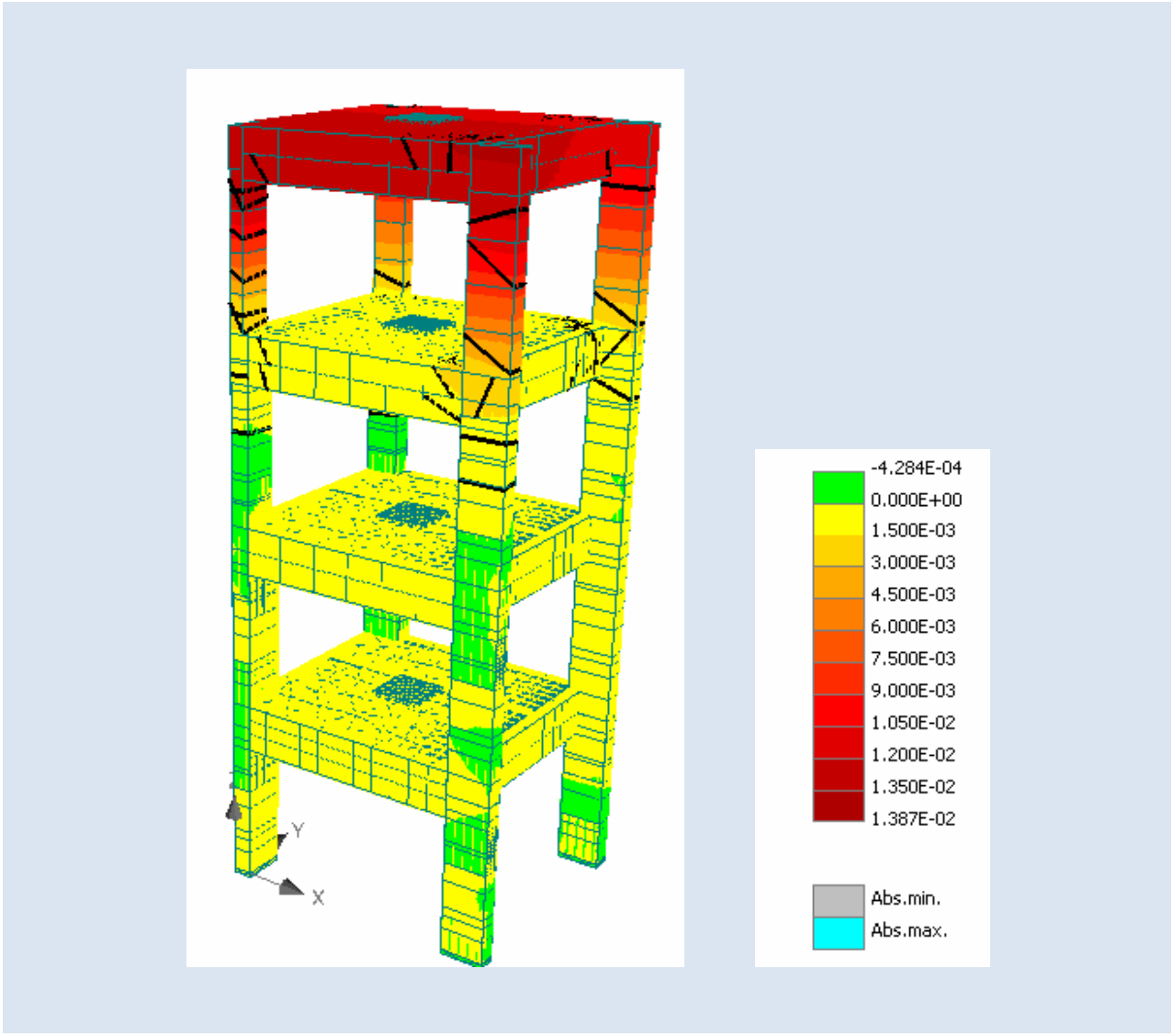

Fig5.29 Crack Pattern at Step-19 (Perspective view)

CRACK PATTERNS AT STEP-22 MAX. CRACK SIZE 2.40 MM

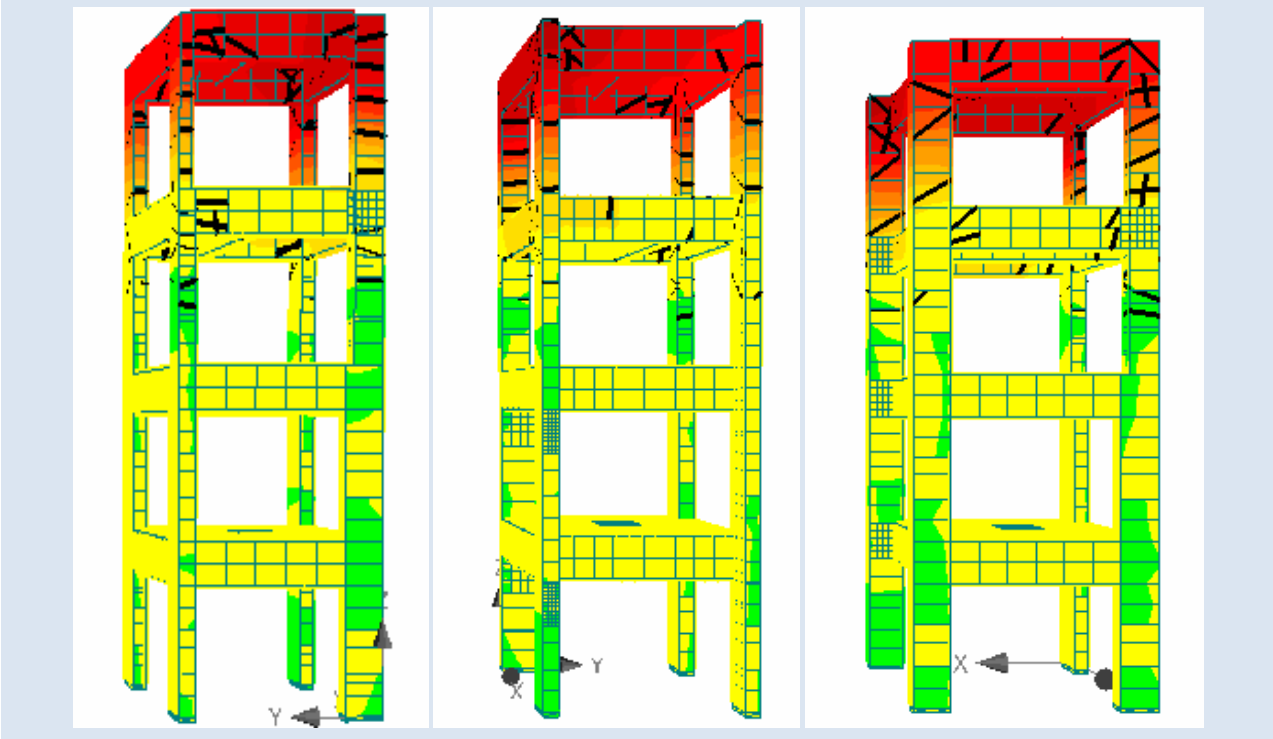

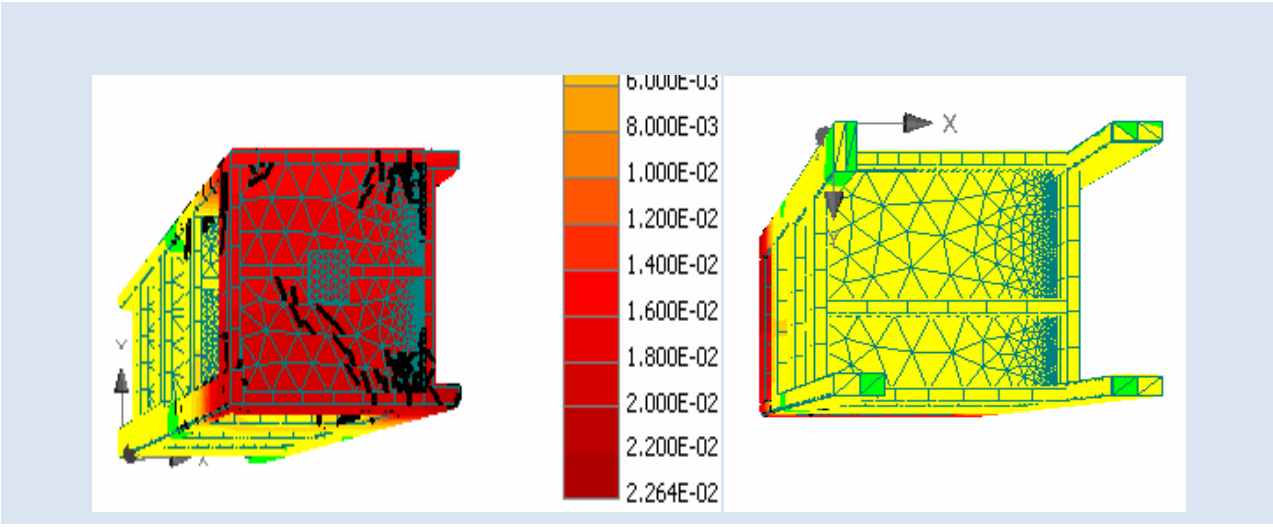

Fig5.30 Crack Pattern at Step-22 at Base- shear 1150 KN

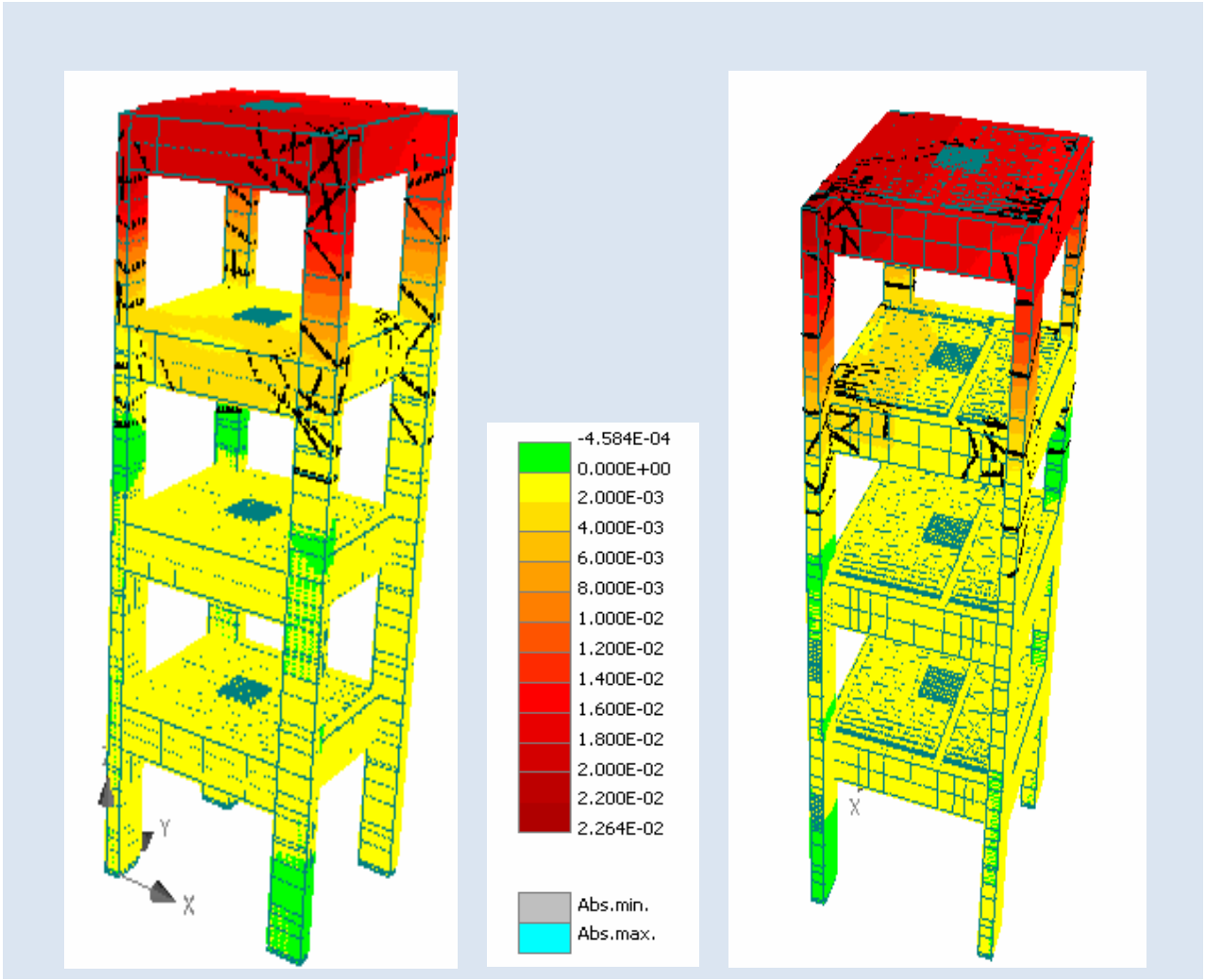

Fig5.31 Crack Pattern at Step-22 (Perspective view)

5.4 COMPARISON BETWEEN THE RESULTS OF CONTROL AND RETROFITTED RC FRAME

The comparison in the base shear v/s deflection between experimental control frame, FE control frame and retrofitted frame has been plotted in **Figure 5.32.** Comparison of cracking patterns between the control and retrofitted frame has been presented in **Figure 5.33.**

- The retrofitted model behaved linearly elastic up to the value of base-shear 600KN. The plot has shown almost negligible curvature up to the base-shear 1250 KN. After this it has observed sudden deflection which indicates frame entering the plastic zone. Fast increase in the value of displacements at fourth floor level has been observed. The value of deflection at base shear of 1350 KN has been observed as 87mm. which is very less in comparison with the value of maximum deflection of control frame at ultimate load.
- It has been observed from the plot that the retrofitted frame has observed brittle failure, as it has shown linear behaviour up to base-shear of 1250 KN and shown sudden increase in deflection at almost negligible increase in load step. The frame has observed total failure at the value of base-shear 1350 KN. This behaviour indicates decrease in ductility of the frame.
- The pattern of cracks has shown strengthened behaviour of retrofitted frame. Lower level floor slabs and other members have observed minimum cracks opposite to that have been experienced in the case of control frame.
- At ultimate value of base-shear retrofitted frame has observed delamination of FRP wrapping at many places.

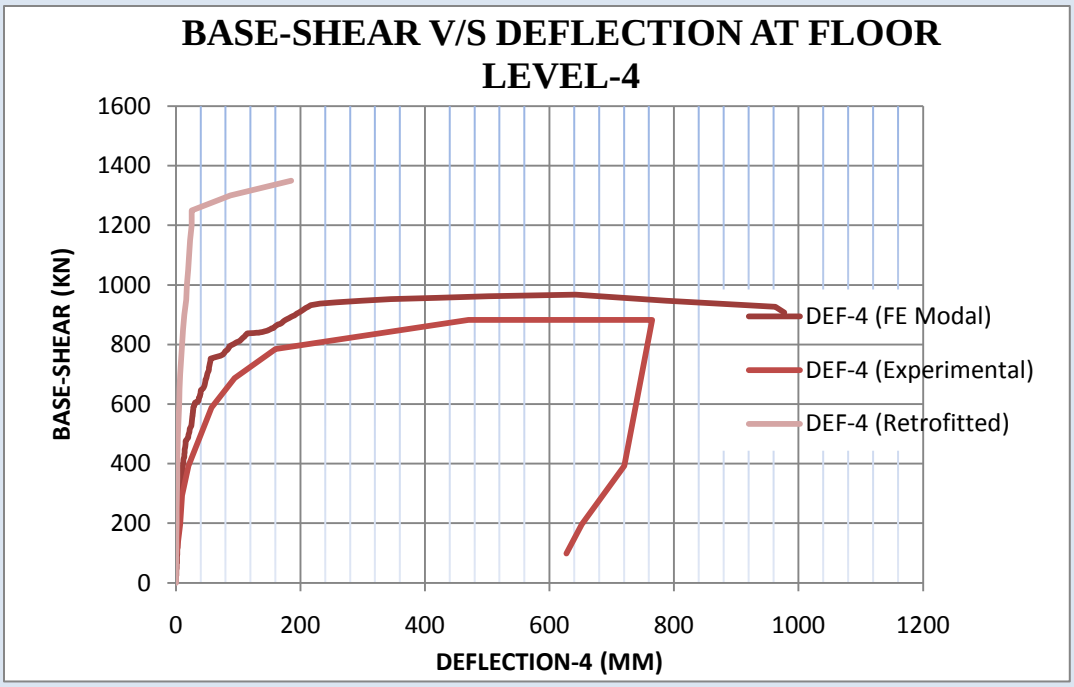

Figure 5.32 Comparison Curve of Base shear v/s Displacement at Floor Level-4

(FE Modal, Experimental & Retrofitted Frame)

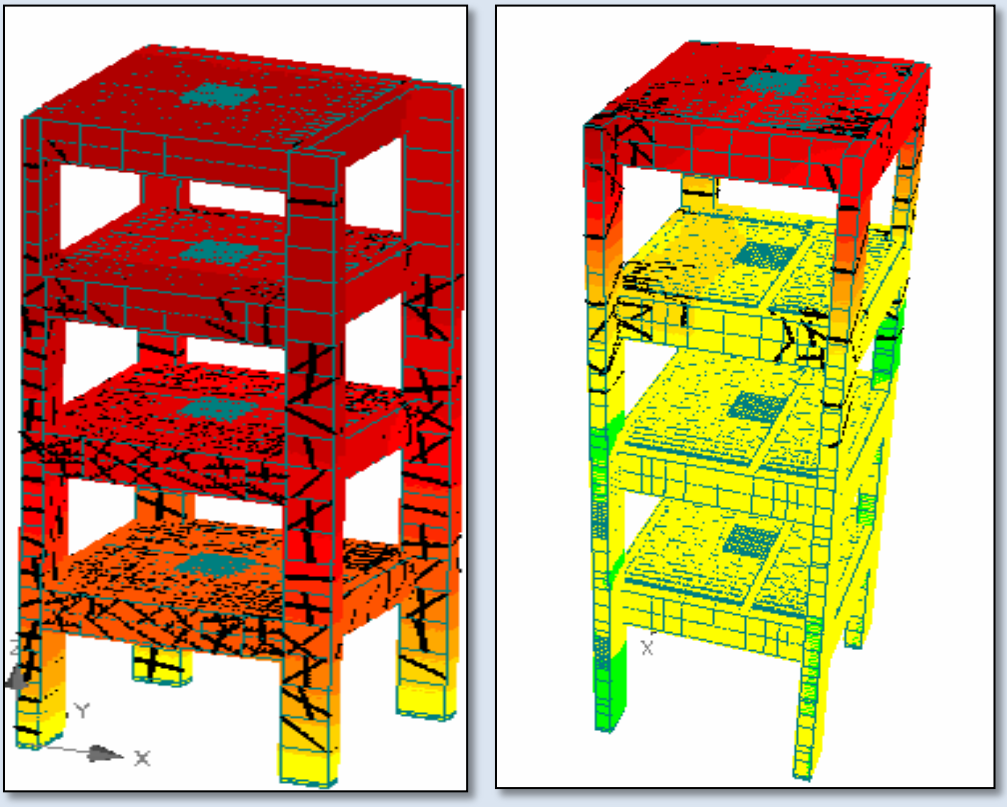

Fig5.33 Comparison between the control and retrofitted frame

Chapter 6

CONCLUSIONS & RECOMMENDATIONS

6.1 GENERAL

In the present study, the non-linear response of RCC control frame and the retrofitted RCC frame using FE Modelling under the incremental loading has been carried out with the intention to study the relative importance of several factors in the non-linear finite element analysis of RC frames.

6.2 CONCLUSIONS

The main observations and conclusions drawn are summarized below:

- *The frame behaved linearly elastic up to a base shear value of around 360 KN. At the value of base-shear 500KN, it depicted non-linearity in its behaviour. Increase in deflection has been observed to be more with load increments at base-shear of 750 KN showing the elasto-plastic behaviour. At value of base-shear 840 KN, a rapid increase in displacement has been observed. It has reached to the value of 175mm when base shear is 880 KN. After this value of base-shear, plastic behaviour has been observed by the frame as a constant increase in deflection has been observed, after the value of base-shear 927 KN. Subsequently deflection started increasing without any significant increment in load; it reaches to the value of 345 mm with the base-shear value 952KN. After this it has kept increasing even at decremental load steps.*
- The joints of the structure have displayed rapid degradation and the inter storey deflections have increased rapidly in non- linear zone. Severe damages have occurred at joints at lower floors whereas moderate damages have been observed in the first and second floors. Minor damage has been observed at roof level as shown in figures.
- The frame has shown variety of failures like beam-column joint failure, flexural failures and shear failures. Prominent failures shown by FE model are joint failures. Flexural failures have been seen in beams due to X-directional loading.

- After comparing experimental and FE Model base-shear v/s deflection curves of the frame at various floor levels the FE model results can be said to be reasonably in close agreement with the experimental data from the full-scale frame test.

- The results of FE model of the control frame have found to be higher by 8% of the experimental results. So it can be concluded that FE model push over results holds good with the experimental results though they are on slightly higher side.
- The retrofitted model has behaved totally linearly elastic up to a value of base shear 250 KN. It has been found to be almost linear till a base shear value of 800 KN, after this the non-linearity in the behaviour of retrofitted frame has been observed. After crossing the value of base shear 800 KN, fast increase in the deflection with load increments has been observed. After reaching the base-shear of 1300 KN, there is constant increase in deflections without any significant increment in load and deflection crosses the value of 87.8mm.The value of ultimate load corresponding to this base shear has been found to be 540 KN.

- Significant increase in the value of base-shear in case of FRP retrofitted FE model has been observed. Base shear v/s deflection curves at floor level-3 depicts lesser deflections as compared to top storey deflections. 1st and 2nd floor levels have experienced very lesser deflections.

- It has been observed that the top storey experienced major damages in this case opposite to the case of control frame.

- Micro cracks have been observed to appear even when the frame is in its elastic zone. The cracks have been found increasing with the increase in deflections

- Decrease in ductility has been observed as the frame has experienced failure at lesser values of deflections at ultimate value of base-shear. Debonding of FRP wrapping has also been observed even at lower value of deflection due to severe failures of beam column joints.

- The results of FE model of the retrofitted frame have found to be higher by 29% of the results obtained in case of control frame.

6.3 Recommendations

The literature review and analysis procedure utilized in this thesis has provided useful insight for future application of a finite element method for analysis. FEM model helps in comparing the results with experimental results data. Modelling the RCC frame in FEM based ATENA software gives good results which can be included in future research.

6.4 Future Scope

In the present study control frame has been studied under monotonic incremental loads. The frame can be studied under cyclic-loading to monitor the variation in load-deflection curves at given time history. Retrofitted frame at various stress levels and with different types of FRP wrapping can be studied to observe their behaviour at different loadings. Dynamic analysis of retrofitted frame can also be incorporated in the study.

REFERENCES

[1] Kwak, H.G., Fillipou, C.F.(1990) **" Finite Element Analysis of Reinforced Concrete Structures Under Monotonic Loading"** Structural Engineering Mechanics and Materials**,** Report no. UCB/ SEMM-90/14.

[2] Habibullah, A., Pyle, S. (1998), **"Practical Three Dimensional Non-near Static Push-Over Analysis"** Structure magazine, winter 1998.

[3] Kachlakev, M., Miller, T., Solomon, PE. Yim, and PE; Chansawat, K., Potisuk, T. (2001). **"Finite Element Modeling of Reinforced Concrete Structures Strengthened with FRP laminates",** Final Report OREGON Department of transportation.

[4] A report on (2010) **"Round Robin Exercise on experiment and analysis of four storey full scale reinforced concrete structure under monotonic pushover loads "** compiled by Ankush Sharma and Dr. G.R. Reddy.

[5] ATENA theory manual, part 1 from Vladimir Cervenka, Libor Jendele and Jan Cervenka.

[6] Amer, M. I., Mohammad, M. (2009) **" Finite Element Modelling of Reinforced Concrete Strengthened with FRP Laminates"** European Journal of Scientific Research, ISSN 1450-216X, Vol-30 No.4 Pg 526-541.

[7] Barbato, M. (2009) **"Efficient finite element modeling of reinforced concrete beams retrofitted with fibre reinforced polymers"** Journal of Computers and Structures, Vol 87, pg 167-176.

[8] Singhal, H. (2009), **"Finite Element Modeling of Retrofitted RCC Beams"** M.E. Thesis, Thapar University, Patiala.

[9] Pannirselvam, N., Raghunath, P.N., and Suguna, K. (2008). "**Strength Modeling of Reinforced Concrete Beam with Externally Bonded Fibre Reinforcement Polymer Reinforcement"** American Journal of Engineering and Applied Sciences, Vol 1(3), pg 192-199.

[10] Camata, G., Spacone, E., Zarnic, R. (2007). "**Experimental and non linear Finite Element studies of RC beams strengthened with FRP plates"** Journal of Composites: Part B, Vol 38, pg 277-288.

[11] Ferracuti, B., Savoia, B.M., Mazzotti, C.(2006). "**A numerical model for FRP-concrete delamination"** Journal of Composites, Vol Part B 37, pg 356-364.

[12] Maheri, M. R., (2005) **"Recent Advances in Seismic Retrofit of RC Frames"** Asian Journal of Civil Engineering (building and housing) vol. 6, NO. 5. Pages 373-391

[13] Perera, R., Recuero, A., De Diego, A., Lopez, C. (2004). "**Adherence analysis of fiber reinforced polymer strengthened RC beams".** Journal of Computers and Structures, Vol 82, pg 1865-1873.

[14] Supaviriyakit, T., Pornpongsaroj, P., and Pimanmas, A. (2004). "**Finite Element Analysis of FRP Strengthened RC beams".** Songklanakarin J. Science Technology, Vol 26(4), pg 497-507.

[15] Santhakumar, R., Chandrasekaran, E. and Dhanaraj, R. (2004). "**Analysis of retrofitted reinforced concrete shear beams using carbon fiber composites".** Electronic journal of structural engineering, Vol 4, pg 66-74.

[16] Cardone, D., Dolce, M., Ponzo, F.C. (2004) **"Experimental behaviour of r/c frames retrofitted with dissipating and recentring braces".** Journal of Earthquake Engineering, Vol. 8, No. 3 (2004) 361-396.

[17] Yang, Z.J., Chen, J.F. and Proverbs, D. (2003). "**Finite Element Modeling of concrete cover separation failure in FRP plated RC beams**" Construction and Building Materials, Vol 17, pg 3-13.

[18] Duthinh, D., and Starnes, M. (2001). **"Strengthening of Reinforced Concrete Beams with Carbon FRP"**, Journal of Composites in Constructions, pg 493-498.

[19] Ma, R., Xiao, Z. and Li, K. N. (2000). "**Column retrofitted with carbon fiber reinforced composites".**

[20] Shahawy, M., Arockiasamy, M., Beitelman, T., and Sowrirajan, R. (1995). **"Reinforced Concrete Rectangular Beams Strengthened with CFRP Laminates"**. Journal of *Composites*, **27**B: 225-233.

[21] Obaidat, Y. Taleb., Heyden, S., Dahblom, O. (2009) **"The effect of CFRP and CFRP/Concrete interface models when modeling retrofitted RC beams with FEM"** Journal of Computers and Structures.

[22] Ayman S. M., Banerjee, S. (2007). "**Shear enhancement of reinforced concrete beams strengthened with FRP composites laminates"** Journal of Composites: Part B, Vol 38, pg 781-793.

[23] Goyal, A. (2007), **"Health Monitoring of Retrofitted Beams by using the Vibration Measurements"** M.E. thesis, Thapar University, Patiala.

[24] Benjeddou, O., Ouezdou, M. B., and Bedday, A. (2007). "**Damaged RC beams repaired by bonding of CFRP laminates"** Journal of Construction and Building Materials, Vol 21, pg 1301-1310.

[25] Einde, L.V.D., Zhao, L., Seible, F.(2003). "**Use of FRP Composites in Structural Applications"** Construction and Building Materials Vol-17, pg389-403.

[26] Mohammad, R. A., Christoph, C., and Motavalli, M. (2007). "**Debonding failure modes of flexural FRP strengthened RC beams"** Journal of Composites: part B, Vol 39, pg 826-841.

[27] Mostofinejad, D., and Talaeitaba, S. B. (2006). "**Finite Element Modeling of RC connections strengthened with FRP laminates"** Iranian Journal of Science and Technology, Transaction B, Engineering, Vol. 30, pg 21-30.

[28] Simonelli, G. (2005). Report on "**Finite Element Analysis of RC Beams retrofitted with Fibre Reinforced Polymers"** Pg 1-220.